The tachykinin hemokinin-1 as a mediator in neuronal- and immune functions in mouse models of pain, arthritis, and dermatitis

Doctoral (PhD) Thesis

Agnes Hunyady MD

Science of Pharmacology Doctoral School

Neuropharmacology Program

Program Director: Erika Pintér MD, PhD, DSc

Supervisors: Zsuzsanna Helyes MD, PhD, DSc

Éva Borbély MD, PhD

UNIVERSITY OF PÉCS, MEDICAL SCHOOL

DEPARTMENT OF PHARMACOLOGY AND PHARMACOTHERAPY AND

JÁNOS SZENTÁGOTHAI RESEARCH CENTER

Pécs, 2021

1 Table of Contents

2 List of abbreviations

ANOVA – Analysis of variance

CFA – complete Freund's adjuvant

CGRP – calcitonin gene related peptide

CNS – central nervous system

DAB – diaminobenzidine

DAPI – 4',6-diamidino-2-phenylindole

(d)DC – (dermal) dendritic cell

pDC – plasmacytoid dendritic cell

DMARDs – disease-modifying antirheumatic drugs

DPA – dynamic plantar aesthesiometer

DRG – dorsal root ganglion

ECS – extracellular solution

EKA, -B, -C, -D – endokinin-A, -B, -C, -D

ELISA – enzyme-linked immunosorbent assay

FMT® – fluorescence molecular tomographic imaging

GABA – gamma-aminobutyric acid

GFAP – Glial fibrillary acidic protein

GPCR – G-protein coupled receptor

HK-1 – hemokinin-1

hr-NGF – human recombinant NGF

i.p. – intraperitoneal

i.v. – intravenous

Iba1 – Ionized calcium binding adaptor molecule 1

IL – interleukin

IVIS – in vivo imaging system

KO – knock out

L – lumbar

LL-37 – human cathelicidin-derived antimicrobial peptide

MAPK – mitogen-activated protein kinase

MCT – mast cell tryptase

MPO – myeloperoxidase

Mrgpr – mouse Mas-related G-protein coupled receptor

MrgprB2 – mouse Mas-related G-protein coupled receptor type B2

MRGPR – human Mas-related G-protein coupled receptor type

MRGPRX2 – human Mas-related G-protein coupled receptor type X2

NFκB – nuclear factor kappa-light-chain-enhancer of activated B cells

NGF – nerve growth factor

NK1, 2, 3 – tachykinin neurokinin 1, -2, or -3 receptor

NKA – neurokinin-A

NKB – neurokinin-B

NMDA – N-methyl-D-aspartate

NO – nitrogen monoxide

NSAID – nonsteroidal anti-inflammatory drugs

PAG – periaqueductal gray matter

PAR2 – protease-activated receptor 2

PBS – phosphate-buffered saline

PCR – polymerase chain reaction

PFA – paraformaldehyde

PMSF – phenylmethanesulfonyl fluoride

PSL – partial sciatic nerve ligation

PTX – pertussis toxin

RA – rheumatoid arthritis

ROI – region of interest

RTX – resiniferatoxin

s.c. – subcutaneous

SEM – standard error of the mean

SNSR – sensory neuron-specific G protein-coupled receptors

SP – substance P

Tac1 – tachykinin precursor 1 or preprotachykinin-A gene

Tac3 – tachykinin precursor 3 or preprotachykinin-B gene

Tac4 – mouse tachykinin precursor 4 or preprotachykinin-C gene

TAC4 – human tachykinin precursor 4 or preprotachykinin-C gene

Tacr1 – tachykinin receptor 1 gene

TCR – T cell receptor

TG – trigeminal ganglion

Th1 – T helper 1 cell

Th17 – T helper 17 cell

Th2 – T helper 2 cell

TNFα – tumor necrosis factor alpha

TRPA1 – Transient Receptor Potential Ankyrin-1 (TRPA1) ion channel

TRPV1 – Transient Receptor Potential Vanilloid-1 (TRPV1) ion channel

WT – wild type

3 Introduction

3.1 Pain, inflammation, and the immune system

Pain is one of the most common complaints for people seeking medical help with an annual economic toll of over 600 billion dollars reported in the USA alone[1]. While in most cases the underlying problem can be resolved, and short term pain medication is sufficient, about 10-20% of pain can becomes chronic, with prevalence increasing among older adults[2–4]. Chronic pain can result in detrimental effects on a person's sociopsychological state, and so there are continuous efforts to better define and diagnose these conditions[5]. The currently used main groups of analgesic drugs are nonsteroidal anti-inflammatory drugs (NSAIDs), opioids, and adjuvant analgesics (e.g., antidepressants, anticonvulsants). These medications are not effective in every case, and especially long-term administration can lead to a variety of side-effects[6], necessitating non-pharmacological approaches in pain management[7], and fueling research to identify new targets for the development of new analgesics. While most research concentrates on structures of the nervous system, it is important to note that many forms of chronic pain begin with (autoimmune) inflammation adding a difficult to treat neurogenic component, and vice versa, damage to the nervous system potentially resulting in chronic pain can lead to local inflammation as well[8,9]. The long-held belief that the nervous system is an immunologically isolated area has been challenged on multiple points. Nociceptors have been shown to release neuropeptides that regulate immune cells[10]; microglia (the resident macrophages of the brain) as well as other immune cells and immune-related signaling molecules influence the developing brain[11], and lymphatic vessels have been discovered in the meninges[12,13]. Exploring the interactions between the nervous- and immune system and the molecules involved in the crosstalk between them could advance our knowledge of both neurological and autoimmune conditions (especially ones with painful symptoms) whose therapy hold unmet medical needs today.

Pain is transmitted by specialized sensory neurons called nociceptors. Nociceptors can be quick conducting (12-30 m/s) thin myelin sheathed Aδ-fibers responsible for somatic pain, or slow conducting (0.5-2 m/s) C-fibers without a myelin sheath responsible for secondary, diffuse pain[14]. The cell body of nociceptors can be found in the dorsal root ganglion (DRG), after entering the spinal cord the central branch ends in the lamina I-II of the dorsal spinal horn. This nociceptor is

the first part of the ascending pain tract which transmits the painful stimulus through the contralateral spinothalamic tract to the thalamus, then to the somatosensory cortex[15]. The descending pathways modulate the sensation (Figure 1). The periaqueductal grey matter (PAG) in the mid-brain integrates the descending inhibitory pathways, where serotonin and endogenous opioids are the most important neurotransmitters, as well as norepinephrine from the locus coeruleus and gamma-aminobutyric acid (GABA)[16].

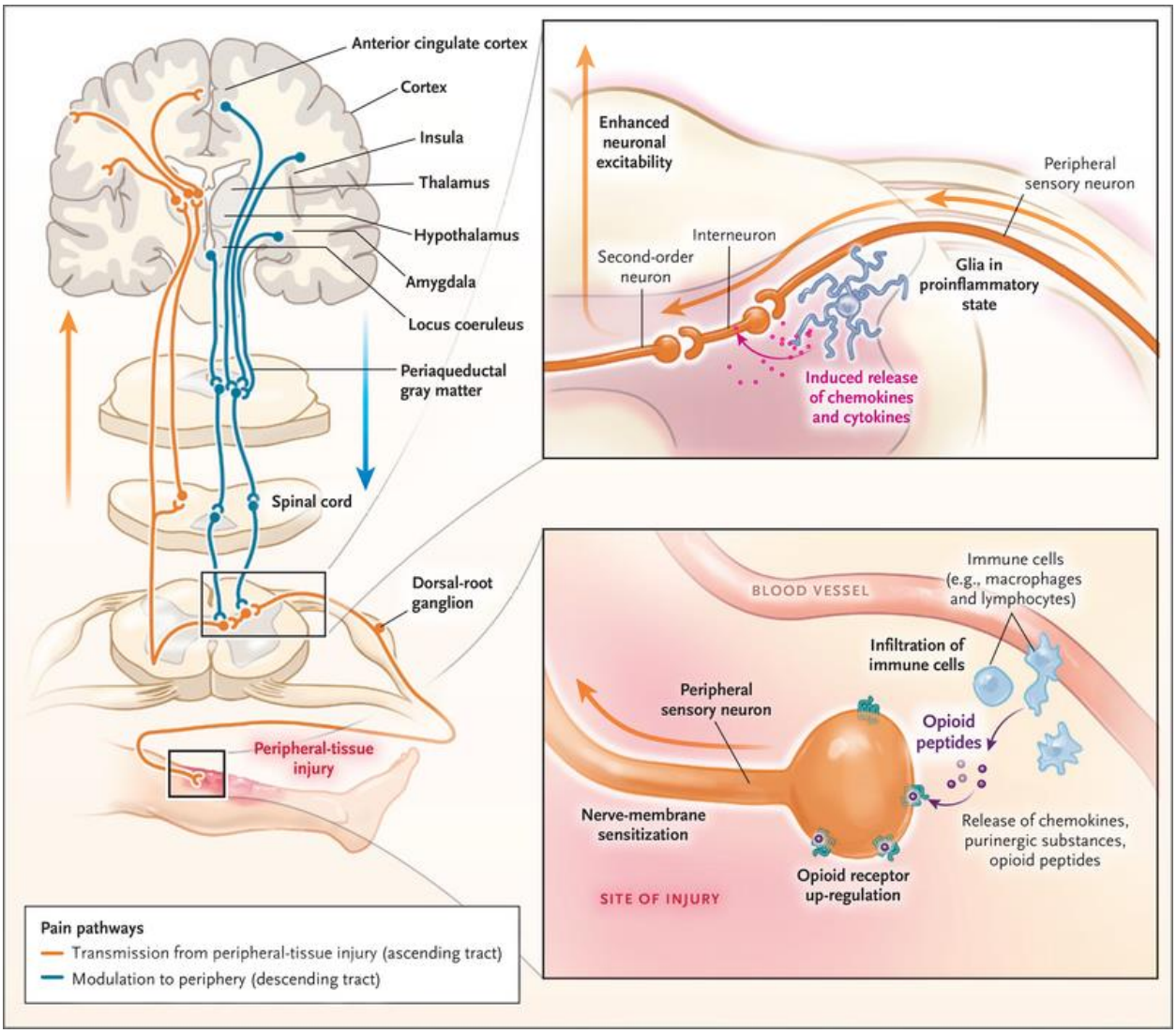

Figure 1. Ascending (orange) and descending (blue) pain pathways of the central nervous system. Upper insert shows glia activation and consequent neuroinflammation sensitizing neurons in the dorsal horn of the spinal cord and lower insert shows peripheral sensitization in the injured tissue. (Martyn et al., 2019.)[15]

A subtype of the nociceptors is the capsaicin sensitive nerve ending which expresses the Transient Receptor Potential Vanilloid-1 (TRPV1) ion channel on its surface[17]. These are polymodal nerve fibers which can be activated by several different types of stimuli like heat-, mechanical- and chemical stimuli. Aside from these classical afferent functions, they also have an efferent function which is activated without a reflex mechanism[18]. This local efferent function is called neurogenic inflammation when inflammatory neuropeptides like tachykinins (substance P = SP and neurokinin-A = NKA) and calcitonin gene related peptide (CGRP) are released from the nerve endings. In addition, as a systemic efferent function, anti-inflammatory agents like somatostatin are released into the systemic circulation which counteract the neurogenic inflammation[19].

In response to continuous stimulation nociceptors become sensitized through both peripheral and central mechanisms[20]. Peripheral sensitization occurs in the tissues, in the vicinity of the nociceptors. Mediators (H^+, NO, histamine, nerve growth factor = NGF, tumor necrosis factor alpha = TNFα) released from the leukocytes and the nerve endings activate their receptors on the nerve terminals, leading to direct action potential generation (activation), and/or sensitization. As a result of sensitization, the threshold of the nociceptor decreases and the reaction to stimuli becomes more intense resulting in hyperalgesia (a mildly painful stimulus causing intensive pain reaction)[21], and spontaneous pain can develop as well.

Persistent nociceptive activity can lead to central sensitization, where the modulation in the central nervous system (CNS) plays a crucial role as well (amplification, emotional component), so the pain sensation is not decided exclusively by the activation of the nociceptor[22]. Descending facilitatory pathways can become enhanced and overcome the descending inhibitory pathways[23]. In the spinal cord the wind-up mechanism occurs in the synapse between the nociceptor and the secondary neuron. The N-methyl-D-aspartate (NMDA) receptor of glutamate becomes free on the post-synaptic cleft due to a series of molecular reactions involving the tachykinin SP and its tachykinin neurokinin 1 (NK_1) receptor [24]. Since SP and NK_1 receptor play such a pivotal role in pain transmission, efforts have been made to develop an NK_1 receptor antagonist as a new type of analgesic drug, however, while NK_1 receptor antagonists were effective in animal models of pain, they had no effect in human pain conditions and have been repurposed as antiemetics[25].

Apparently, some additional complexity in the human tachykinin system was able to circumvent these new types of analgesics, and years of research have uncovered new peptides and tachykinin receptors, adding further nuances to the relationship between the nervous- and immune systems as well.

3.2 Hemokinin-1, the newest member of the tachykinin family

3.2.1 Tachykinins and receptors

Tachykinins represent a classical neuropeptide family, their members include SP, NKA and neurokinin-B (NKB). The name tachykinin refers to the ability of SP to produce rapid contraction of smooth muscle as opposed to the slow contraction caused by bradykinin, while the "neurokinin" name reflects the earliest data regarding their role in the nervous system: SP and NKA could be found primarily in the CNS and primary sensory neurons, NKB in brain and spinal cord. Tachykinins consist of 10-11 amino acids with a conserved FXGLM-NH2 sequence (X being an aromatic or an aliphatic amino acid) on their C-terminal end which is responsible for receptor activation. The C-terminal end is amidated and deamination results in the decrease of their activity[26]. The N-terminal region is hydrophilic and varies between tachykinins. Their molecular targets are G-protein coupled receptors: NK_1-, NK_2- and NK_3 receptors. Every tachykinin can bind to each receptor, but with different affinities: SP shows preference to NK_1 receptor, NKA to NK_2 receptor and NKB to NK_3 receptor. They are encoded by the tachykinin precursor genes: preprotachykinin-A gene (*Tac1*) encodes both SP and NKA by alternative splicing, preprotachykinin-B gene (*Tac3*) encodes NKB (Table 1).

Gene	Tachykinin	Receptor	Main localization
Tac1	SP	NK_1	Primary sensory neuron, central nervous system (CNS)
	NKA	NK_2	
Tac3	NKB	NK_3	Uterus, placenta, CNS
Tac4	HK-1	NK_1, ?	Immune cells, cerebellum

Table 1. Genes, prefered receptors and main localisations of tachykinins

In later years evidence increased of these peptides being expressed in non-neuronal tissues. SP and NKA were found in the airways[27], SP in the endothel[28] and leukocytes[29], and NKB was discovered in the entirely nerve-free placenta[30]. In 2000 the newest member of the tachykinin family, hemokinin-1 (HK-1) was discovered in the (also non-neuronal) lymphopoietic bone marrow stem cells of mice[31].

3.2.2 HK-1 and endokinins

HK-1 is an undecapeptide which has the characteristic C terminus of tachykinins (Phe-X-Gly-Leu-Met-NH2) (Figure 2). It shows a remarkable structural resemblance to SP, so much so that the effort to reliably differentiate them from each other continues to date[32].

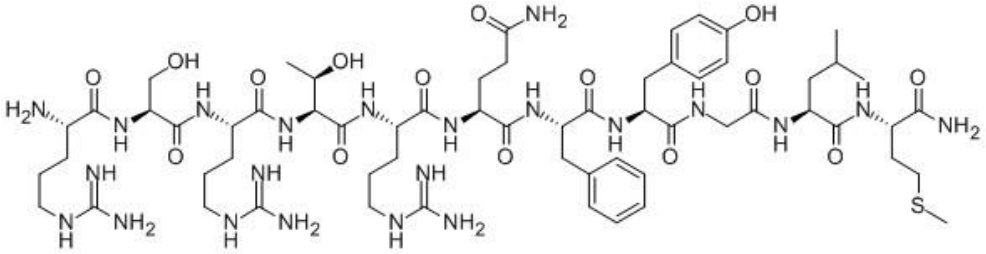

Figure 2. Molecular structure of HK-1 from https://www.mybiosource.com/Hemokinin-1-peptide

It is encoded by the preprotachykinin-C gene (*Tac4*), which is not an evolutionarily conserved gene; different peptides are derived from it in different species. In mice the *Tac4* gene product is a single peptide, the rat/mouse HK-1, whereas in humans several isoforms can be found. There are 4 splice variants, the α-, β-, γ-, δ*TAC4* that result in a diverse group of peptides (Table 2)[33].

species	gene	locus	splice variant	product
mouse	Tac4	11D		**r/mHK-1**
rat		10q31		
human	TAC4	17q21.33	αTAC4	**EKA**, EKC
			βTAC4	**EKB**, EKD
			γTAC4	**EKB**
			δTAC4	**EKB**, hHK-1, hHK-1(4-11)

Table 2. Genes, splice variants ang gene products of HK-1. Products in bold: classic tachykinins with FXGLM-NH_2 motif, products in regular font: tachykinins with GLL-NH_2 motif. EKA, -B, -C, -D: endokinin A, B, C, D; hHK-1: human hemokinin-1; r/mHK-1: rat/mouse hemokinin-1; hHK-1(4-11): truncated human HK-1

3.2.3 HK-1: molecular mechanism of action

Predictably, HK-1 shows the highest affinity to the NK_1 receptor, though HK-1 is a full agonist on all three tachykinin receptors[34]. The NK_1 receptor is G-protein coupled, has several isoforms, and can activate different types of signal transduction in different cells. Phosphorilation of the serine/threonine residues at the C-terminal end can deactivate the receptor, and a truncated isoform exists as a result of alternative pre-mRNA splicing, where the loss of the last 96 C-terminal amino acids results in weakened function[35] and decreased ligand affinity[36]. The glicosilation of the N-terminal site elicits signal transduction and ligand binding as well as prevents receptor internalization.[37] (Figure 3)

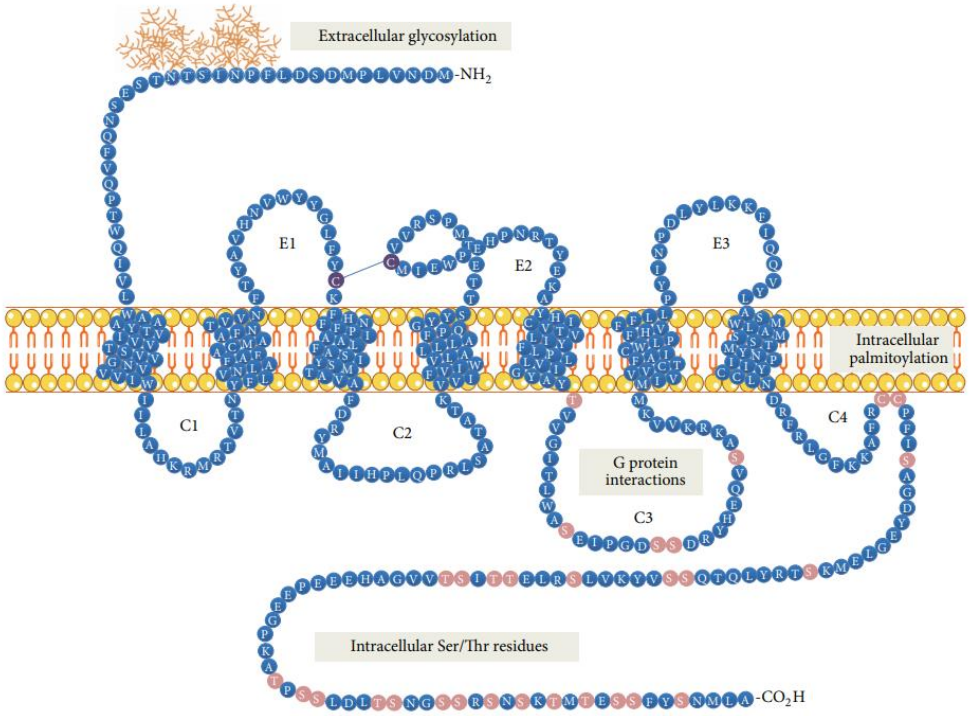

Figure 3. Structure of NK_1-receptor. The extracellular N-terminal part shows glycosylation, the serine/threonine amino acids marked with red on the intracellular C-terminal part are possible sites of phosphorylation resulting in weakened function. (Garcia-Recio et Gascón, 2015.)[38]

The signal transduction of the activated NK_1 receptor is complex and tissue specific. Proposed signaling pathways include adenyl cyclase enzyme activation and inhibition, activating phospholipase C and consequently increasing intracellular Ca^{2+} level, and activation of Rho/Rock pathway leading to cytoskeleton reorganization and cell migration[38] (Figure 4).

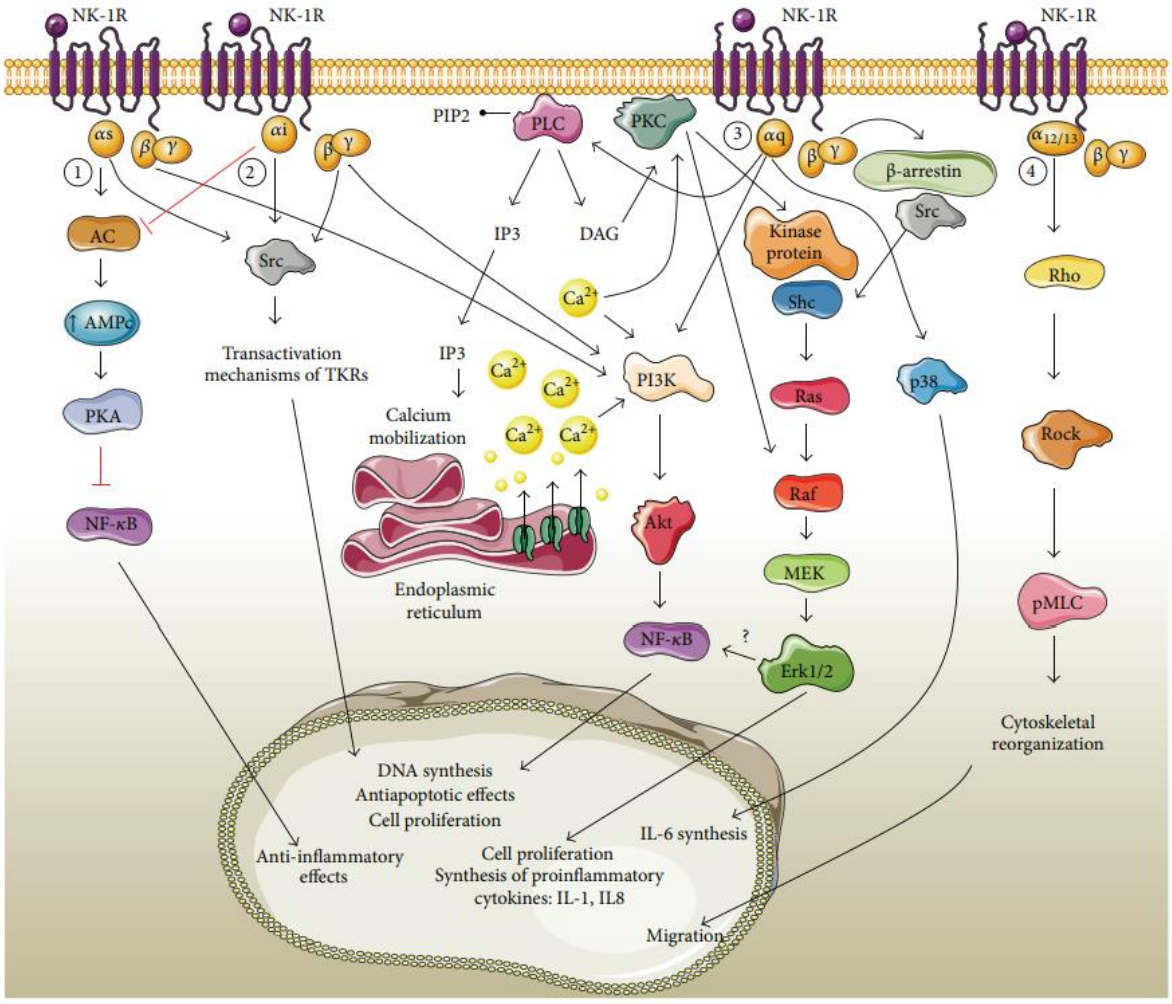

Figure 4. Possible signal transduction pathways activated by the NK_1 receptor (Garcia-Recio et Gascón, 2015.)[38] *AC: adenyl cyclase; AMPc: cyclic adenosyl monophosphate; PKA: protein kinase A; NF-κB: nuclear factor kappa-light-chain-enhancer of activated B cells; PLC: phospholypase C; PKC: protein kinase C; PIP2: Phosphatidylinositol 4,5-bisphosphate; IP3: inositol 1,4,5-trisphosphate; DAG: diacylglycerol; PI3K: Phosphoinositide 3-kinases; MEK: mitogen-activated protein kinase kinase; pMLC: phosphorylated myosin light chain; IL: interleukin*

HK-1 can activate the NK_1 receptor as its N-terminal region binds to the extracellular loop and helps the insertion of the C-terminal region into the transmembrane part of the receptor.[39] While the affinity of HK-1 to NK_1 receptor was comparable to SP, it was 500 times less potent at activating NK_2 receptor and NK_3 receptor than SP[34], and also showed differences in the molecular mechanism, as HK-1 did not elicit the desensitization and internalization of the receptor[40]. The

other *TAC4* gene products found in humans further vary the picture of receptor-ligand interactions: while EKA and EKB also show the highest affinity toward the NK_1 receptor, EKC and EKD do not seem to bind to any of the known NK receptors[33]. These variations can be explained in part by the NK_1 receptor subtypes, since beyond the "classic" receptor, "septide sensitive" and "new NK_1-sensitive" subtypes also exist[41], however other evidence has suggested the presence of unidentified molecular target(s) of HK-1. Studies of gene knock-out (KO) mice showed that HK-1-deficient and NK_1 receptor-deficient mice do not behave the same in certain disease models. HK-1-deficient *Tac4* KO mice showed milder inflammation of the airways, while NK_1 receptor-deficient *Tacr1* KO mice did not[42]. Recently it has been discovered that tachykinins can act on Mas-related G-protein coupled receptors (MRGPR). These are a family of receptors formerly known as sensory neuron-specific G protein-coupled receptors (SNSR)[43], which were identified in the early 2000s[44], and are located mainly on primary sensory neurons and mast cells[45]. Older NK_1 receptor antagonists such as aprepitant can inhibit both NK_1 receptor and Mrgpr in mice, but not in humans, whereas novel dual action antagonists can inhibit human MRGPR as well[46]. Since these receptors play a role in nociception[47], this observation is a possible explanation for the ineffectiveness of NK_1 receptor antagonists as analgesics in humans despite being effective in rodents. HK-1 contributes to the development of asthma in murine models through NK_1 receptor on mast cells, while in human mast cells it acted through MRGPRX2 receptor, not NK_1 receptor[48], making MRGPRs a likely candidate for HK-1's missing target molecule.

3.2.4 Physiological and pathophysiological role of HK-1

As opposed to the other tachykinins, HK-1 was suggested to play an important role in the periphery rather than the nervous system. In humans *TAC4* mRNA was found by PCR analysis in visceral and reproductive organs, skeletal muscle, thyroid gland, skin while in mice *Tac4* mRNA was found in visceral organs, brain, thymus, spleen, and skin. Interestingly, HK-1 was scarcely

found in most regions of the brain, SP being the predominant tachykinin everywhere, except for the cerebellum. Here HK-1, and not SP showed a more remarkable expression (Figure 5)[49].

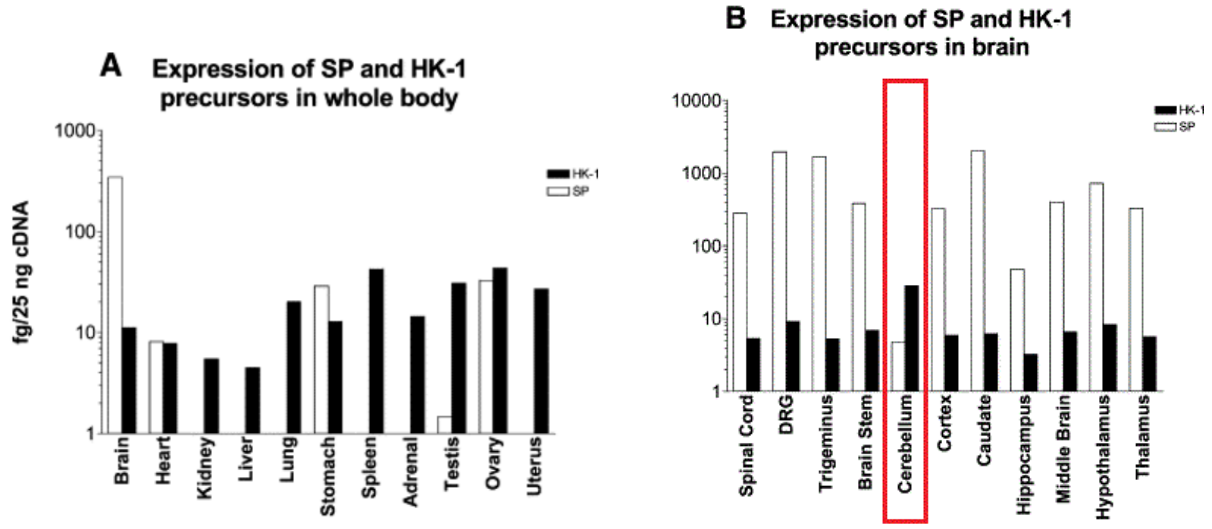

Figure 5. Expression pattern of HK-1 and SP in different organs (A) and brain regions (B). HK-1 is predominantly peripheral, while SP is mainly found in the brain, except in the cerebellum, where HK-1 shows a higher expression. (Duffy et al., 2003.)

As its name suggests, HK-1 is the predominant tachykinin in the bone marrow as it is expressed in both myeloid and lymphoid precursor cells like monocytes, macrophages, dendritic cells, T cells, and B cells[50,51]. Its preferential expression in such peripheral tissues can be explained by the regulatory mechanism in its promoter region, as well as NFκB promoting increased *Tac4* transcription in T cell lines[52]. HK-1 can enhance the maturing of B cells in the transition to antigen developing cells[53], activate the mitogen-activated protein kinase (MAPK) pathway and act as a co-stimulator in mature B cells[54]. HK-1 (and SP) can be found in the synapse between T cells and dendritic cells as NK_1 receptor interacts with the T cell receptor to promote T cell maturation and survival[55]. Through the NK_1 receptor HK-1 could also upregulate IL17A and IFNγ production in CD4+ T cells and contributes to the development of T helper (Th) 17 cells. HK-1 enhanced IL1β, IL6, and TNF-α, and IL23 production as well[56].

Since its discovery, some roles of HK-1 in the CNS have also been revealed: evidence points to the nociceptive effect of HK-1 (with some notable exceptions), as well as its interactions with

well-established components of the pain pathway like opioids and glutamate. Intracerebroventricular administration of low dose (1–10 pmol) HK-1 caused nocifensive behavior, while high dose (≥0.1 nmol) caused analgesia, all of which could be counteracted by an NK_1 receptor antagonist, as well as opioid antagonists[57]. Other studies have shown that lumbar intrathecal administration of 0.1 nmol HK-1 caused pain reaction in mice which could be inhibited by an NMDA receptor antagonist[58], but not an NK_1 receptor antagonist[59]. These results suggest that high doses of HK-1 might have non-specific actions resulting in divergent (e.g., analgesic) outcomes. Beyond this, HK-1 can potentiate the effects of TRPV1 activation, suppress TRP melastatin 8 (TRPM8) mediated cold-induced nociception, but has no influence on the effects of TRP ankyrin 1 (TRPA1) channels[60]. An increased amount of HK-1 was detected in the blood of patients with fibromyalgia[61], a pathological condition with heightened pain sensitivity due to alterations in the central and peripheral pain pathways[62]. It has been suggested that a brain-specific N-terminal acetylation of HK-1 can increase its potency in the CNS[63].

Tachykinins and their receptors are also known to promote tumor proliferation, growth, and survival, neovascularization, and metastatic progression and accordingly, some data regarding HK-1 has emerged as well[64]. An increased amount of HK-1 was detected in nasal lavage fluid of patients with nasal polyposis[65]; and in leiomyoma samples alongside an increased expression of truncated NK_1 receptor isoform[66]. It promotes glioblastoma cell migration via the NK_1 receptor[67], as well as the migration of melanoma cells[68]. Other notable effects of HK-1 include contribution to immune and inflammatory responses in the gastrointestinal tract, and it is expressed in the human airways. It can decrease blood pressure, increase heart rate, and is involved in angiogenesis. It has an uterotonic effect on the non-pregnant uterus, and promotes sperm motility[69].

3.3 Arthritis

Rheumatoid arthritis (RA) is the most common autoimmune disorder of the joints characterized by chronic inflammation and severe pain. Although the inflammation can be effectively controlled by NSAIDs, steroids, disease-modifying antirheumatic drugs (DMARDs) and biologic agents[70], pain is often resistant to these drugs[71]. Persistent pain has resulted in an increased use

of opioids among RA patients[72], though opioids are not effective in all cases[73] suggesting more complex pain pathomechanisms in RA and making pain management an unmet medical need. The joints are densely innervated by capsaicin-sensitive peptidergic sensory nerves[74] expressing, among others, the TRPV1 and TRPA1 ion channels activated by a broad range of inflammatory mediators[10] (Figure 6). These nerves play an important role in complex neurovascular-immune interactions resulting in chronic pain[75]. Recently, intensive investigations have been initiated to reveal sensitization processes at molecular[76] and histological levels alike[77] that convert inflammatory to central pain, contributing to persistent arthritic pain[78]. Exploration of these pathophysiological processes is hindered by the fact that no single animal model can mimic every aspect of RA, conclusions drawn from a single model might not necessarily apply to the human disease[79]. Studying the role of endogenous molecules of the sensory-vascular-immune interactions is essential to identify key mediators and potential novel drug targets.

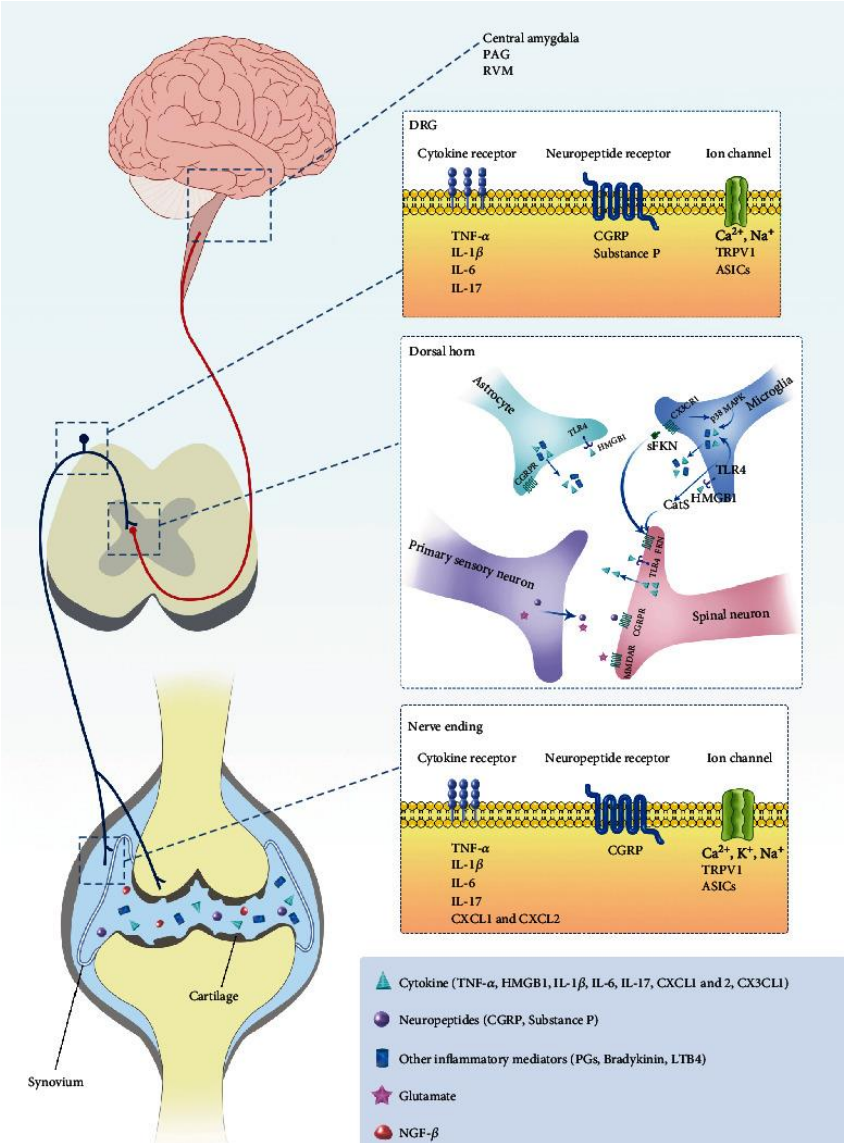

Figure 6. Peripheral and central mechanisms of RA pain (Cao et al., 2020.). Proinflammatory cytokines released in the joint and CGRP sensitize sensory neurons. Activated glia in the spinal cord release mediators which contribute to neuroinflammation and central sensitization.

PAG=periaqueductal grey matter; RVM=rostral ventromedial medulla; DRG: dorsal root ganglion; TNF: tumor necrosis factor; IL: interleukin; TRPV1: transient receptor potential vanilloid 1; ASICS: acid-sensing ion channels; CGRP(R): Calcitonin gene-related peptide (receptor); CXC(L/R): chemokine (C-X-C motif) ligand/receptor; TLR: toll-like receptor; HMGB1: high-mobility group box 1 protein; MAPK: p38 mitogen-activated protein kinase; MMDAR: (s)FKN: (soluble) fractalkine; Cats: cathepsin S

3.4 Neuropathic pain

Pain can originate from several sources like trauma, inflammation, cancer, metabolic diseases, but the most debilitating and therapeutically challenging form is neuropathic pain, which is a very typical symptom of diabetes, genetic diseases and nerve injury[80]. Neuropathy can be central (injury to the spinal cord or brain) or peripheral nerve damage; mononeuropathy if one nerve is affected (e.g., carpal tunnel syndrome) or polyneuropathy. There can be sensory-, motor- or vegetative symptoms based on what type of nerve has been involved. We can also classify it by etiology (diabetic, traumatic, chemotherapy induced, genetic etc.), or the cellular damage (axon and/or myelin damage)[81]. Gliosis can be an accompanying mechanism, both microglia and astrocytes can become activated at the site of nerve damage, or in the spinal cord where the central branch of the neuron ends[82] (Figure *7*).

NGF can be highlighted as a critical factor in nerve development, survival, and regeneration, as well as a transmitter of pain. Based on this contradictory action, both human recombinant NGF (hr-NGF) and the antagonist of TrkA, an NGF receptor have been tried as analgesics. The TrkA antagonist showed promising results in alleviating pain, while hr-NGF somewhat improved neuropathic pain, but increasing the dosage was not possible due to hyperalgesia, muscle- and joint pain occurring as side effects. In the pharmacological treatment of neuropathy NSAIDs are ineffective, and opioids have only limited use. The adjuvant analgesics currently in use (tricyclic antidepressants, antiepileptics) have common and severe side effects[83], and in many cases the presently available pharmacotherapy is not satisfactory, there are several therapy-resistant patients[84]. Therefore, neuropathic pain is still an unmet medical need; understanding the underlying mechanisms and finding new key molecules is essential in determining new therapeutic targets.

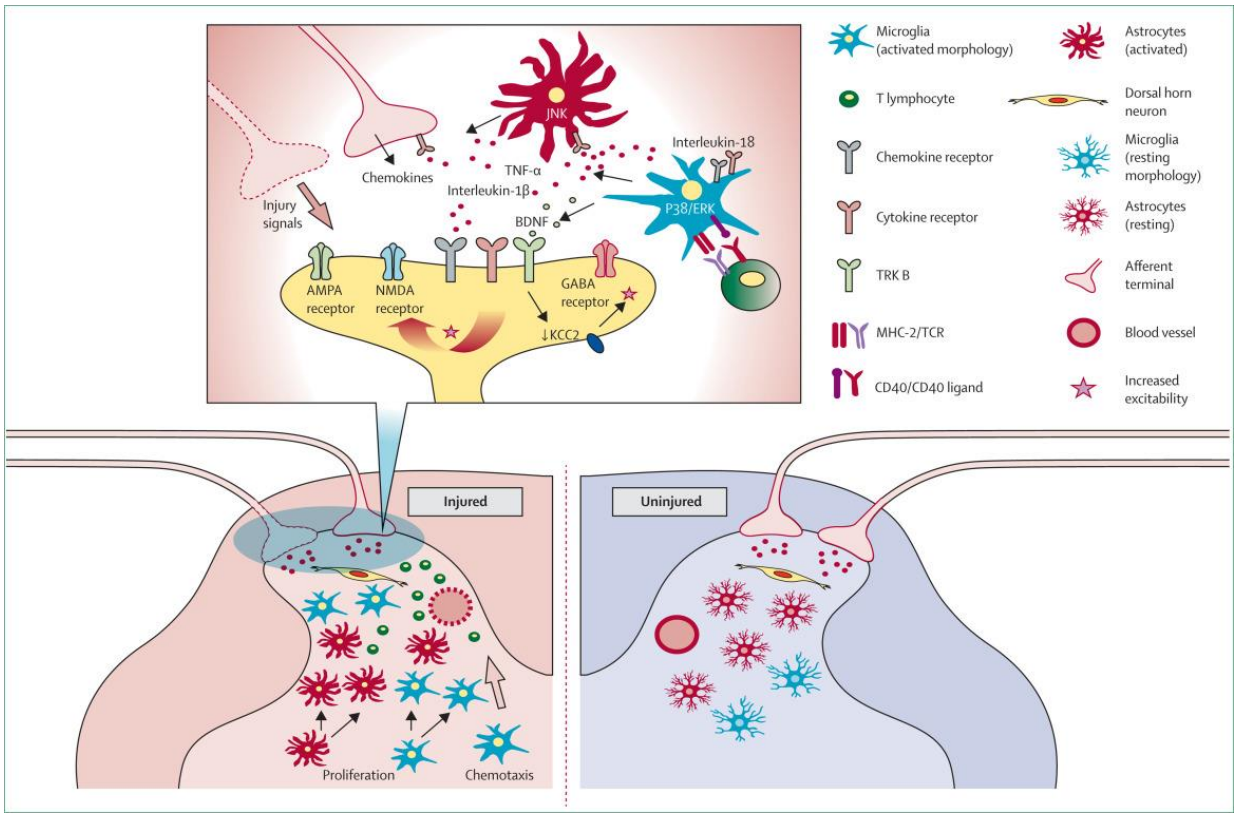

Figure 7. Glia cells in the spinal cord with and without injury. Factors released after peripheral nerve injury activate microglia and astrocytes and stimulate T cell response. The released cytokines and chemokines disrupt the transmitter balance and result in enhanced excitation and sensitization (Calvo et al., 2012.)[85]

TNF: tumor necrosis factor; BDNF: Brain-derived neurotrophic factor ; GABA: gamma-Aminobutyric acid; AMPA: α-amino-3-hydroxy-5-methyl-4-isoxazolepropionic acid; NMDA: N-Methyl-D-aspartate; KCC: chloride potassium symporter; TRK B: tropomyosin receptor kinase B; TCR: T cell receptor

3.5 T-cell mediated skin pathologies: allergic contact dermatitis and psoriasis

3.5.1 Allergic contact dermatitis

Allergic contact dermatitis is a type IV delayed hypersensitivity reaction caused by a contact allergen in 2 main phases: a sensitization phase, and an elicitation phase. A contact allergen is usually a small molecule that cannot induce an immune reaction by itself, but after entering the skin it can bind to local proteins. In the sensitization phase this hapten-protein conjugate will be taken up by the Langerhans cells (LC) or dermal dendritic cells d(DC), transported to the local lymph nodes and presented to T-cells[86] (Figure 8). The activation and maturation of the T-cells takes about 7 days in mice and 14 days in humans. The elicitation phase happens after the second encounter with the allergen, activating the T-lymphocytes and leading to redness, swelling, itching of the skin with cellular infiltration, skin lesions. Both Th1 and Th2 cells and cytokines may play a role in mouse models of allergic contact dermatitis[87]. This pathological immune response is modulated by the nervous system as well, TRPA1 on sensory neurons of the skin and NK_1 receptor playing a role in the integration of immune and neuronal mechanisms[88,89].

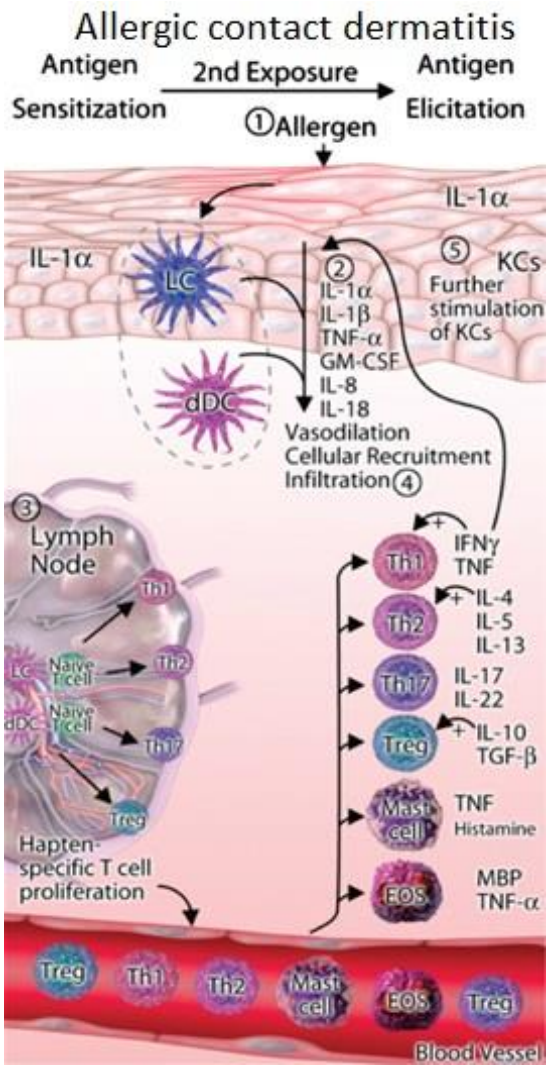

Figure 8. Development of allergic contact dermatitis. The contact allergen is taken up by LCs or dDCs, to be presented in the lymph node to T cells in the sensitization phase. After the 2nd exposure, in the elicitation phase, these T cells will be responsible for symptom development. (Dhingra et al., 2013.)LC: Langerhans cell; dDC: dermal dendritic cell; IL: interleukin; KC: keratinocyte; TNF: tumor necrosis factor; IFN: interferon; GM-CSF: granulocyte-macrophage colony-stimulating factor; Th: T helper cell; Treg: regulatory T cell; EOS: eosinophile granulocyte

3.5.2 Psoriasis

Psoriasis is an autoimmune disease mediated by Th1-cells affecting the skin and/or joints, with characteristic elevated, dry, itchy and scaly skin lesions[90]. Psoriasis can develop when LL-37 (human cathelicidin-derived antimicrobial peptide) produced by keratinocytes binds bacterial or own DNA after injury. This protein-DNA complex will be taken up by plasmacytoid dendritic cells (pDC) in the skin. Furthermore, dermal dendritic cells stimulate the migration of autoimmune Th17 and Tc17 cells into the epidermis, where they produce IL17 and IL22 cytokines; and neutrophil infiltration mediated by IL17 can lead to pustular psoriasis[91] (Figure 9). DCs in the skin are in close contact with sensory nerve endings and inhibiting the subset of TRPV1 and Nav1.8 ion channel expressing fibers can stop the IL23 dependent formation of psoriasis[92]. Human case reports provide evidence that nerve injury was able to ameliorate psoriatic skin lesions in the affected dermatome, with recurrence of lesions after nerve recovery[93]. SP and NKA and their receptors have been reported in psoriatic biopsy samples in immune cells, and NKA in nerve endings as well[94]. There is some information regarding the role of HK-1 in T-cells. HK-1 plays a role in T-lymphopoiesis, it is expressed in dendritic cells, and NK_1 receptor interacts with the T cell receptor (TCR) promoting the maturation and survival of T-cells[55].

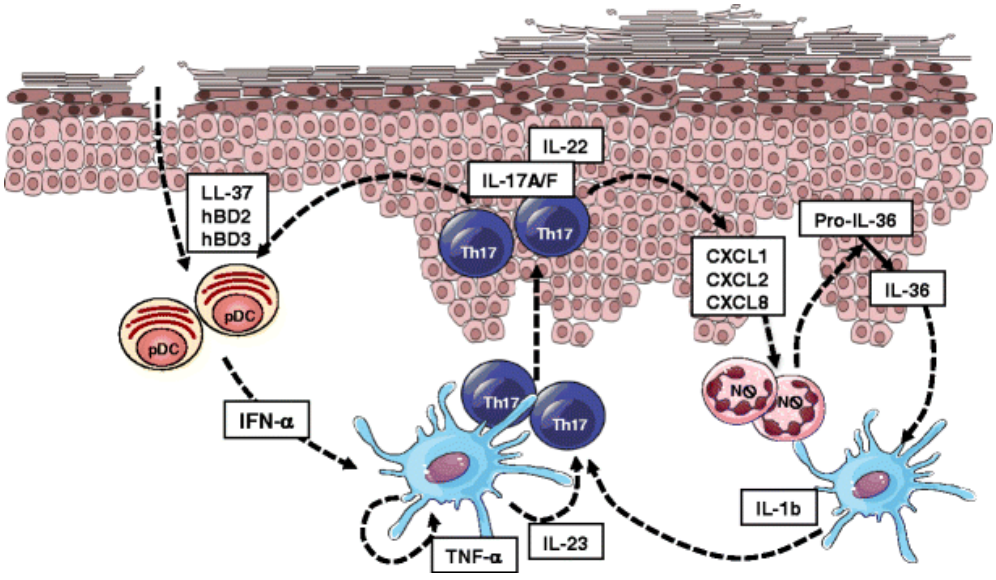

Figure 9. Th17 cells in the development of psoriasis. The pDC cells produce mediators that contribute to Th17 activation and the development of psoriatic lesions. (Conrad et al., 2018.)

pDC: plasmacytoid dendritic cells; LL-37: human cathelicidin-derived antimicrobial peptide; CXCL: chemokine ligands; IL: interleukin; IFN: interferon; TNF: tumor necrosis factor; hBD: human beta defensin

4 Primary aims

1. Determining the role of HK-1 in acute and chronic models of arthritis in relation to nervous system alterations.
2. Analyzing the effect of HK-1 on primary sensory neuronal cultures.
3. Investigating the role of HK-1 in acute pain conditions and peripheral traumatic mononeuropathy.
4. Examining the role of HK-1 in T-cell mediated autoimmune models as allergic contact dermatitis and psoriasis.

5 Methods

5.1 Animals

Experiments were carried out on *Tac1* (*Tac1*$^{-/-}$), *Tac4* (*Tac4*$^{-/-}$) gene-deficient, NK_1 receptor knockout (*Tacr1*$^{-/-}$) mice and C57Bl/6 wild types (WT) of both sexes (8–12 weeks, 20–30 g). The original breeding pairs of the *Tac1*$^{-/-}$ and *Tacr1*$^{-/-}$ mice were obtained from the University of Liverpool, UK[95,96], while those of the *Tac4*$^{-/-}$ mice were donated by Berger et al.[97] Transgenic mice with deletion of *Tac1*, *Tac4* or *Tacr1* were generated on a C57Bl/6 background and backcrossed to homozygosity for > 5 generations prior to using C57Bl/6 mice as controls, purchased from Charles-River Ltd. (Hungary). Germline transmission of the mutated allele and excision of the selection cassette were verified by PCR analysis. Animals were bred and kept in conventional animal house of the Department of Pharmacology and Pharmacotherapy, University of Pécs at 24–25 °C, 12 h light/dark cycles. Animals were provided standard diet and water *ad libitum*. Mice were housed in groups of 5–10 in polycarbonate cages (330 cm^2 floor space, 12 cm height) on wood shaving bedding. Behavioral tests and perfusion were carried out in the laboratory of the Department in the morning. The animals had a 60-min period prior each experiment for acclimatization. Anesthesia was performed by intraperitoneal (i.p.) administration of ketamine and xylazine (100 mg/kg and 10 mg/kg, respectively). The investigator was always blinded to the treatments and the genotypes of the mice.

5.2 Ethics

All experiments were carried out according to the European Communities Council Directive of 2010/63/EU and Consideration Decree of Scientific Procedures of Animal Experiments (243/1988). The studies were approved by the Ethics Committee on Animal Research of Pécs University according to the Ethical Codex of Animal Experiments (BA 02/2000-9/2011), (BA 02/2000–2/2012), (BAI/35/55-76/2017).

5.3 Experimental models

The measurement methods of the models are described in chapter 5.4. (Investigational techniques).

5.3.1 Induction of arthritis

5.3.1.1 K/BxN serum transfer arthritis (chronic)

K/BxN are a strain of mice that express the T cell receptor transgene KRN and the MHC class II molecule (A^{g7})[98] and spontaneously develop joint inflammation reminiscent of human rheumatoid arthritis[99]. Administering the serum of these animals to other mouse strains evokes a passive serum transfer arthritis as the IgG class autoantibodies in their serum target the glucose-6-phosphate isomerase in the recipient mouse leading to the activation of the cells innate immune system as well[100]. We gave an i.p. injection of 150-150 µl K/BxN serum on day 0 and day 3 of the experiment. The resulting arthritis spontaneously resolves 3-4 weeks after treatment. Mice in the control group received 150-150 µl of non-arthritogenic BxN serum. We also added a group of non-treated (intact) mice for the *Tac4* mRNA PCR measurement (Figure 10).

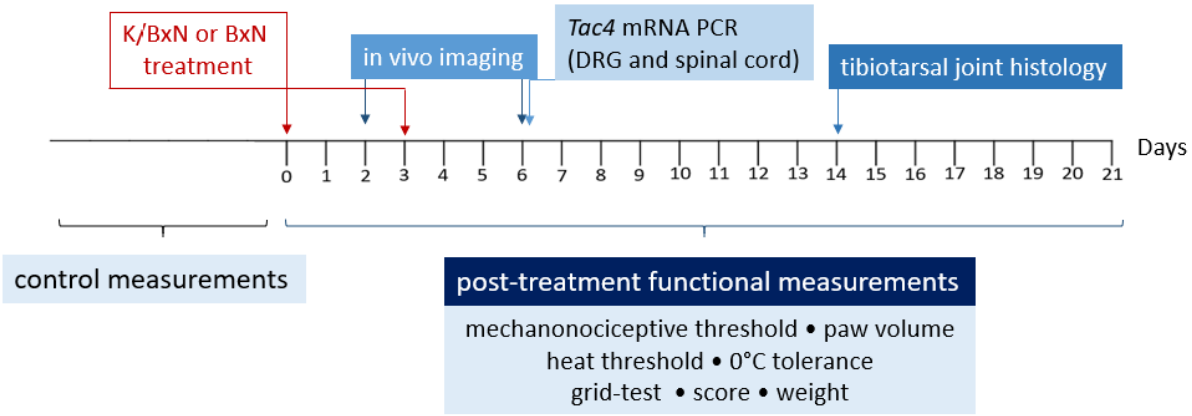

Figure 10. K/BxN-induced arthritis experiment protocol

We measured the mechanonociceptive threshold with dynamic plantar aesthesiometry (DPA), paw volume with plethysmometry, cold tolerance by measuring paw withdrawal latency from 0°C water, heat threshold with hot plate and arthritis disease severity by grid-test, visual score, and weight monitoring. Control measurements were performed the week before treatment. Plasma extravasation was measured with fluorescence molecular tomographic imaging (FMT)

and MPO-activity with the *in vivo* imaging system (IVIS). The DRG and spinal cord of WT mice were processed on day 6 to measure *Tac4* mRNA level by PCR, tibiotarsal joints were obtained on day 14 from all groups for histological staining and evaluation.

Histology was performed by Éva Borbély, *Tacr1*$^{-/-}$ measurements by Báint Botz. PCR was performed with the help of Krisztina Pohóczky, DRG extraction was done by Éva Szőke.

5.3.1.2 Tryptase-induced arthritis (acute)

Mast cell tryptase (MCT) can be found in abundance in synovial fluid contributing to the inflammation in different types of arthritis (RA, osteoarthritis, spondyloarthritis) by activating the protease-activated receptor 2 (PAR2) on the sensory nerves and inflammatory cells. To investigate acute inflammatory synovial microcirculatory changes, 1 h after guanethidine (12 mg/kg i.p., Sigma) pretreatment, MCT (Merck Millipore) was applied topically to the synovial membrane of the knee joint (12 µg/ml, 20 µl), after removing the skin under anesthesia. Contralateral knee joint was treated with 0.9% saline. Blood flow was continuously monitored by laser Speckle imaging for 40 min after the treatment, and the differences compared to the baseline values of the respective area were calculated. To measure acute inflammatory hyperalgesia and edema, MCT was injected intra-articularly (20 µl, 12 µg/ml) into the right knee joint. The paw mechanonociceptive threshold and knee diameter were measured at 2, 4, and 6 h post-injection (Figure 11).

These measurements were performed by Éva Borbély and Katinka Békefi.

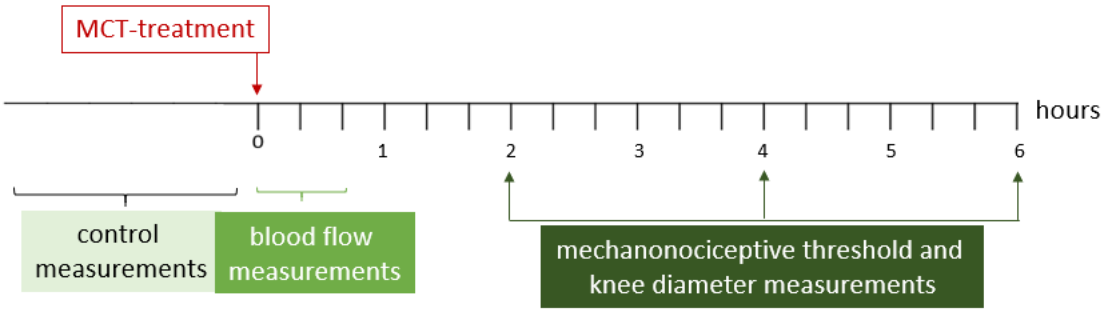

Figure 11. MCT-induced arthritis experiment protocol

Complete Freund's adjuvant (CFA) arthritis (acute)

CFA is heat-killed Mycobacterium tuberculosis suspended in paraffin oil (1 mg/ml; Sigma-Aldrich) which is taken up by macrophages, activating their reactive oxygen species, cytokine and enzyme generation within a few hours causing localized arthritis of the injected joint without severe systemic symptoms. CFA (20 µl) was injected into the right mouse knee joint under ketamine-xylazine anaesthesia. Contralateral knee joint was treated with 20 µl 0.9% saline. Paw mechanonociceptive threshold and antero-posterior knee diameter were measured 2, 6, and 24 h after CFA administration, changes were expressed as percentage of change compared to the pre-injection values. Myeloperoxidase (MPO) activity was measured 24 h after treatment (Figure 12).

These measurements were performed by Éva Borbély and Katinka Békefi.

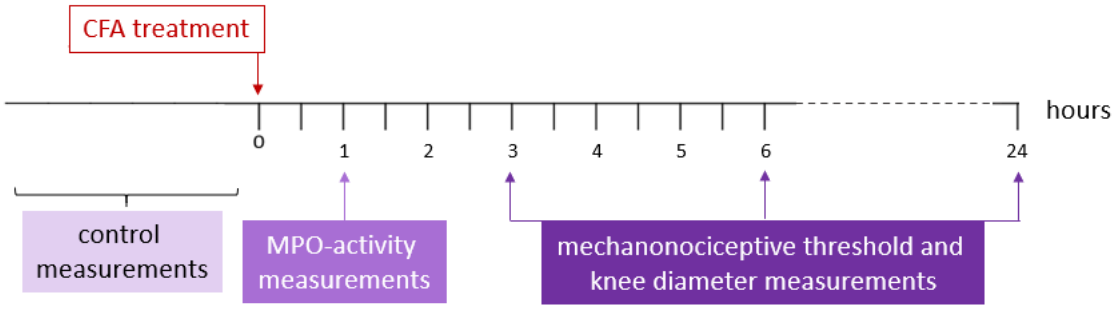

Figure 12. CFA-induced arthritis experiment protocol

5.3.2 Pain models

5.3.2.1 Examination of formalin-induced acute somatic nocifensive behavior

Acute somatic chemonociception was elicited by formalin (Formaldehydum solutum 37%; Ph.Hg. VII.; 50 µl, 2.5%) injected subcutaneously (s.c.) into the plantar surface of the right hind paw. Nocifensive behavior – lifting, licking, and shaking movement of the treated hind paw – developed in two phases. The evolvement of the first phase (0–5 min, early phase) is thought to occur due to a direct activation of sensory nerve terminals, while the second one (20–45 min, late phase) develops mainly as a result of the release of acute inflammatory mediators.[101] In both periods: the duration of nocifensive behavior was determined (Figure 13).[102,103]

These measurements were performed by Zsófia Hajna and Tímea Gubányi

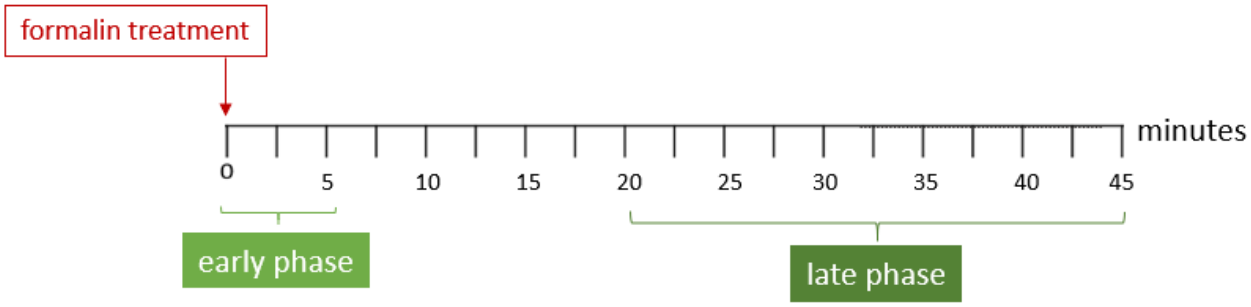

Figure 13. Examined phases of nocifensive behavior after formalin treatment

5.3.2.2 Investigation of acetic acid-evoked acute visceral nocifensive reaction (writhing test)

In order to investigate acute visceral chemonociception, i.p. administration of acetic acid (0.2 ml per mouse, 0.6%) was carried out. As a result of chemical irritation of the peritoneum, abdominal contractions (writhing movements) occurred, regarded as typical sign of visceral nocifensive behavior. For quantitative assessment of this reaction, animals were placed in a transparent plastic box immediately after the injection and the amount of writhing movements was counted during the 0–5, 5–20 and 20–30 min time intervals (Figure 14).[104]

These measurements were performed by Zsófia Hajna and Tímea Gubányi

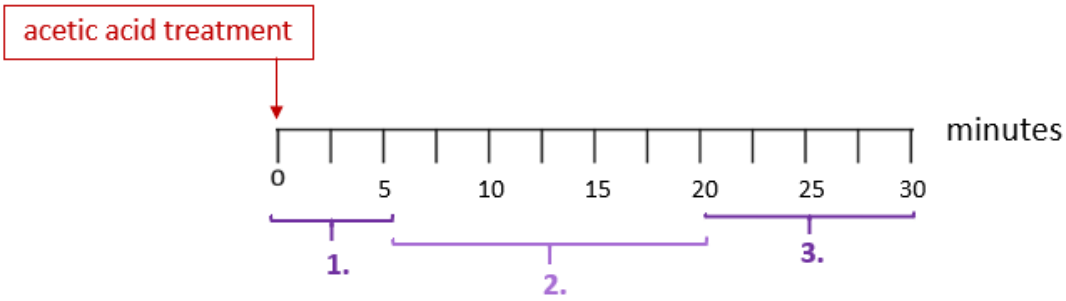

Figure 14. Acetic acid-evoked visceral pain experiment protocol

5.3.2.3 Resiniferatoxin (RTX)-induced thermal allodynia and mechanical hyperalgesia

Acute neurogenic inflammation of the right hind paw was evoked by intraplantar injection of the ultrapotent TRPV1 receptor agonist RTX (20 µl, 0.03 µg/ml i.pl.). RTX evokes an acute neurogenic inflammatory reaction including the evolvement of a rapid thermal allodynia, and a subsequent mechanical hyperalgesia.[105] Heat threshold was examined with hot plate, mechanonociceptive threshold with DPA. Both parameters were expressed as % of change compared to the pre-treatment control values (Figure 15).[103]

These measurements were performed by Zsófia Hajna and Tímea Gubányi

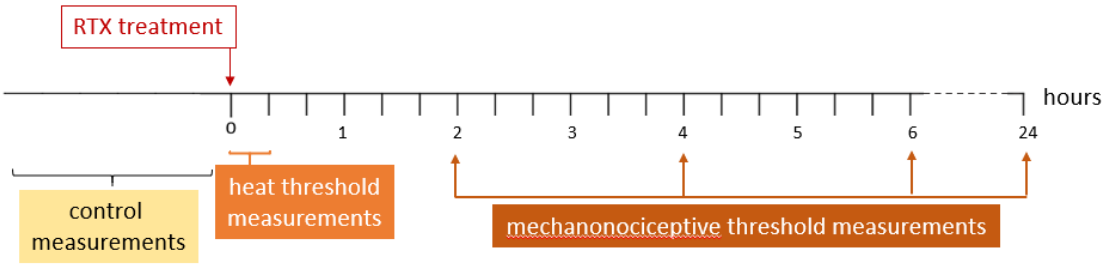

Figure 15. RTX-induced pain experiment protocol

5.3.2.4 Investigation of neuropathic pain (partial sciatic nerve ligation, PSL)

Several methods of evoking traumatic neuropathic pain are available, in our lab the partial sciatic nerve ligation has been established as a reliable method[106]. About 1/3–1/2 of the right sciatic nerve was ligated under anesthesia (Figure 16). In sham-operated group sciatic nerve was located, but not ligated, and an intact group was added for CNS immunohistochemistry examination.

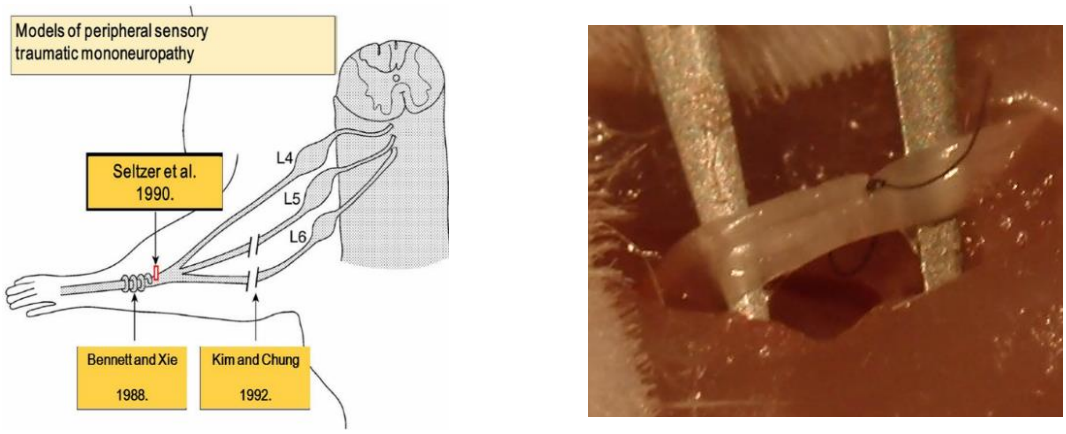

Figure 16. Surgical procedure of PSL

Before and after operation, we measured mechanonociceptive threshold with DPA, cold tolerance by measuring path withdrawal latency from 0°C water, motor coordination with accelerating rotarod. Decrease in mechanonociceptive threshold and cold tolerance were expressed as percentage change in comparison to the preoperative baseline values. On the 7th day paw homogenates were obtained to examine NGF-levels with Enzyme-linked immunosorbent assay (ELISA). On the 14th day after operation brain and spinal cord were removed for immunohistochemistry processing (Figure 17).

Removal of spinal cord and brain, as well as immunohistological staining were performed with the help of Balázs Gaszner and Izabella Orbán.

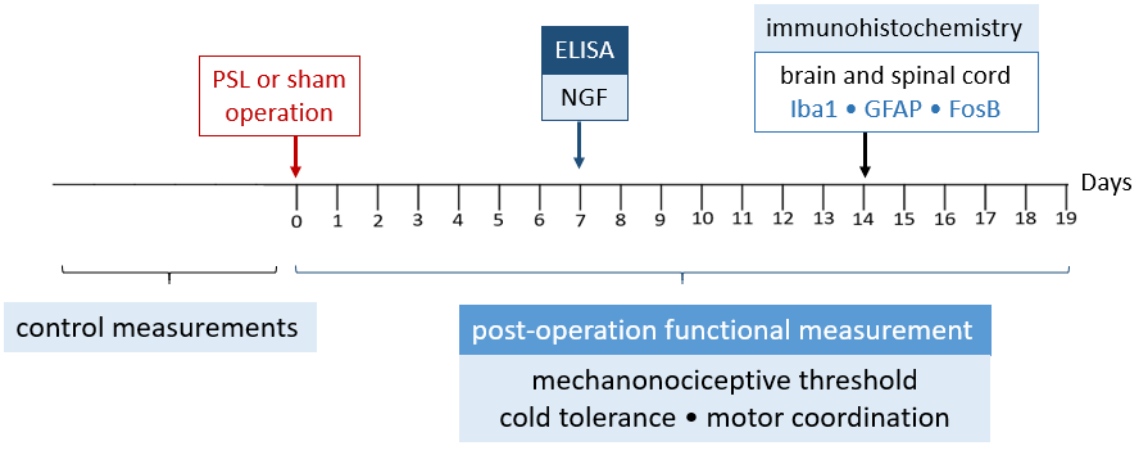

Figure 17. PSL-induced neuropathic pain experiment protocol

5.3.3 In vitro primary sensory neuron experiments

5.3.3.1 Primary Cultures of Trigeminal Ganglion (TG) Neurons

TG cultures were prepared from neonatal NMRI mice. Ganglia were excised in ice-cold phosphate-buffered saline (PBS), incubated in PBS containing collagenase Type XI (1 mg/ml) and then in PBS with deoxyribonuclease I (1,000 units/ml) for 8 min. Cells were plated on poly-D-lysin-coated glass coverslips in a medium containing Dulbecco's-Modified Eagle Mediumlow glucose, 5% horse serum, 5% newborn calf serum, 5% fetal bovine serum, 0.1% penicillin-streptomycin, 200 ng/ml NGF. Cells were maintained at 37°C in a humidified atmosphere with 5% CO_2[107].

These measurements were performed by Éva Szőke and Maja Payrits.

5.3.3.2 Ratiometric Technique of Intracellular Free Calcium Concentration ($[Ca^{2+}]i$) Measurement with the Fluorescent Indicator Fura-2 AM.

One-two-day-old neurons were incubated for 30 min at 37° C with 1 µM of fluorescent Ca^{2+} indicator dye, fura-2-AM. Cells were washed with extracellular solution (ECS). Calcium transients were detected with microfluorimetry as described elsewhere[107]. Fluorescent imaging was performed with an Olympus LUMPLAN FI/x20 0.5 W water immersion objective and a digital camera (CCD, SensiCam PCO) and a Monochromator (Polychrome II., Till Photonics) (generated light: 340 and 380 nm, emitted light: 510 nm). Axon Imaging Workbench 2.1 (AIW, Axon Instruments) software was used, R F340/F380 was monitored, data were subsequently processed by the Origin software version 7.0 (Originlab Corp.). Ratiometric response peak magnitude was measured. Capsaicin (330 nM), allyl isothiocyanate (100 µM), HK-1 (500 nM, 1 µM) and SP (500 nM, 1 µM) were administered during the experiments. CP99994, AMG 9810 and HC 030031 were administered in 10 µM concentration.

These measurements were performed by Éva Szőke and Maja Payrits.

5.3.4 Induction of skin diseases

5.3.4.1 Allergic contact dermatitis

After hair removal with electric shaver 50-50 µl oxazolone solution (2% with 96% ethanol as solvent) was applied to the shaved abdominal skin of the mice on day -6 and day -5 under ketamine-xylazine anaesthesia. On day 0 mice were again anaesthetized, ear thickness was measured with micrometer and 15-15 µl oxazolone solution was applied to the inner and outer surface of the right ear of each mouse, while 15-15 µl 96% ethanol was applied to the left ear. Ear thickness was repeatedly measured at the 6h, 24h, 48h and 72h timepoints. In vivo imaging was performed at 24h and 48h before the ear thickness measurement. N = 6 mice were terminated at 24h, 48h and 72h, ears were excised, flash frozen in liquid nitrogen and stored at -80 °C until processing for cytokine Luminex ELISA. Oxazolone- and ethanol-treated and intact ears of WT mice were obtained 24 hours after treatment as well as inguinal lymph nodes from oxazolone treated mice for RNAscope in situ hybridization (Figure 18).

These measurements were performed with the help of Ágnes Kemény and Szabina Horváth. RNAscope was performed with the help of Angéla Kecskés, Viktória Kormos and János Konkoly. Imaging studies were performed by Ádám Horváth.

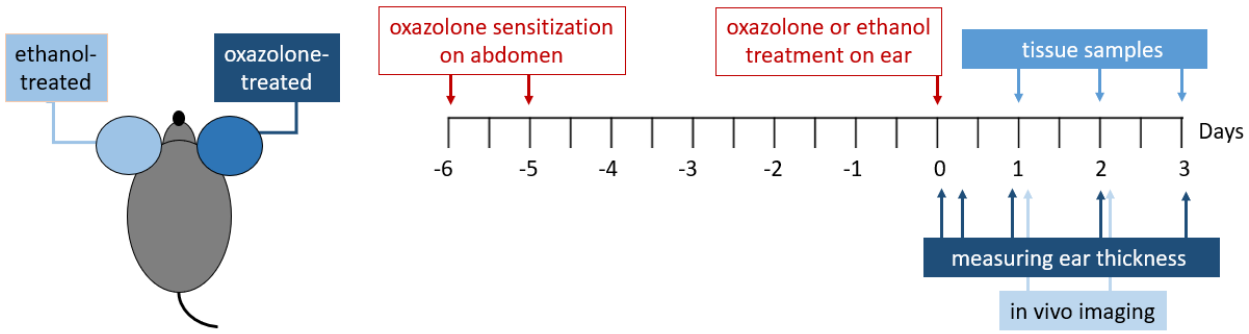

Figure 18. Oxazolone-induced allergic contact dermatitis experiment protocol

5.3.4.2 Psoriasiform dermatitis

Mice were anaesthetized with i.p. ketamine-xylazine on every day of the experiment. On day -1 hair was removed from the back of the mice with an electric shaver then remaining hair was removed with depilation cream. From day 0 and onward every day the mice were anaesthetized, blood flow of the back was registered with laser speckle, then skinfold thickness was measured. After measurements we applied a Finn chamber filled with 25 mg of imiquimod containing Aldara cream to the upper right half of the back to evoke psoriatic skin reaction. The lower left side of the back was treated with 25 mg vaseline in a Finn chamber as control area. Afterward mice were left on a 37°C heating pillow until awakening then returned to their home cage[108]. Tissue samples were obtained at 24 and 96 hours after first treatment, flash frozen in liquid nitrogen and stored at -80 °C until processing for cytokine Luminex ELISA. Tissue samples from WT mice were collected at 96 h for RNAscope in situ hybridization (Figure 19).

These measurements were performed with the help of Ágnes Kemény and Szabina Horváth. RNAscope was performed with the help of Angéla Kecskés, Viktória Kormos and János Konkoly.

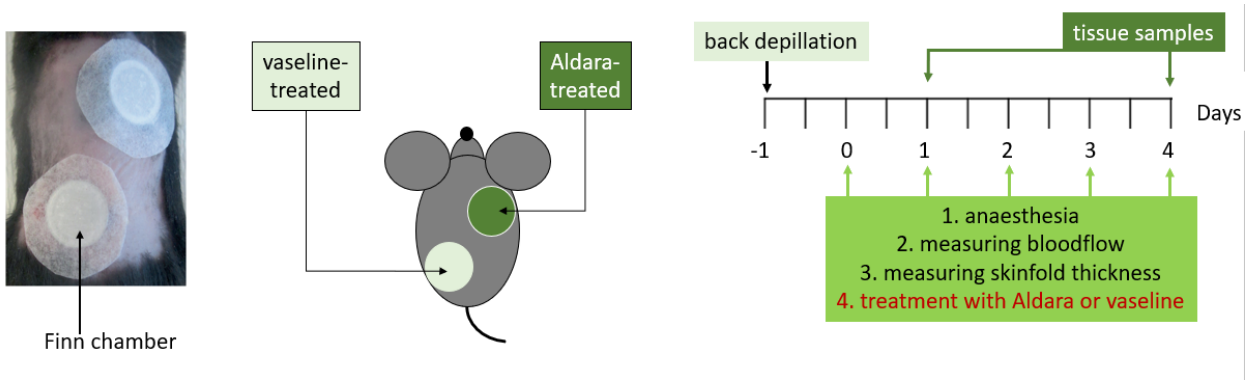

Figure 19. Aldara-induced psoriasiform dermatitis experiment protocol. Photo of Finn chamber placement from Horváth et al., 2020.

5.4 Investigational techniques

5.4.1 Functional measurements

5.4.1.1 Measuring pain

5.4.1.1.1 MECHANONOCICEPTIVE THRESHOLD (DPA)

Figure 20. DPA device

The mechanonociceptive threshold was measured with the dynamic plantar aesthesiometer (PA; Ugo Basile 37000) before (to determine baseline nociceptive threshold) and after treatment (Figure 20). In this technique mice are placed in individual boxes on a wire mesh. The DPA machine elevates a blunt needle from underneath which presses into the underside of the paw applying pressure that continuously increases until 10 g equivalent of pressure in 4 seconds. When the mouse feels pain, it will withdraw its foot and the machine registers the corresponding g value. The average of 3 values constituted the mechanonociceptive threshold of a paw. The baseline threshold is given as the average of 3 threshold measurements performed on separate days. The post-treatment values are shown as the percentage of threshold-decrease of the individual mouse compared to its baseline thresholds.[109]

5.4.1.1.2 HEAT THRESHOLD

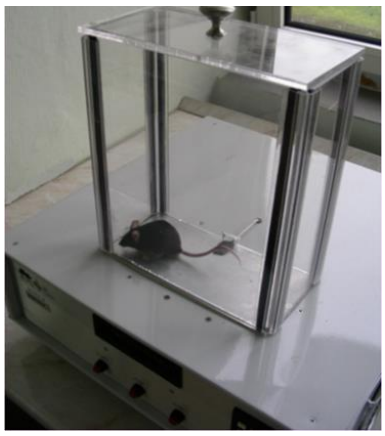

Figure 21. Hot plate device

Heat threshold was determined with the hot plate device (IITC Life Sciences, Figure 21). The mouse was placed on the metal plate and temperature of the plate steadily increased until the 53 °C cut-off value. When the mouse indicated pain by licking, shaking, or lifting the hind paw the heat increase was stopped and automatically began to cool down while the device registered the heat threshold. Control measurements were performed 3 times on separate days to determine the baseline heat threshold of a mouse.

5.4.1.1.3 PAW WITHDRAWAL LATENCY FROM 0°C WATER

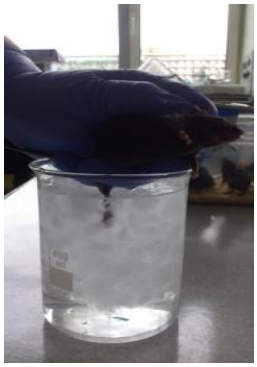

Figure 22. Measuring 0 °C tolerance of hind

Cold tolerance was given as the latency to paw-withdrawal from 0° C water (Figure 22). The mouse was held firmly and one hind limb at a time was submerged in icy (0°C) water while time was measured. When the mouse felt pain, it could withdraw its hind limb from the water and the time passed was registered in seconds. Cut off value was set at 180 sec. Control measurements were performed 3 times on separate days to determine the baseline cold tolerance of a mouse.[110]

This method was performed by Dóra Ömböli.

5.4.1.2 Determining disease severity

5.4.1.2.1 CHANGE IN PAW VOLUME (PLETHYSMOMETRY)

Figure 23. Plethysmometry

Paw edema was quantified using plethysmometer (Ugo Basile 7140, Figure 23). The device has two cylinders filled with fluid, one cylinder containing the sensor. We dipped the hind limb of the mouse into the other cylinder until the fur-skin border. The two cylinders are connected as communicating vessels so the sensor could register the volume of the hind limb based on the change of water level in its own cylinder. Three measurements were performed on separate days to determine the control hind limb volume[111].

5.4.1.2.2 BODY WEIGHT

Bodyweight was measured as a parameter of general well-being. Weight loss was given as the percentage of lost weight compared to pretreatment control values.

5.4.1.2.3 TIME SPENT ON GRID

To assess joint function mice were placed on a horizontal grid, the grid was turned upside-down and the latency to fall was measured (Figure 24). The grasping ability needed to perform this task correlates with the joint function. Cut-off value was set at 30 sec.

Figure 24. Grid test

5.4.1.2.4 VISUAL ARTHRITIS SCORE

Arthritis severity was scored using a semiquantitative visual scale where 0–0.5 was no change and 10 was maximal inflammation.[112] Swelling and redness of all four limbs were considered for the score.

5.4.1.3 Measuring motor coordination

Motor coordination was examined with the accelerating rotarod (Ugo Basile, Comerio, Italy). Mice were placed on the rotating drum of the rotarod (Figure 25). The speed of the wheel gradually accelerated, when the mouse fell off the drum onto a lever, the lever triggered the stop of the counter and time spent on the wheel was registered. Cut-off value was set at 5 minutes.[113]

Figure 25. Mice on the rotarod device

5.4.1.4 Measuring skin and ear thickness

Ear thickness was measured with an engineer's micrometer (Moore and Wright, Sheffield, England) (Figure 26A). To measure the thickness of the double skin fold of the back one experimenter pinched the skin in a rostrocaudal direction above the spine while the other experimenter measured it with the same device[108] (Figure 26B).

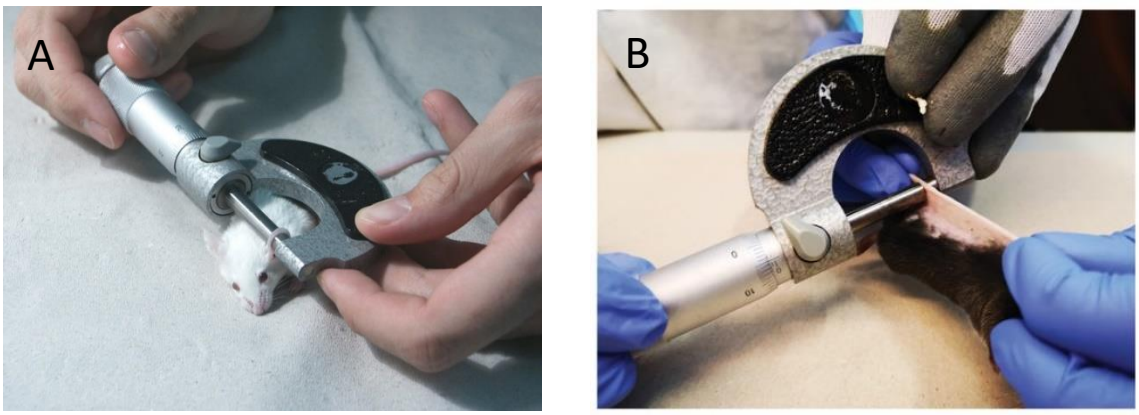

Figure 26. Measuring ear- (A) and skinfold thickness (B) with engineer's micrometer. Photo from Horváth et al., 2020.

5.4.2 In vivo imaging

5.4.2.1 Assessment of neutrophil myeloperoxidase (MPO) activity and vascular leakage

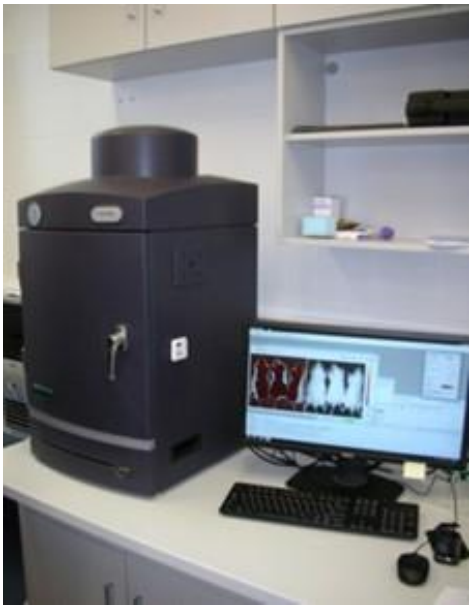

Figure 27. IVIS system for in vivo imaging

Mice were anesthetized with ketamine-xylazine anesthesia (100/5 mg/kg, i.p.) for in vivo optical imaging with IVIS Lumina II instrument (PerkinElmer; 120s acquisition, F/stop 1, Binning 8) (Figure 27). Luminol (5-amino2,3-dihydro-1,4-phthalazine-dione) sodium salt (GoldBio, 150 mg/kg) was given i. p. in sterile PBS solution (30 mg/ml), which interact with neutrophil MPO and the produced reactive oxygen species resulting in luminescent signals. Luminescence was measured 10 min postinjection and expressed as total radiance (total photon flux/s) in identical Regions of Interests (ROIs) drawn around the ankle joints or ears.

To examine vascular leakage fluorescent IR-676 dye (Spectrum-Info Ltd., 0.5 mg/kg) dissolved in 5 v/v% aqueous solution of Kolliphor HS 15 (polyethylene-glycol-15-hydroxystearate; Sigma-Aldrich) was given intravenously (i.v.) as a retro-bulbar injection. Measurement was performed 20 minutes postinjection and fluorescence was expressed as Total Radiant Efficiency [p/s] / [µW/cm^2] in identical Regions of Interest.

5.4.2.2 Measuring skin perfusion with laser speckle device

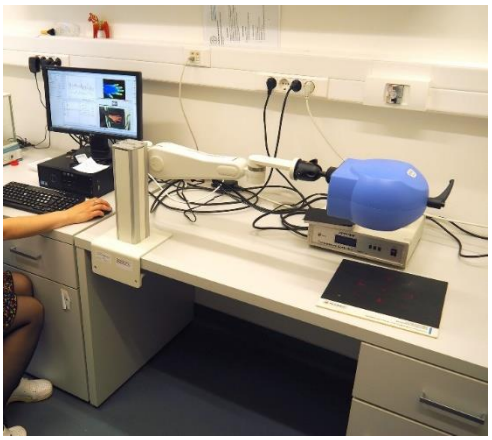

Figure 28. Laser speckle device

Blood perfusion can be monitored by laser speckle contrast analysis imaging (Figure 28). The laser light emitted by the device scatters on objects (e.g., blood cells) and the fluctuation caused by the movement of these cells is registered by the device. Since the movement of these cells correlate to the blood flow velocity the method can be used to measure blood flow (perfusion) in superficial tissues. The mice were placed on a heated pad and sufficiency of anesthesia was monitored carefully to ensure that involuntary movements of the animal would not influence the result.

5.4.3 Histology staining and evaluation

5.4.3.1 Safranin stain

After euthanasia, the tibiotarsal joint was removed and fixed for 8 hours in 4% buffered formalin solution. Afterwards, joints were decalcified by placing in a solution of 7 V/V% AlCl3-, 5 V/V% formic acid and 8,5 V/V% HCl for 8 hours on 4 °C[114]. After washing for 8 hours in Sörensen-phosphate buffer and dehydrating for 8-8 hours on 4 °C in 10 V/V% then 15 V/V% sacharose-solution specimens were set in paraffin then cut with microtome to 5-7 µm sections and stained with safranin[109]. Fibroblast proliferation; leukocyte invasion; thickness of synovium and collagen deposition were evaluated by giving each parameter a 0–3 score depending on severity, the maximum possible score being 9.

5.4.3.2 Immunohistochemistry (Iba1, FosB, GFAP)

The mice had their last pain threshold measurement on the 7th day after PSL and returned to the animal house for 7 days of rest to allow the increase in FosB protein caused by handling to subside. On the 14th day after operation, the mice were perfused with 4% paraformaldehyde, and their spinal cord and brain were removed. Sections were cut for free-floating diaminobenzidine (DAB; Sigma-Aldrich Ltd, Missouri, USA) immunohistochemistry after marking the operated (right) side of the tissues with alcian blue stain (Merck, Darmstadt, Germany). Polyclonal rabbit antiserum against Iba1 (Wako Biochemicals, Osaka, Japan) and FosB (Santa Cruz Biotechnology Inc., Dallas, USA), monoclonal mouse antibody against glial fibrillary acidic protein (GFAP) (Leica Biosystems, Wetzlar, Germany) were used. Goat anti-rabbit IgG was applied to detect activated neurons and microglia, horse anti-mouse IgG to detect astrocytes.[115] Photographs were taken with a digital camera (Spot RT; Nikon, Tokyo, Japan). Immunopositive cells were quantified in pain-related brain regions with microscope (Nikon Microphot FXA) and Inform software (Massachusetts, USA). The locations of the investigated areas were determined based on the Paxinos and Franklin brain atlas (2003)[116].

5.4.3.3 RNAscope in situ hybridization on skin, ear, and lymph node samples

WT mice were anesthetized and perfused transcardially after PBS rinse with 4% paraformaldehyde in Millonig's phosphate buffer. After rinsing in 1xPBS, dehydrating, and embedding in paraffin, 5 µm sections were cut using sliding microtome (HM 430, Thermo Fisher Scientific, USA). Lymph nodes were cryoprotected in 30% sucrose in 4% PFA at 4 °C for 24 hrs then frozen on dry ice in tissue freezing media (Leica Biosystems, Wetzlar, Germany) before cutting 20 µm sections using cryostat (CM1850, Leica Biosystems). RNAscope was performed using RNAscope Multiplex Fluorescent Reagent Kit v. 2 (Advanced Cell Diagnostics, Newark, CA, USA). Sections were hybridized with probes specific to mouse *Tac4* mRNA then sequential signal amplification and channel development were performed. Tissues were treated with 4',6-diamidino-2-phenylindole (DAPI) counterstain then with ProLong Diamond Antifade Mountant (Thermo Fisher Scientific) for confocal imaging. Mouse positive and negative control probes ensured reliability of the experiment. Blue for DAPI and red for *Tac4* mRNA virtual colors were selected to visualize fluorescent signals.

5.4.4 Molecular biology essays of tissue samples

5.4.4.1 Real time PCR

L3-L5 lumbar spinal cord and the respective DRGs (total of six DRGs pooled per mouse) were obtained from WT mice 6 days after treatment when behavioral results showed the greatest difference between WT and *Tac4*$^{-/-}$ animals. Mice were divided into K/BxN treated arthritic (n = 8), BxN serum treated control (n = 5) and intact control (n = 7) groups. Spinal cord samples of *Tac4*$^{-/-}$ mice served as negative (n = 3), while inguinal lymph nodes from WT mice served as positive controls (n = 2). Tissue samples were harvested after cervical dislocation and placed immediately into 500 µl TRI reagent (Molecular Research Center, Inc.), snap-frozen on dry ice, then stored on -80°C until processing. Tissue samples were thawed out on ice and homogenized in TRI reagent. After homogenization, total RNA was extracted using Direct-zol RNA MicroPrep (Zymo Research) according to the manufacturer's instructions.[117] The quantity of the extracted RNA was examined using Nanodrop ND-1000 Spectrophotometer V3.5 (Nano-Drop Technologies, Inc.). RNA samples were treated with dnase I in order to remove contaminant genomic DNA, and 500 ng of RNA was reverse transcribed into cDNA using High Capacity cDNA Reverse Transcription Kit (Thermo Fisher Scientific). SensiFAST™ Probe Lo-ROX Kit (Meridiane Bioscience, Memphis, United States) was used according to the manual in the QuantStudio five Real-Time PCR System (Thermo Fisher Scientific). Transcripts of the reference gene glucuronidase beta (*Gusb*[118]) and the target gene *Tac4* were evaluated using FAM-conjugated specific probes (Mm01197698_m1, and Mm00474083_m1 respectively, Thermo Fisher Scientific). The gene expression was calculated using ΔΔCt method.[119]

5.4.4.2 NGF ELISA

ELISA was applied to determine NGF expression at the protein level using ChemiKine Nerve Growth Factor Sandwich ELISA Kit (Chemicon International, catalog nr: CYT304). Measurement was performed according to the manufacturer's instructions. Shortly, sheep polyclonal antibodies generated against mouse NGF were coated on a 96-well plate. Samples and standards were incubated overnight on the plate to let any NGF present in the sample bound to the immobilized antibodies. After removal of unbound biological components by washing, indirect labelling was performed using mouse anti-mouse NGF monoclonal primary antibody and

peroxidase conjugated donkey anti-mouse IgG polyclonal antibodies. The formed immunocomplex was incubated with TMB/E Substrate. Enzyme reaction was stopped with HCl solution and color intensity was detected immediately using Labsystem Multiscan RC plate reader. Results were calculated after plotting of a standard curve and are given in pg/g tissue homogenate.

5.4.4.3 Cytokine Luminex Assay

Skin and ear samples were thawed and weighted before being placed into a cold solution of 10 mg/ml phenylmethanesulfonyl fluoride (PMSF, Sigma Aldrich, P7626) protease inhibitor in PBS. Tissues in this solution and on ice were homogenized with Miccra D-9 Digitronic device (Art-moderne Laborteknik, Germany). Supernatants obtained after centrifuging homogenates for 10 min (4 °C, 12,500 rpm) were kept at -80 °C until measurement. Cytokines/chemokines were quantified using customized Milliplex Mouse Cytokin/Chemokine Magnetic Bead Panel (Millipore) for Luminex Multiplex Immunoassay. Undiluted 25 µl volume of each sample, control, and standard was added in duplicate to a 96-well plate containing 25 µl of capture antibody coated, fluorescent-coded beads provided with the kit. After the appropriate incubation periods Biotinylated detection antibodies and streptavidin-PE were added to the plate. Sheat fluid (150 µl) was added after washing, the plate was then incubated and read with Luminex100 device. By analyzing the bead median fluorescence intensity, standard curves of analytes were plotted using five-PL regression curves by the xPonent 3.1 software. Results were calculated as pg/g tissue.

5.5 Statistical analysis

The treatments were not randomized within cages to prevent control animals from harming the arthritic animals. Results are expressed as the means ± SEM of n = 4–16 mice per group in case of in vivo functional tests. Data obtained in these experiments were analyzed with repeated measures two-way ANOVA followed by Bonferroni's post hoc test with GraphPad Prism 8 software. In all cases $p < 0.05$ was accepted as statistically significant. The data of the immunohistological staining, due to the larger number of groups, was analyzed with factorial ANOVA and Tukey's post hoc test with Statistica software (TIBCO Inc., Palo Alto, USA). In all cases $p < 0.05$ was accepted as statistically significant.

6 Results

6.1 Arthritis

6.1.1 K/BxN arthritis

6.1.1.1 HK-1 plays a role in arthritis related early and late mechanical hyperalgesia and paw edema

The greatest decrease in mechanonociceptive threshold developed on day 11 in WT (-47.93±2.8 %) and day 13 in *Tac4*$^{-/-}$ group (-35.67±2.56 %) and resolved in both groups by day 21. *Tac4*$^{-/-}$ group had a significantly milder threshold decrease throughout the experiment, including the last phase of arthritis on day 14-21 (-33.25±2.48 % in WT and -18.3±1.69 in *Tac4*$^{-/-}$ on day 17) (Figure 29A). Paw volume measured by plethysmometry reached its peak on day 8 in WT (87.55±6.15 %) and *Tac4*$^{-/-}$ (63.37±8.11 %) alike, and spontaneously resolved by day 14 in both groups. The paw volume of *Tac4*$^{-/-}$ animals was significantly lower in the first 8 days of the experiment. (Figure 29B)

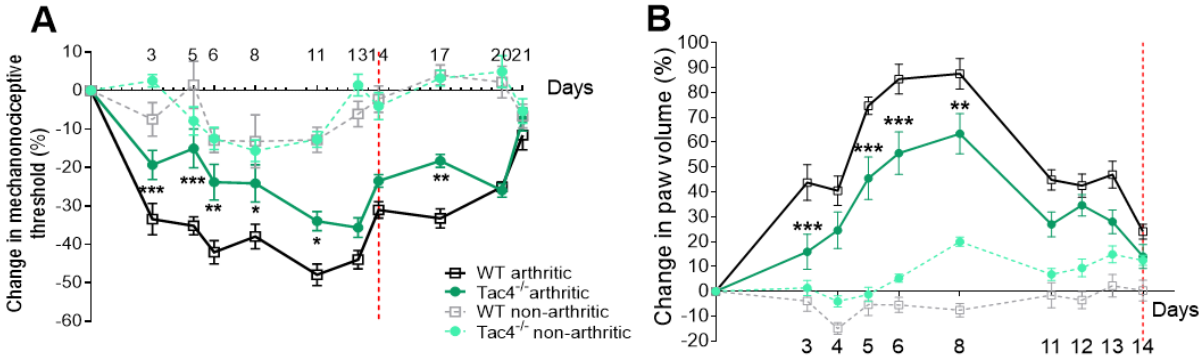

Figure 29. Change in mechanonociceptive threshold (A) and paw volume (B) after K/BxN (arthritogenic) or BxN (control) serum treatment in WT and hemokinin-1-deficient (Tac4$^{-/-}$*) mice, red line signifying day 14 (n = 4–10 per group; *p < 0.05, **p < 0.01, ***p < 0.001 vs. arthritic WT, repeated measures two-way ANOVA + Bonferroni's post hoc test).*

6.1.1.2 HK-1 plays a role in arthritis related heat threshold decrease

Tac4$^{-/-}$ mice had a significantly higher heat pain threshold on day 4 (47.6 ± 1.3°C in WT vs 50.6 ± 0.8°C in *Tac4*$^{-/-}$) (Figure 30A). Paw withdrawal latency decreased until day 6 of the experiment but showed no difference between the groups. (Figure 30B).

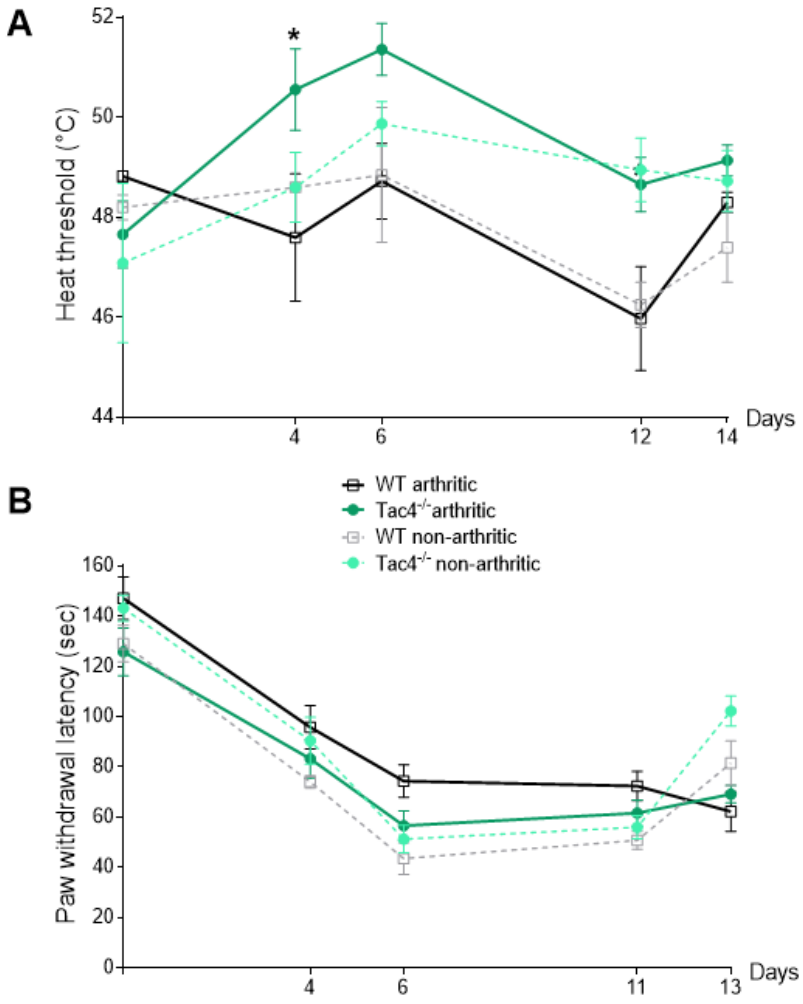

Figure 30. Heat threshold (A) and paw withdrawal latency from 0°C water (B) after K/BxN (arthritogenic) or BxN (control) serum treatment in WT and hemokinin-1-deficient (Tac4$^{-/-}$*) mice (n = 4–10 per group; *p < 0.05 vs. arthritic WT, repeated measures two-way ANOVA + Bonferroni's post hoc test).*

6.1.1.3 HK-1 did not influence the grid grasping ability or change in body weight of arthritic mice

The grid grasping ability of the mice deteriorated severely by day 3 (1 ± 1 sec in arthritic WT mice) and nearly returned to control value by day 14 (Figure 31A). Body weight reached its lowest value after 1 week (-13.38±1.32 % in WT arthritic mice on day 5) and began to increase on the 2nd week (Figure 31B). The absence of HK-1 did not influence either values.

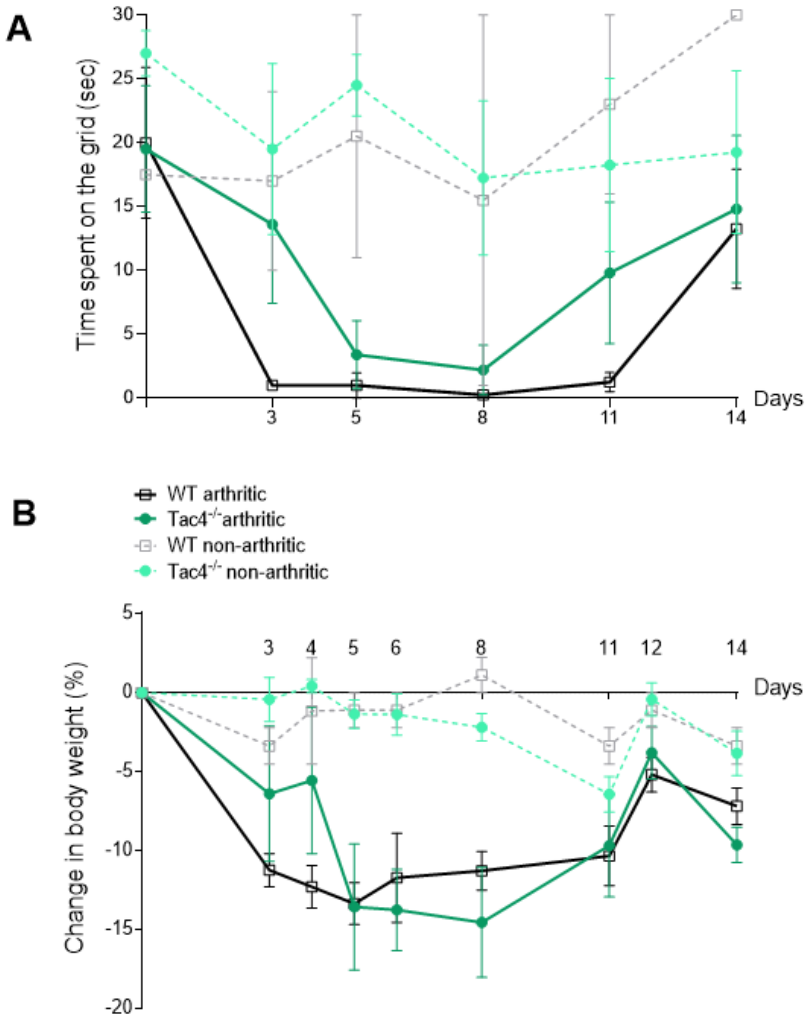

*Figure 31. Time spent on grid (A) and change in body weight (B) after K/BxN (arthritogenic) or BxN (control) serum treatment in WT and hemokinin-1-deficient (Tac4$^{-/-}$) mice (n = 4–10 per group; *p < 0.05 vs. arthritic WT, repeated measures two-way ANOVA + Bonferroni's post hoc test).*

6.1.1.4 NK_1 receptor does not play a role in arthritis related mechanical hyperalgesia and paw edema

The greatest decrease in mechanonociceptive threshold developed on day 10 in both groups (-45.88±3.92 % in WT and -49.06±4.91% in *Tacr1*$^{-/-}$) with no significant difference in the absence of NK_1 receptor. (Figure 32A)

Paw volume measured by plethysmometry reached its peak on day 8 both in WT (49.48±9.05 %) and *Tacr1*$^{-/-}$ (87.84±12.08 %) mice without significant differences between the groups. (Figure 32B)

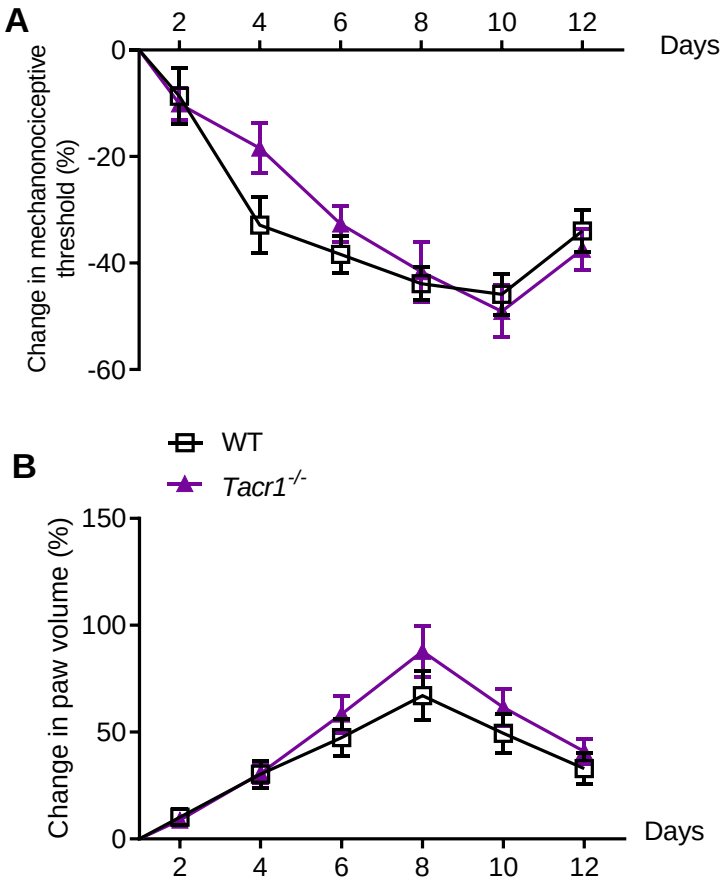

Figure 32. Change in mechanonociceptive threshold (A) and paw volume (B) after K/BxN (arthritogenic) or BxN (control) serum treatment in WT and NK_1 receptor-deficient (Tacr1$^{-/-}$*) mice (n = 14–16 per group; repeated measures two-way ANOVA + Bonferroni's post hoc test).*

6.1.1.5 NK_1 receptor does not influence grid grasping ability and weight change in arthritis

The grasping ability was worst from day 6 in WT (11.14±5 sec) and day 8 in *Tacr1*$^{-/-}$ mice (0.71±0.47 sec). There was no significant difference between groups and began to improve after the 8th day (Figure 33A).

WT group reached the lowest average weight on day 5 (-12.88±2.06) and day 8 in *Tacr1*$^{-/-}$ group (-16.71±1.13) with no significant difference between them (Figure 33B).

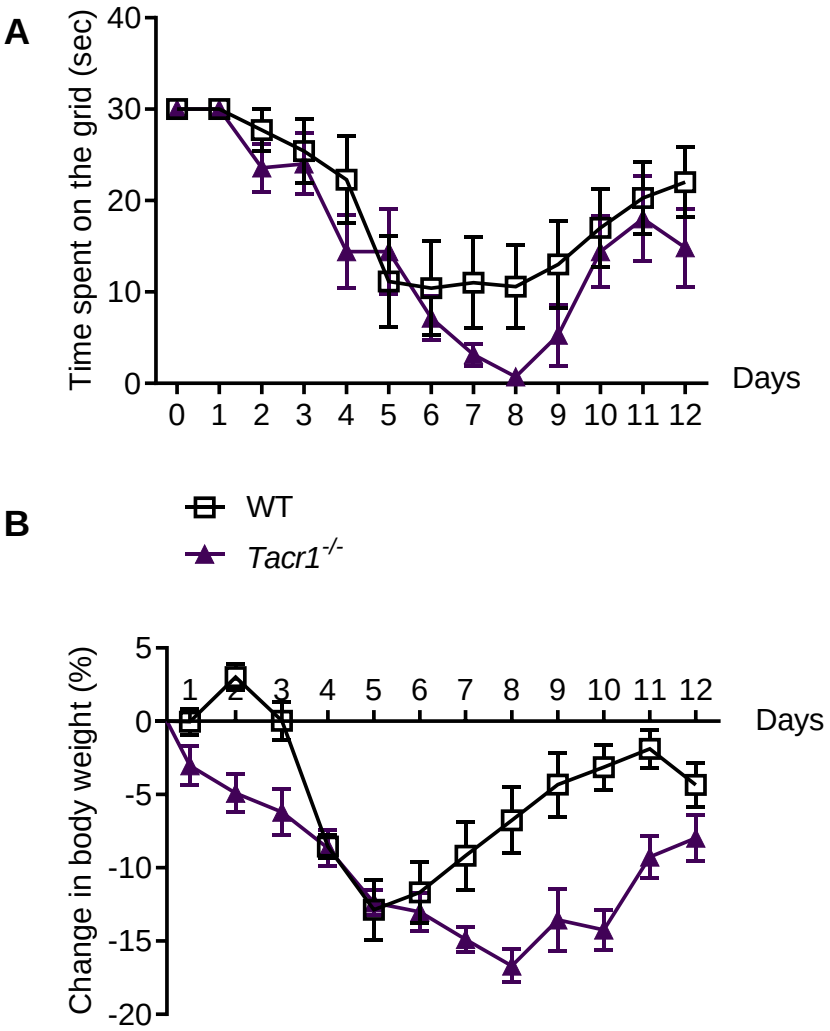

Figure 33. Time spent on grid (A) and change in body weight (B) after K/BxN (arthritogenic) or BxN (control) serum treatment in WT and NK_1 receptor deficient (Tacr1$^{-/-}$) mice (n = 7-8 per group; repeated measures two-way ANOVA + Bonferroni's post hoc test).

6.1.1.6 NK_1 receptor did not influence the arthritis score or cold tolerance of arthritic mice

Arthritis score and paw withdrawal latency did not show any difference between WT and *Tacr1*$^{-/-}$ groups throughout the experiment (Figure 34).

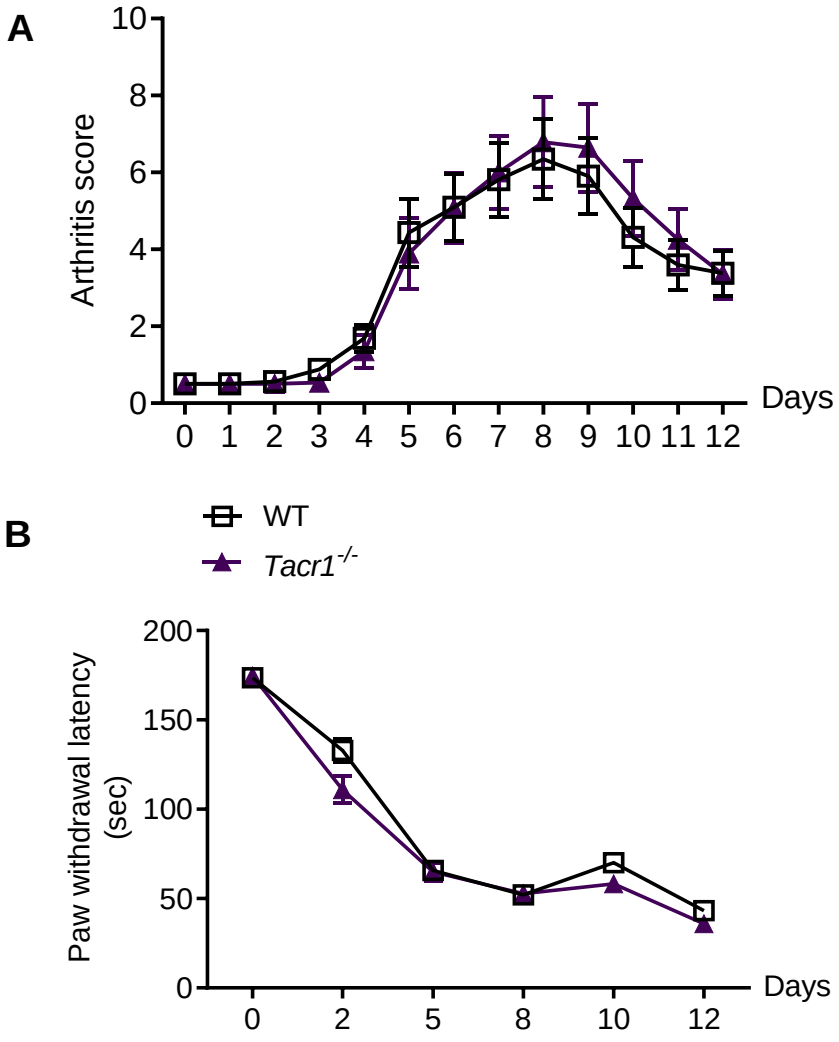

Figure 34. Arthritis score (A) and paw withdrawal latency from 0°C water after K/BxN (arthritogenic) or BxN (control) serum treatment in WT and NK_1 receptor-deficient (Tacr1$^{-/-}$) mice (n = 14–16 per group; repeated measures two-way ANOVA + Bonferroni's post hoc test).

6.1.1.7 HK-1 Decreases MPO-Activity in K/BxN Serum-Transfer Arthritis

MPO-activity showed a significant increase after 2 days in *Tac4*$^{-/-}$ mice (6.16 × 10^5 ± 6.83 × 10^4 p/s), while in WT mice it became significant compared to its control after 6 days (4.1 × 10^5± 5.67 × 10^4) (Figure 35A). Both groups had an increased rate in plasma extravasation on day 2 and 6, but no effect of the gene-deletion could be observed (Figure 35B). Representative pictures of MPO-activity can be seen on Figure 35C.

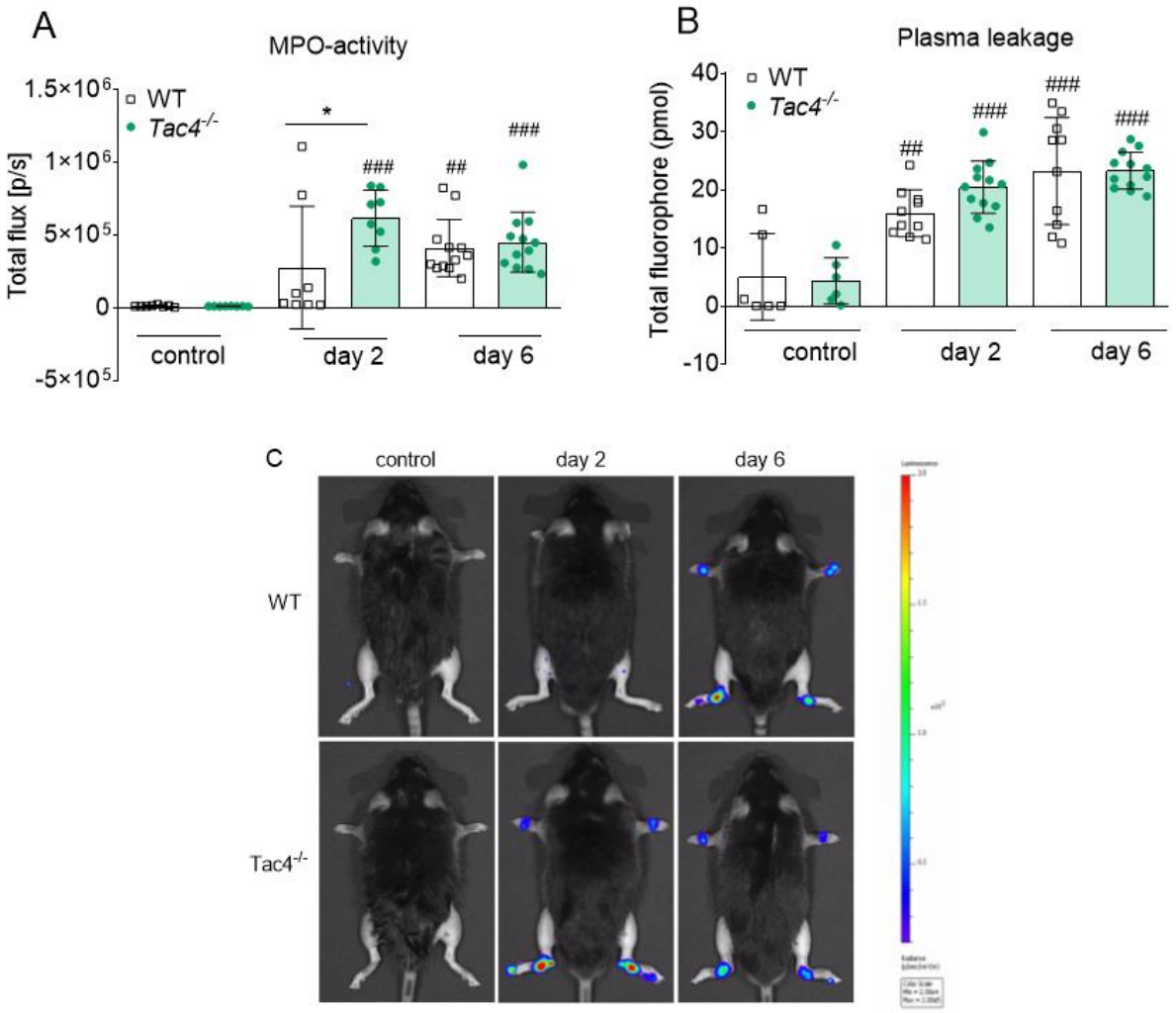

Figure 35. MPO-activity (A) and plasma leakage (B) after K/BxN (arthritogenic) or BxN (control) serum treatment in WT and hemokinin-1-deficient (Tac4$^{-/-}$*) mice with representative photos from MPO-activity (C) (n = 6–12 per group; *p < 0.05 vs. arthritic WT, repeated measures two-way ANOVA + Bonferroni's post hoc test).*

6.1.1.8 HK-1 Increases Histopathological Arthritis Severity

Representative photos of histopathological staining from mice terminated on the 14th day of the experiment with larger magnification of the synovium in the 2 pictures on the right (Figure 36A). Based on the semiquantitative scoring with a maximum of 9 points *Tac4*$^{-/-}$ mice had a significantly lower score of 2.5 ± 0.5 compared to WT mice (4.0 ± 0.5) (Figure 36B).

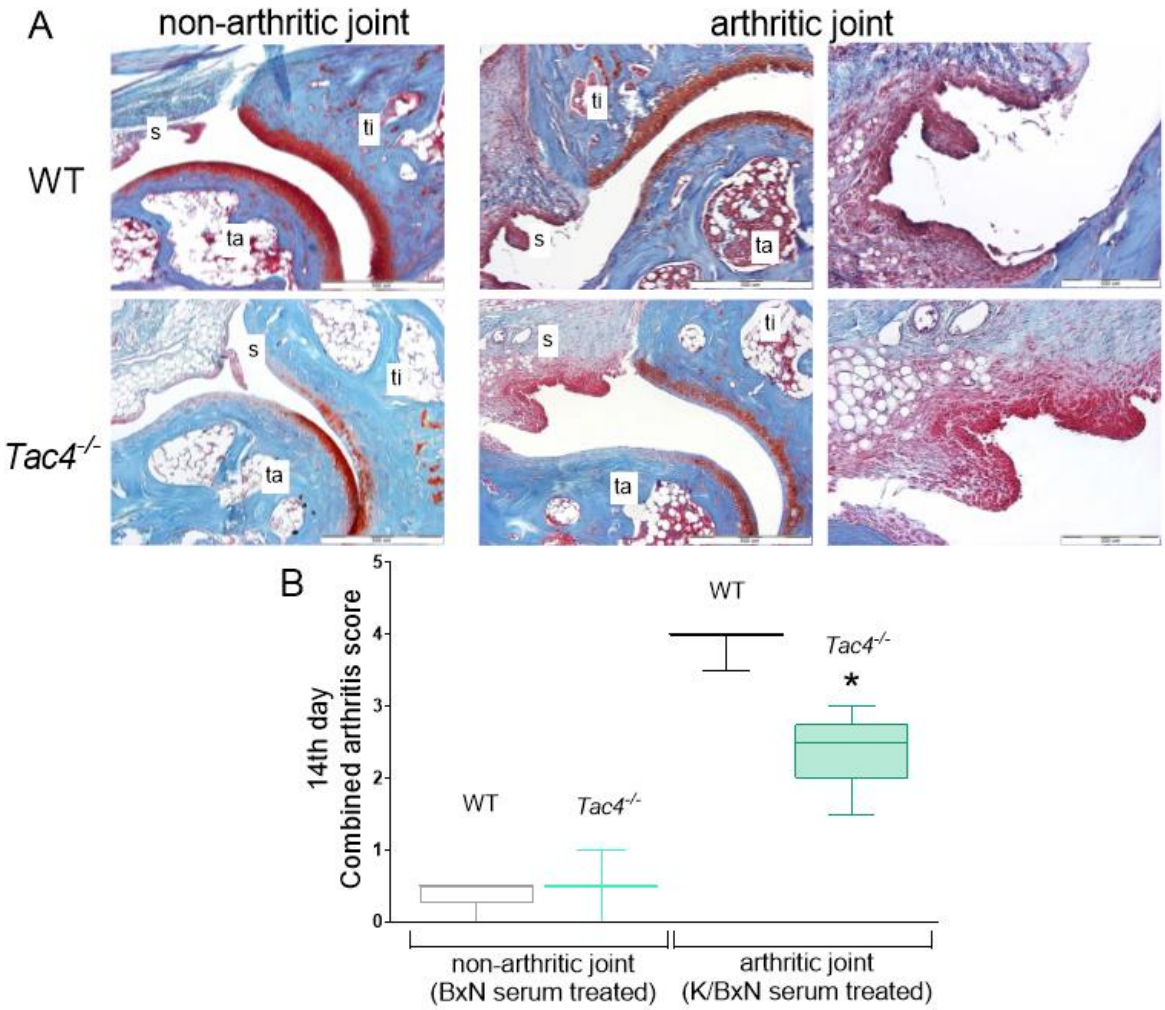

Figure 36. Representative photos of safranin-stained histological preparations of the tibiotarsal joints 14 days after K/BxN (arthritogenic) or BxN (control) serum treatment in WT and hemokinin-1-deficient (Tac4$^{-/-}$*) mice. The 4 pictures on the left with a scale bar of 500 µm, the right 2 pictures a scale bar of 200 µm included in the lower right corner (n = 3-5 per group; *p < 0.05 vs. arthritic WT, repeated measures two-way ANOVA + Bonferroni's post hoc test).*

6.1.1.9 *Tac4* mRNA Expression in DRG and Spinal Cord

Tac4 mRNA expression could be seen on day 6 in the L4-6 DRGs of intact, BxN- and K/BxN serum treated mice with a non-significant decrease of expression in the K/BxN treated arthritic group (Figure 37). We could not detect *Tac4* mRNA in the lumbar spinal cord samples.

Tac4 mRNA expression could be seen in lymph nodes serving as positive control, and there were no amplification products observed with the applied probes in samples of *Tac4*$^{-/-}$ mice serving as negative control (data not shown).

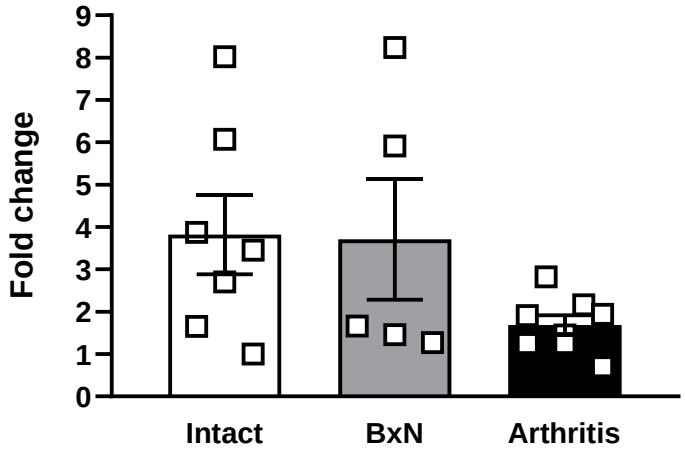

Figure 37. Fold change of Tac4 mRNA in the L4-6 DRGs of intact, BxN-, and K/BxN treated WT mice (n = 5-7 per group; repeated measures one-way ANOVA + Tukey's post hoc test).

6.1.2 HK-1 contributes to pain and edema in MCT-induced acute monoarthritis

Mechanical hyperalgesia developed in WT mice 2 days after MCT administration (-11.8 ± 4.0%; Figure 38A), while knee edema developed on the 4th day (13.3 ± 1.6; Figure 38B). Both parameters were significantly less severe in *Tac4*$^{-/-}$ mice. Increase in blood flow was detectable in the first 40 min after treatment but showed no significant difference between the groups (Figure 38C).

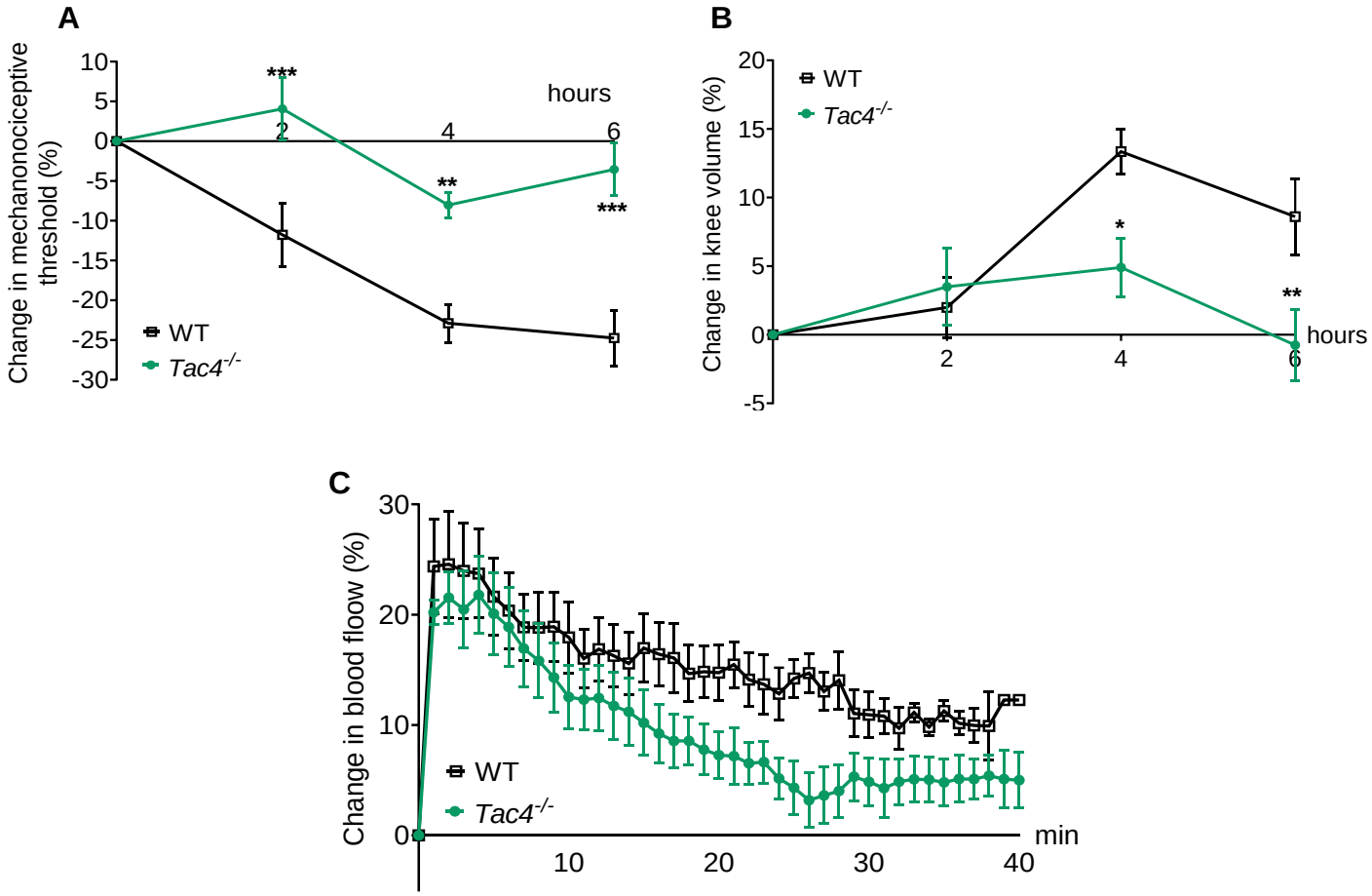

Figure 38. Change in mechanonociceptive threshold (A), knee volume (B) and blood flow (C) after MCT-treatment in WT and HK-1-deficient (Tac4$^{-/-}$*) mice (n = 5–10 per group; *p < 0.05, **p < 0.01, ***p < 0.001 vs. WT, repeated measures two-way ANOVA + Bonferroni's post hoc test).*

6.1.3 Acute CFA arthritis

6.1.3.1 HK-1 Mediates Mechanical Hyperalgesia and Knee Edema, but Decreases MPO Activity in CFA-Induced Subacute Knee Inflammation

Mechanical hyperalgesia and knee edema were detectable 2, 6 and 24 h after the CFA administration (Figure 39A,B). *Tac4*$^{-/-}$ mice had a significantly milder mechanical hyperalgesia at every time point and less severe knee edema at 24 h. *Tac4*$^{-/-}$ mice showed a significant increase in MPO-activity (457,125 ± 94397) (Figure 39C).

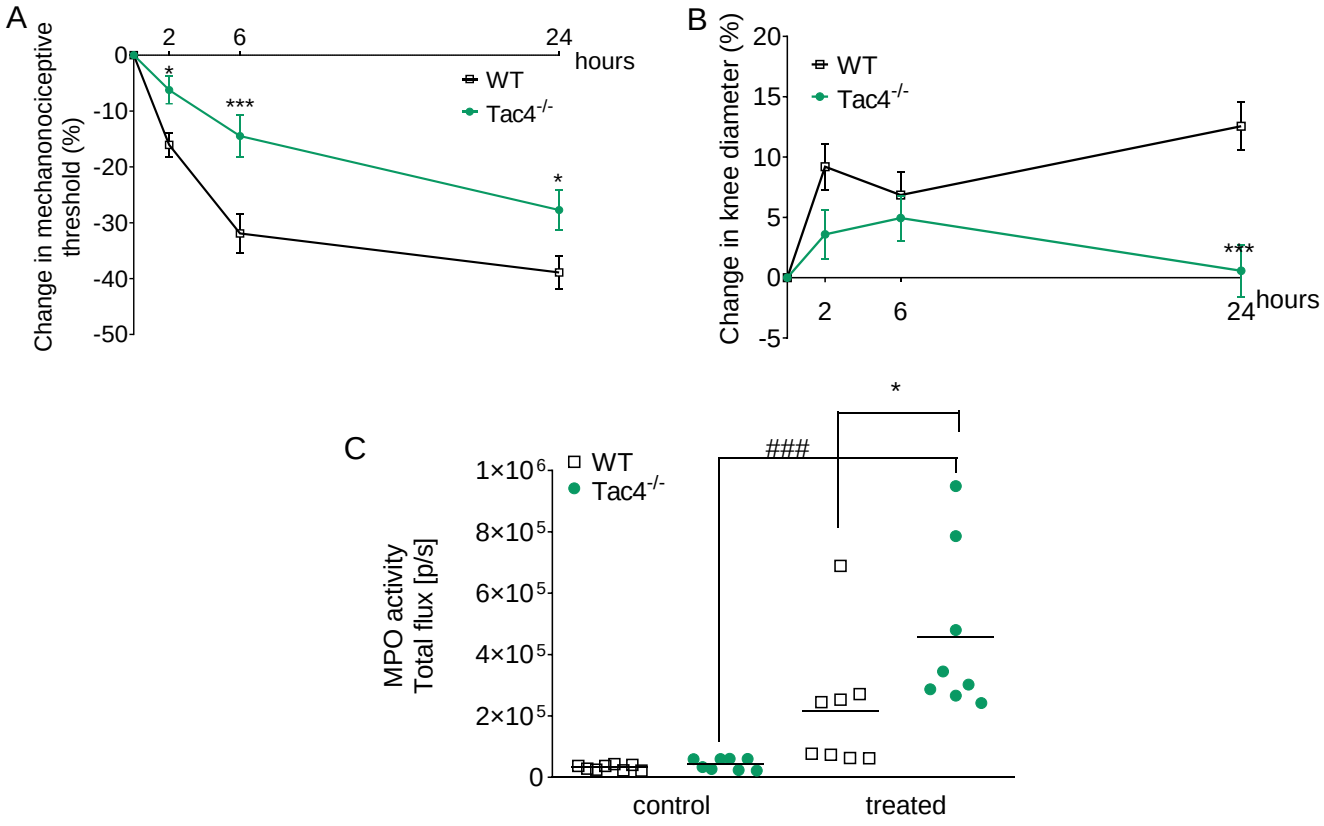

Figure 39. Change in mechanonociceptive threshold (A), knee diameter (B) and MPO-activity (24 hours) (C) after CFA-treatment in WT and HK-1-deficient (Tac4$^{-/-}$*) mice (n = 7–15 per group; *p < 0.05, **p < 0.01, ***p < 0.001 vs. WT, repeated measures two-way ANOVA + Bonferroni's post hoc test).*

6.1.3.2 NK_1 receptor does not play a role in CFA-Induced Subacute Knee Inflammation

Changes in mechanonociceptive threshold and knee volume did not show significant difference to WT mice in NK_1 receptor-deficient mice (Figure 40).

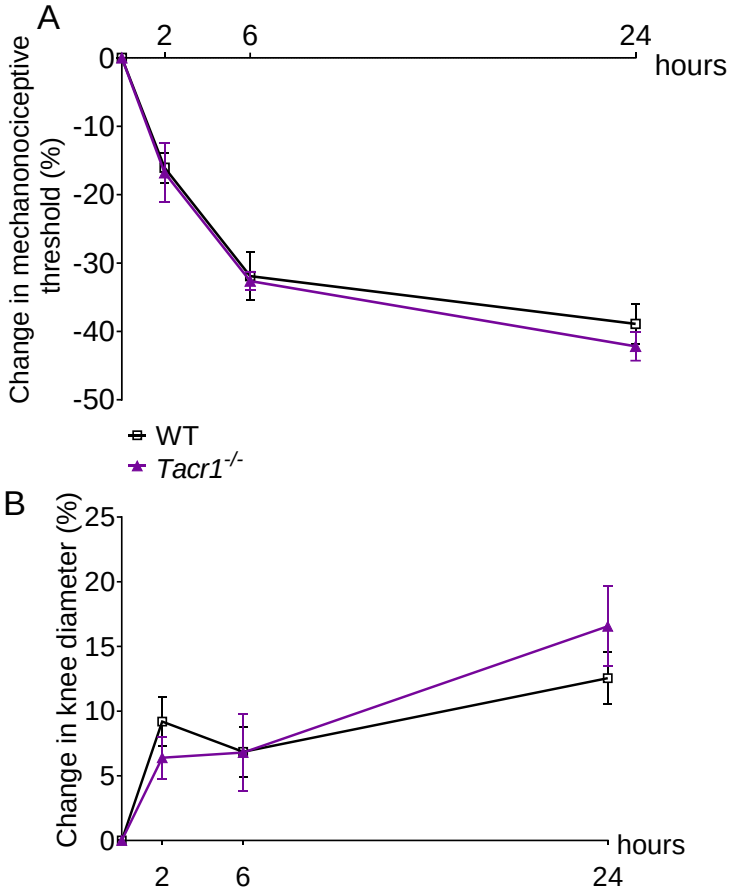

Figure 40. Change in mechanonociceptive threshold (A), knee diameter (B) and MPO-activity (C) after CFA-treatment in WT and NK_1 receptor-deficient ($Tacr1^{-/-}$) mice (n = 7–15 per group; vs. WT, repeated measures two-way ANOVA + Bonferroni's post hoc test).

6.2 In vitro primary sensory neuron experiments

6.2.1 HK-1 Directly Activates Primary Sensory Neurons

HK-1 applied to a culture of primary sensory neurons in 1 µM concentration caused Ca^{2+}-influx (R 0.67 ± 0.07) in 26.39 ± 4.5%, whereas 500 nM HK-1 and 500 and 1 µM SP had no effect (data not shown). The NK_1 receptor antagonist CP99994 did not influence the HK-1 response (20.93 ± 3.8%, R = 0.62 ± 0.08). This was similar in neurons of NK_1 receptor gene-deleted mice (21.4 ± 3.5%, R = 0.49 ± 0.04). The G-protein coupled receptor (GPCR) blocker pertussis toxin (PTX) influenced neither the ratio (24.49 ± 3.6%;) nor the extent of the response (R = 0.74 ± 0.03) to HK-1; neither did the TRPV1 antagonist AMG8910, (22.7 ± 4%; R = 0.7 ± 0.28) nor the TRPA1 antagonist HC 030031 (19.2 ± 4.7%, R = 0.32 ± 0.26). No Ca^{2+}- signal was detected in Ca^{2+} free ECS (Figure 41).

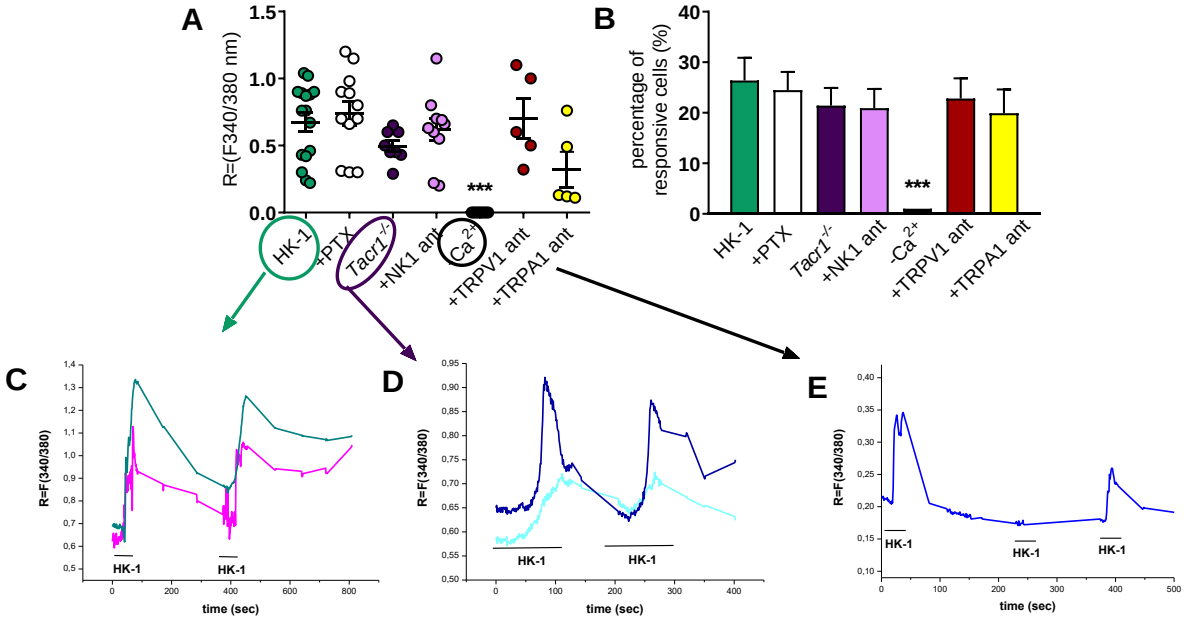

*Figure 41. Change in the fluorescence ratio (A) and percentage of responsive primary sensory neurons (B) to HK-1, HK-1+PTX, HK-1 in TG from NK_1 receptor-deficient $Tacr1^{-/-}$ animals, HK-1+ NK_1 receptor antagonist CP99994, HK-1 in Ca^{2+}-free condition, HK-1 + TRPV1 receptor antagonist AMG9810 and HK-1 + TRPA1 receptor antagonist HC 030031. Two different original Ca^{2+}-imaging registrations after HK-1 administration: increases of R 340/380 fluorescence (C), primary sensory neurons from $Tacr1^{-/-}$ mice (D) and one in Ca^{2+}-free solution (E). The percentage of responsive cells' Ca^{2+}-responses are presented in % of total number of examined neurons (n= 19-49 per group; ***p < 0.001, vs. HK-1, one-way ANOVA with Bonferroni's multiple comparison post hoc test).*

6.2.2 HK-1 can counteract the desensitization caused by repeated capsaicin administration

Four or five repeated treatments of capsaicin on the same cultured sensory neurons were performed, and the effect of 500 nM HK-1 was investigated on capsaicin-evoked Ca^{2+}-influx. The first application of 330 nM capsaicin induced transient Ca^{2+}-accumulation which gradually decreased in response to the second capsaicin stimulus due to TRPV1 desensitization. Meanwhile, HK-1 administered in separate cultures after the second capsaicin stimulus diminished the desensitization as shown by the third and fourth capsaicin-evoked responses (Figure 42).

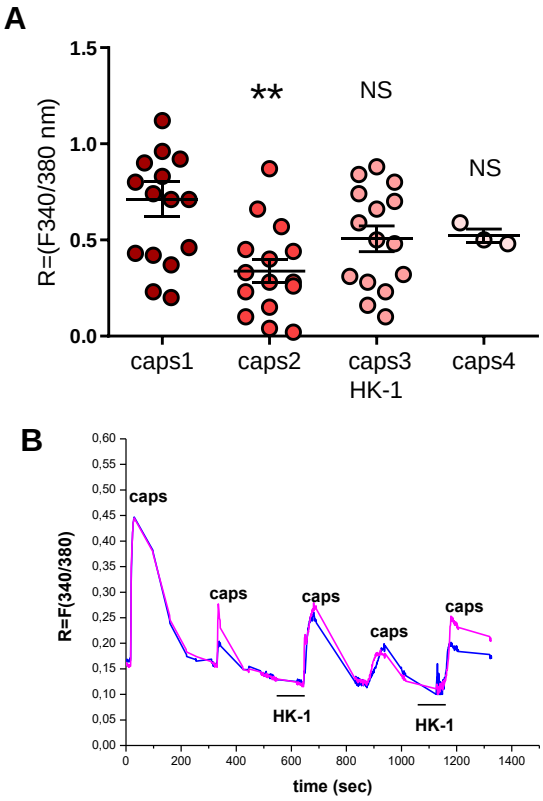

*Figure 42. Effect of HK-1 on capsaicin-induced Ca^{2+}-influx. Increases of R 340/380 fluorescence in fura-2 loaded neurons are presented, **p < 0.01, NS (vs. caps1, one-way ANOVA with Bonferroni's multiple comparison post hoc test, n = 16) (A). Two original Ca^{2+}-imaging registrations after capsaicin and HK-1 administration (B).*

6.2.3 SP can counteract the desensitization caused by repeated capsaicin administration

Capsaicin was applied *in vitro* to primary sensory neurons as described above, and the effect of 500 nM SP was investigated on capsaicin-evoked Ca^{2+}-influx. SP administered in separate cultures after the second capsaicin stimulus diminished the desensitization as shown by the third and fourth capsaicin-evoked responses (Figure 43).

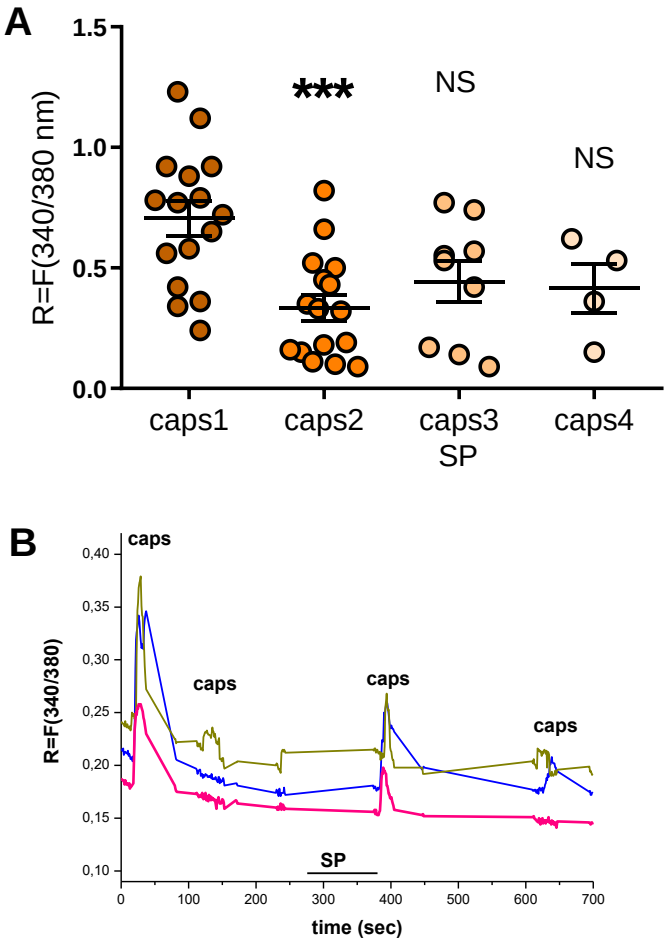

*Figure 43. Effect of SP on capsaicin-induced Ca^{2+}- influx. Increases of R 340/380 fluorescence in fura-2 loaded neurons are presented, ***p < 0.001, NS (vs. caps1, one-way ANOVA with Bonferroni's multiple comparison post hoc test, n = 17) (A). Three original Ca^{2+}-imaging registrations after capsaicin and SP administration (B).*

6.3 Neuropathy and acute pain

6.3.1 Acute pain

6.3.1.1 HK-1 contributes to acetic acid-evoked visceral pain

In WT mice, the total duration of formalin-induced paw lickings, liftings and shakings was 128.54 ± 16.80 s in the early phase referring to acute somatic chemonociception and 440.69 ± 35.74 s in the late phase evoked by neurogenic inflammatory mechanisms. There was no significant difference between *Tac4* gene-deleted mice and WT mice in either phase (Figure 44A). The number of acetic acid-induced abdominal contractions were 0.75 ± 0.48, 19.25 ± 0.85 and 5.75 ± 0.63 in WT mice in the 0–5, 5–20 and 20–30 min time periods, respectively. However, in *Tac4*$^{-/-}$ mice writhing movements were significantly decreased in the second observational period, indicating a less intensive visceral nocifensive reaction (Figure 44B).

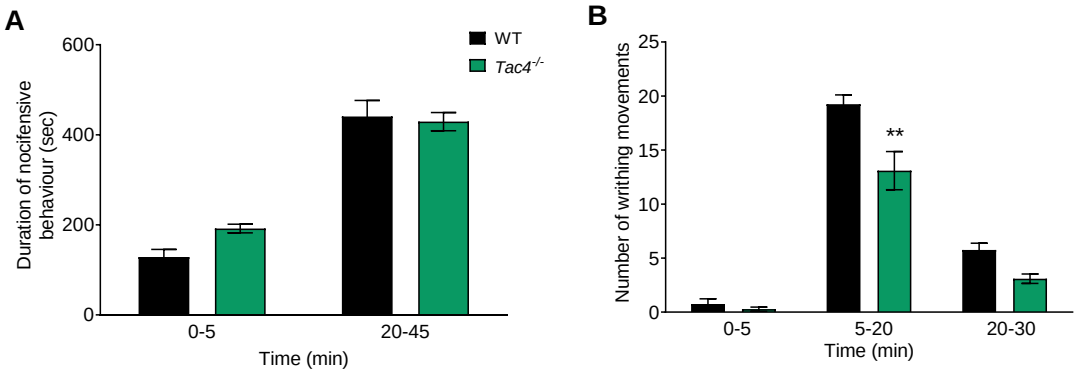

Figure 44. Assessment of formalin-induced nocifensive behavior (A) and acetic acid-evoked writhing movements in WT and HK-1-deficient (Tac4$^{-/-}$*) mice (n = 4–13 per group, **p < 0.01, vs. WT, repeated measures two-way ANOVA + Bonferroni's post hoc test.)*

6.3.1.2 HK-1 contributes to heat- and mechanical hyperalgesia in RTX-induced neurogenic inflammation

Compared to the basal thermonociceptive thresholds of WT (45.38 ± 0.86 °C) and *Tac4*$^{-/-}$ mice (46.03 ± 0.82 °C) intraplantar RTX injection induced an 8.79 ± 1.48 °C decrease of the thermonociceptive threshold in WTs, which was maintained at a stable level throughout the 20-min investigation period. In contrast, in *Tac4*$^{-/-}$ mice this thermal allodynia was significantly attenuated (*Figure 45*A). The basal mechanonociceptive thresholds of WT and *Tac4*$^{-/-}$ mice were 7.26 ± 0.16 g and 8.13 ± 0.17 g, respectively. This decreased by 34.05 ± 2.47% at 2 h and 20.67 ± 2.97% by the 24 h time point in WTs after RTX injection However, in *Tac4*$^{-/-}$ mice this was also significantly reduced in comparison to the WTs during the whole investigation period (*Figure 45*B).

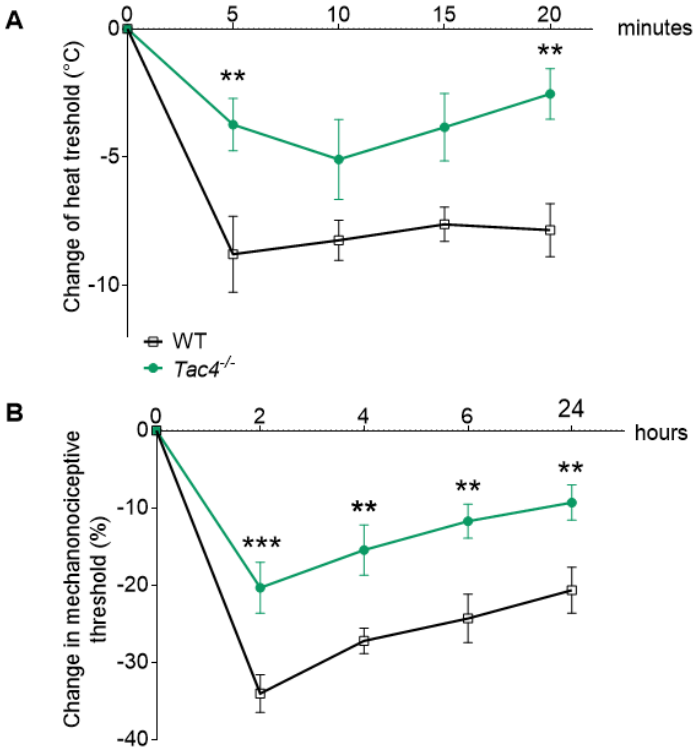

Figure 45. RTX-induced decrease in thermal allodynia (A) and mechanonociceptive threshold (B) in WT and HK-1-deficient (Tac4$^{-/-}$*) mice. (n = 14 per group, **p < 0.01, ***p < 0.001 vs. WT, repeated measures two-way ANOVA + Bonferroni's post hoc test).*

6.3.1.3 Formalin-induced nocifensive behavior and acetic acid-evoked visceral pain in the absence of SP/NKA and NK_1 receptor

Formalin-induced somatic nocifensive behavior was significantly reduced in the late phase in *Tac1*$^{-/-}$ mice, but not in *Tacr1*$^{-/-}$ ones (Figure 46A). Acetic acid-evoked writhing movements were significantly decreased both in the *Tac1*$^{-/-}$ and *Tacr1*$^{-/-}$ mice in the second and third phases (Figure 46B).

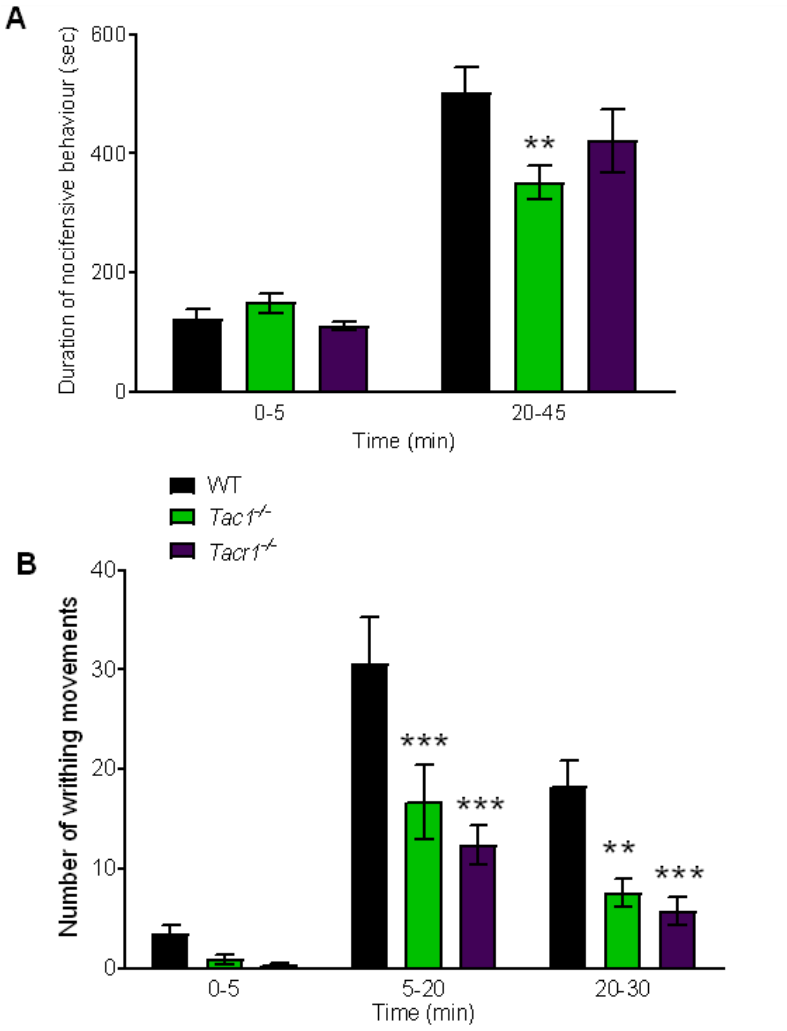

Figure 46. Assessment of formalin-induced nocifensive behavior (A) and acetic acid-evoked writhing movements in WT, SP/NKA-deficient (Tac1$^{-/-}$*) and NK_1 receptor-deficient (Tacr1*$^{-/-}$*) mice (n = 6-10 per group, **p < 0.01, ***p < 0.001 vs. WT, repeated measures two-way ANOVA + Bonferroni's post hoc test).*

6.3.1.4 RTX-induced neurogenic inflammation in the absence of SP/NKA and NK_1 receptor

RTX-induced thermal hyperalgesia was abolished in the *Tac1*$^{-/-}$ mice but in the *Tacr1*$^{-/-}$ group significant decrease was only detected at the last, 20 min time point (Figure 47A). However, mechanical hyperalgesia in this model was significantly attenuated in the *Tacr1*$^{-/-}$ mice, but not in the *Tac1*$^{-/-}$ group (Figure 47B).

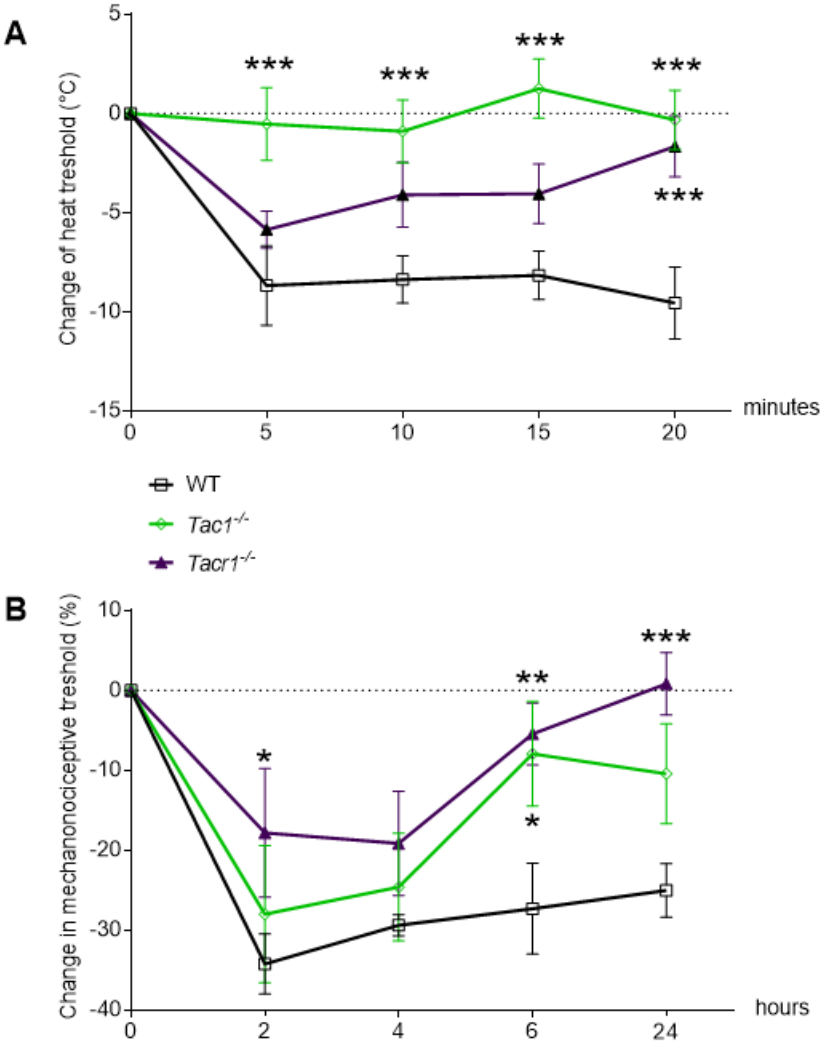

Figure 47. RTX-induced decrease in thermal allodynia (A) and mechanonociceptive threshold (B) in WT and SP/NKA-deficient (Tac1$^{-/-}$*) and NK_1 receptor-deficient (Tacr1*$^{-/-}$*) mice (n = 6-8 per group, *p < 0.05, **p < 0.01, ***p < 0.001 vs. WT, repeated measures two-way ANOVA + Bonferroni's post hoc test).*

6.3.2 PSL-experiment results

6.3.2.1 Decrease in mechanonociceptive threshold and cold tolerance is milder in the absence of HK-1

Compared to the pre-operation control values (9.29 ± 0.07 g in the WT and 9.10 ± 0.09 g in the *Tac4*$^{-/-}$ group), significant mechanical hyperalgesia developed by day 5 after the sciatic nerve ligation in the WT group, reaching its maximum of −48.46 ± 4.01% on day 10, which was maintained until the end of the study. In the *Tac4*$^{-/-}$ group neuropathic mechanical hyperalgesia was significantly smaller throughout the whole experiment with the maximum of −29.03 ± 2.30% on day 10 (Figure 48A). The basal withdrawal latency from 0 °C water was 158.60 ± 4.09 and 147.41 ± 3.49 s in the WT and *Tac4*$^{-/-}$ groups, respectively. Decrease in cold tolerance was significantly smaller in the HK-1-deficient mice until day 7 (Figure 48B).

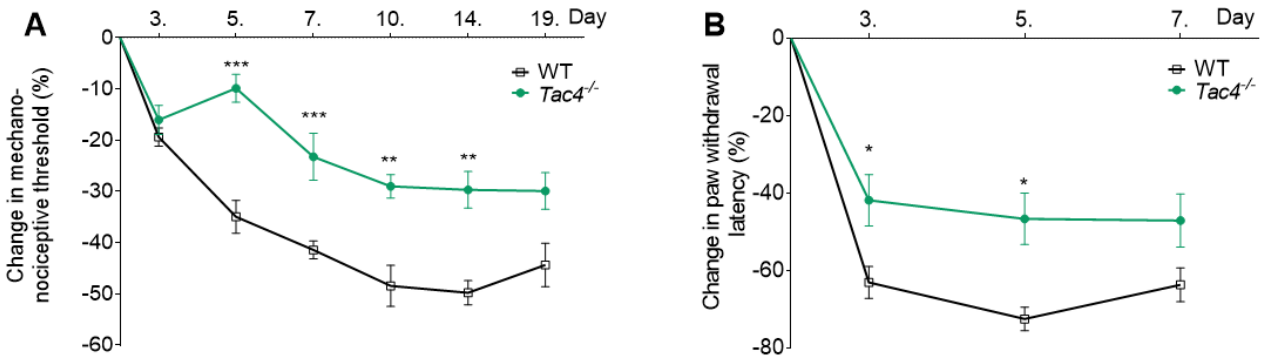

Figure 48. Change in mechanonociceptive threshold (A) and paw withdrawal latency from 0°C water (B) after PSL in WT and HK-1-deficient (Tac4$^{-/-}$*) mice (n = 5–10 per group; *p < 0.05, **p < 0.01, ***p < 0.001 vs. WT, repeated measures two-way ANOVA + Bonferroni's post hoc test).*

6.3.2.2 Motor coordination is worse in the absence of HK-1

The basal motor performance on the accelerating rotarod was 56.64 ± 5.28 s in the WT and 38.13 ± 8.38 s in the *Tac4*$^{-/-}$ group. This did not worsen after PSL, but *Tac4*$^{-/-}$ mice performed worse which reached statistical significance on day 10. (Figure 49).

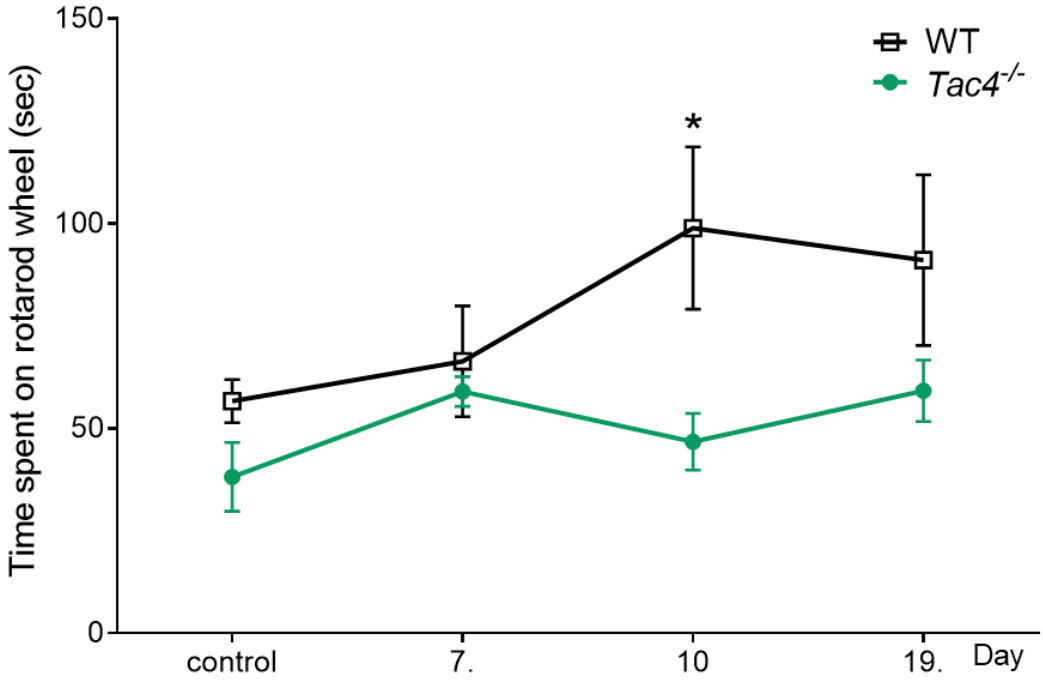

Figure 49. Motor coordination before and after PSL in WT and HK-1-deficient (Tac4$^{-/-}$*) mice (n = 5-6 per group; *p < 0.05, vs. WT, repeated measures two-way ANOVA + Bonferroni's post hoc test).*

6.3.2.3 Lower basal NGF-level which increases significantly after PSL in the absence of HK-1

The NGF concentration of the paw homogenates was significantly lower in intact *Tac4*$^{-/-}$ mice compared to WTs. Under neuropathic condition, 7 days after PSL NGF level was not altered in the WT group but showed an almost 2-fold elevation in the *Tac4*$^{-/-}$ one (Figure 50).

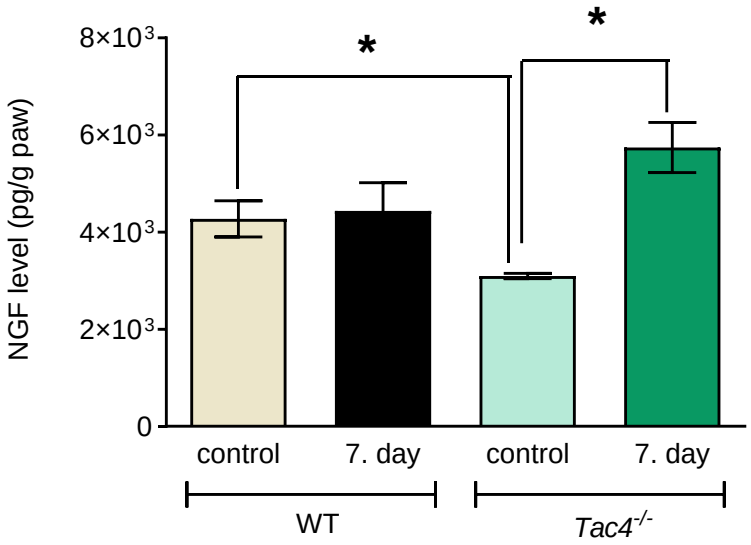

Figure 50. NGF-levels of paw homogenates in PSL and sham operated WT and HK-1-deficient (Tac4$^{-/-}$*) mice (n = 3-6 per group; *p < 0.05, vs. WT, two-way ANOVA + Bonferroni's post hoc test).*

6.3.3 Immunohistochemistry of central nervous system

6.3.3.1 Spinal dorsal horn: number of microglia cells decreased in the lamina I-II of operated mice in the absence of HK-1

In the spinal dorsal horn, the number of Iba1-immunopositive microglia did not differ under intact conditions in the WT and *Tac4* gene-deficient groups. In response to PSL microglia density significantly increased ipsilaterally in WT mice but not in the *Tac4*$^{-/-}$ mice (Figure 51A), there was no change on the contralateral side (Figure 51B, Figure 52). The number of GFAP-positive astrocytes were very similar in the spinal dorsal horn of both WT and *Tac4*$^{-/-}$ mice under intact conditions, astrocyte numbers did not increase significantly in the WT group either ipsi- or contralaterally but interestingly even decreased in the *Tac4*$^{-/-}$ one on both sides (Figure 51). The chronic neuronal activation marker FosB-immunopositivity did not show any changes in relation to genotype, PSL or side (Figure 51).

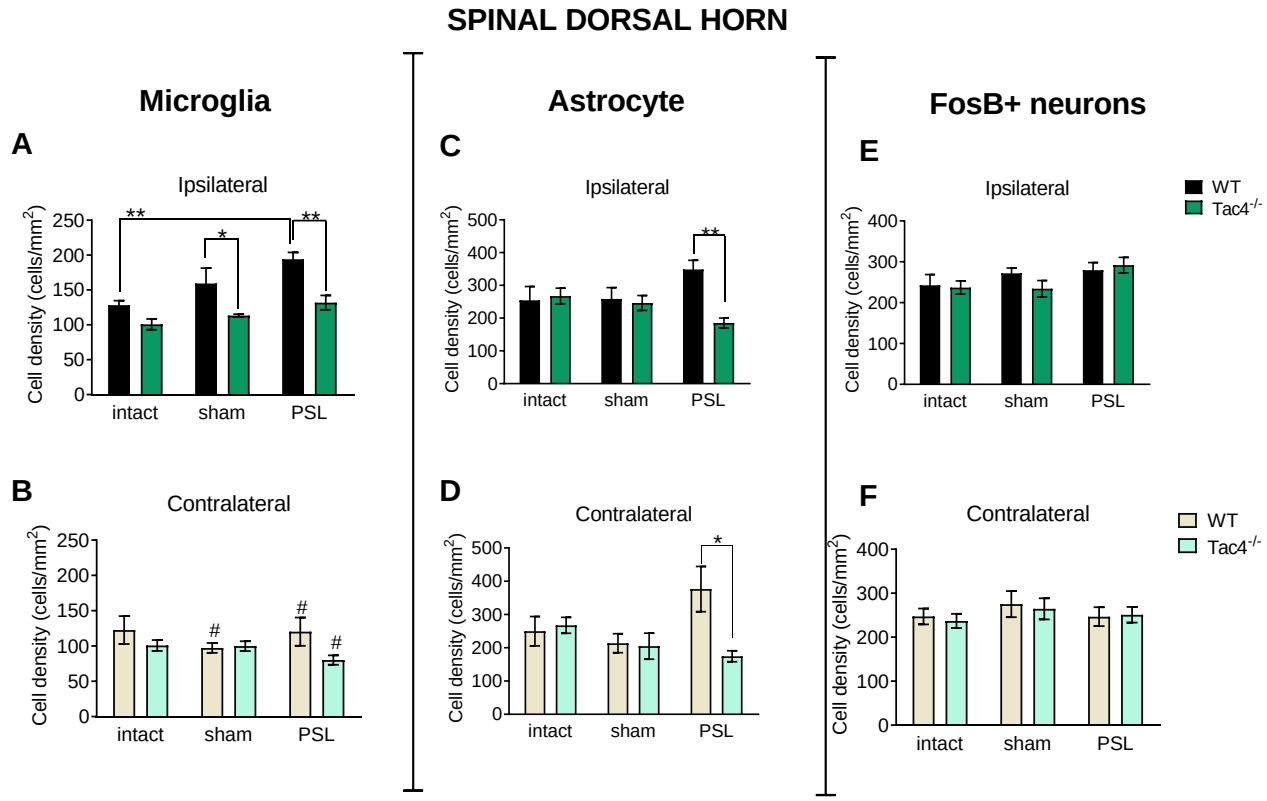

Figure 51. Iba1+ microglia (A, B), GFAP+ astrocytes (C, D) and FosB+ neurons (E, F) in the lamina I-II of L4-L6 spinal dorsal horn of intact, sham- and PSL-operated WT and HK-1-deficient (Tac4$^{-/-}$*) mice (n = 5–8 per group; *p < 0.05, **p < 0.01, factorial ANOVA + Tukey's posttest).*

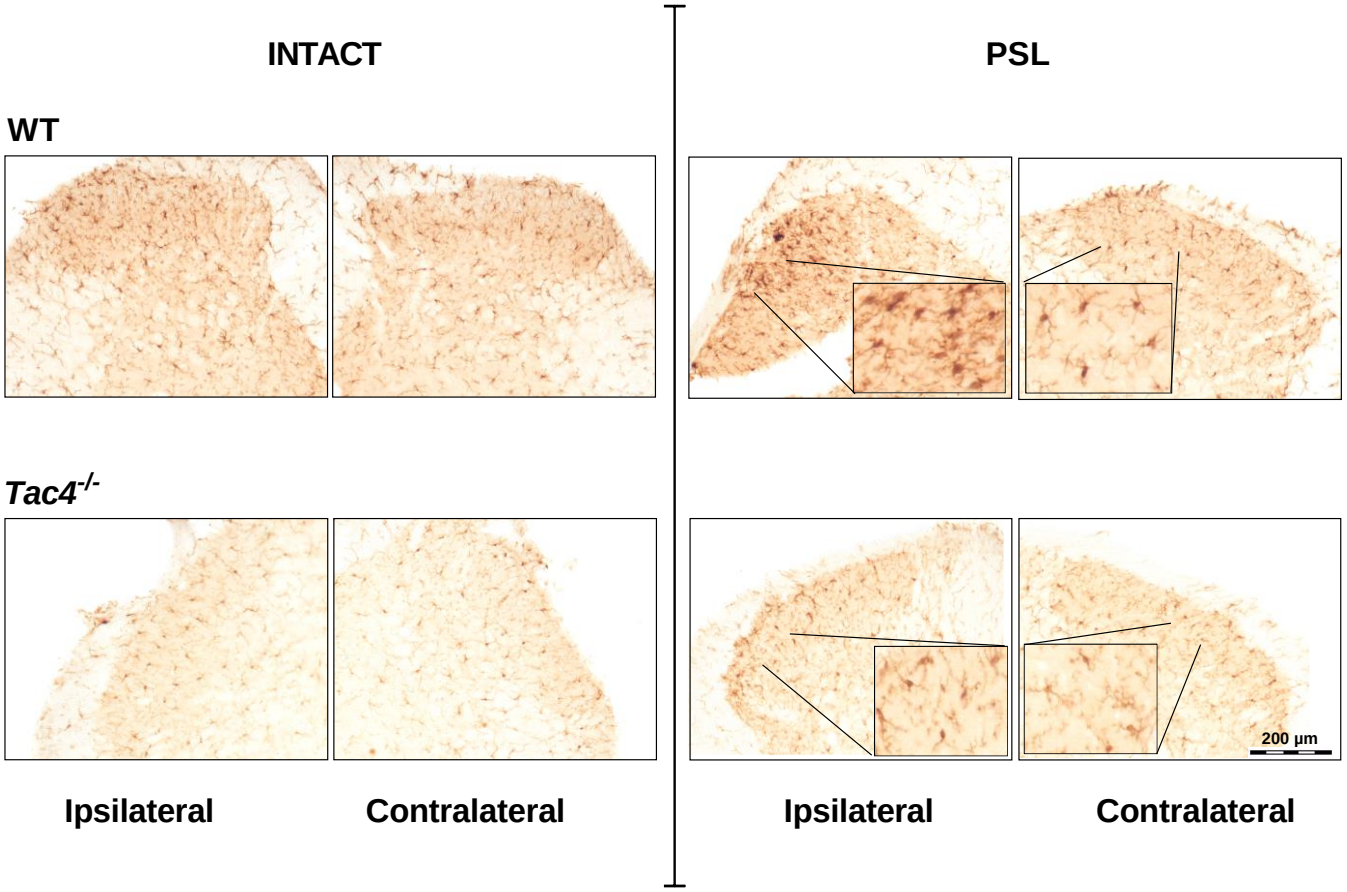

Figure 52. Representative photos of DAB-stained microglia cells in the L4-L6 spinal dorsal horn of intact and PSL operated WT and HK-1-deficient ($Tac4^{-/-}$) mice. A 200 µm bar for scale, inserts showing 2x magnification of microglia cells compared to the original image.

6.3.3.2 Periaqueductal grey matter (PAG)

Microglia- and FosB positive neuron-density did not show differences in either regions of the PAG. In the dorsal and lateral PAG *Tac4*$^{-/-}$ had fewer astrocytes which was statistically significant in intact mice, however it is worth noting that the examined regions had a very low number of astrocytes, 0-4 in every region of interest in every group (Figure 53).

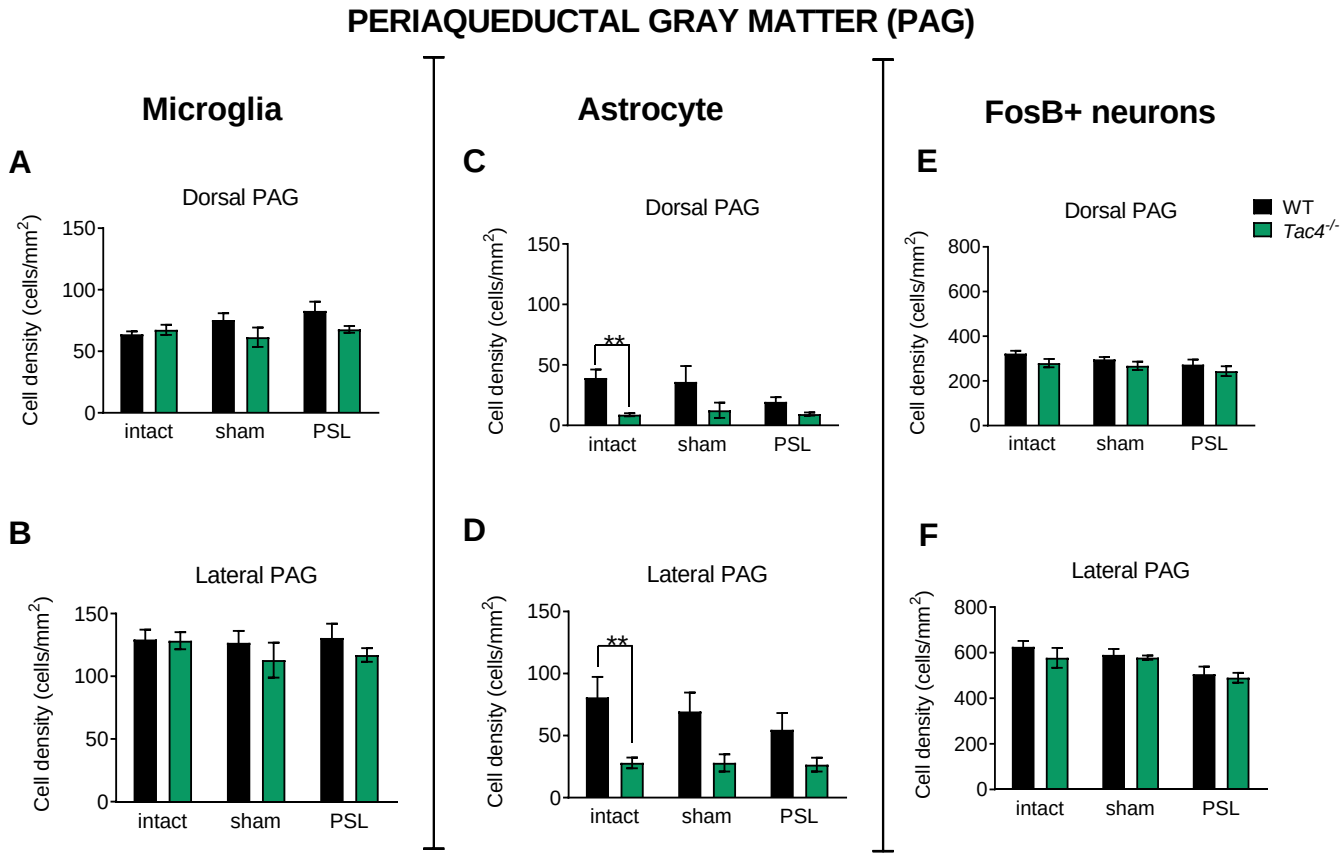

Figure 53. Iba1+ microglia (A, B), GFAP+ astrocytes (C, D) and FosB+ neurons (E, F) in dorsal and lateral PAG of intact, sham- and PSL-operated WT and HK-1-deficient (Tac4$^{-/-}$*) mice (n = 5–8 per group; *p < 0.05, **p < 0.01, factorial ANOVA + Tukey's posttest).*

6.3.3.3 Laterocapsular amygdala

In the laterocapsular amygdala the number of Iba1-positive microglia, GFAP-positive astrocytes and FosB positive neurons were respectively very similar in all groups (Figure 54).

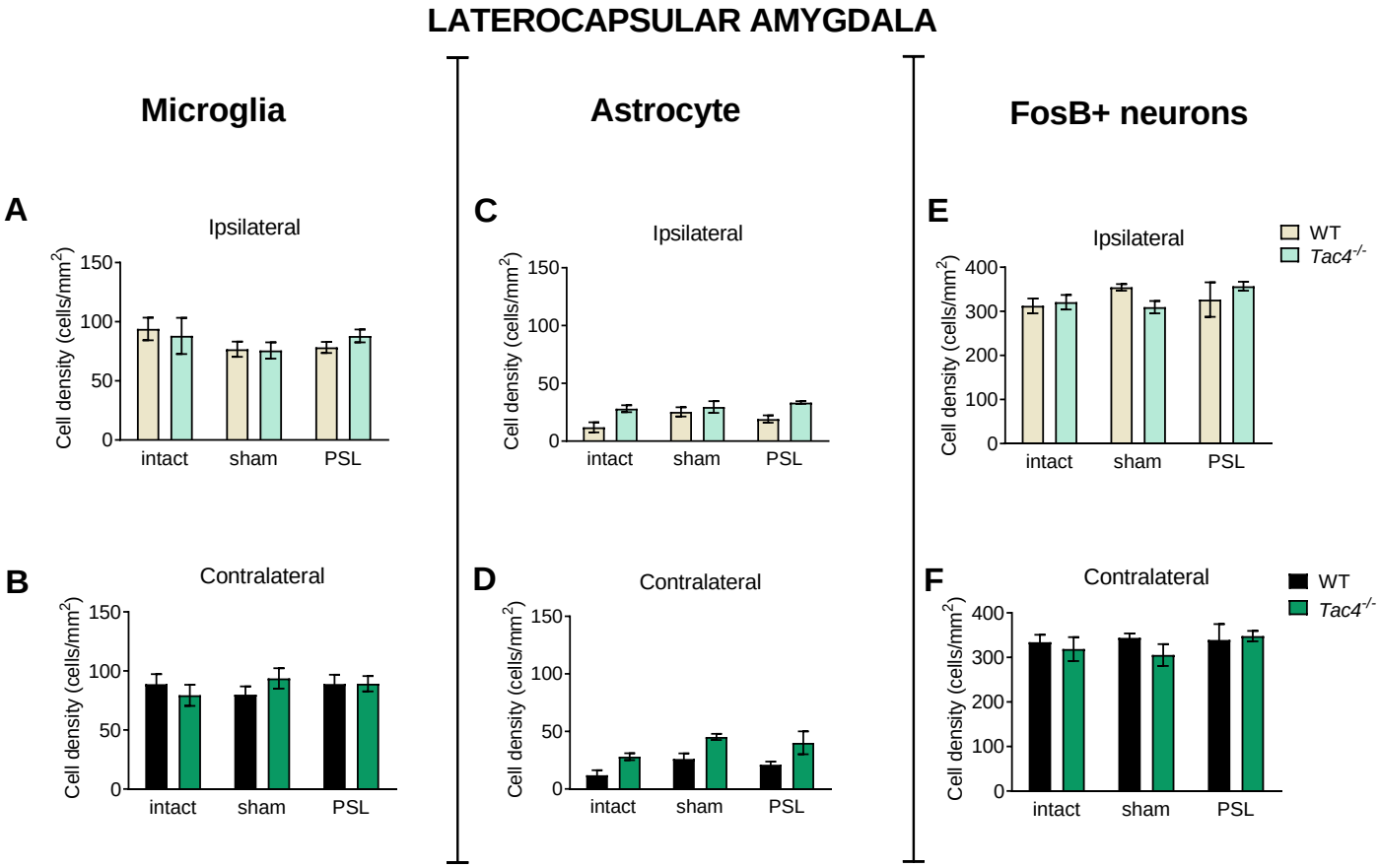

Figure 54. Iba1+ microglia (A, B), GFAP+ astrocytes (C, D) and FosB+ neurons (E, F) in the laterocapsular amygdala of intact, sham- and PSL-operated WT and HK-1-deficient ($Tac4^{-/-}$) mice (n = 5–8 per group; factorial ANOVA + Tukey's posttest). Color hues have been reversed compared to spinal cord figure to indicate the neuronal pathways crossing to the other side of the body.

6.3.3.4 Somatosensory cortex

In the somatosensory representation of the L4-L6 regions the number of Iba1-positive microglia, GFAP-positive astrocytes and FosB positive neurons showed no difference after neither operation nor gene deletion (Figure 55).

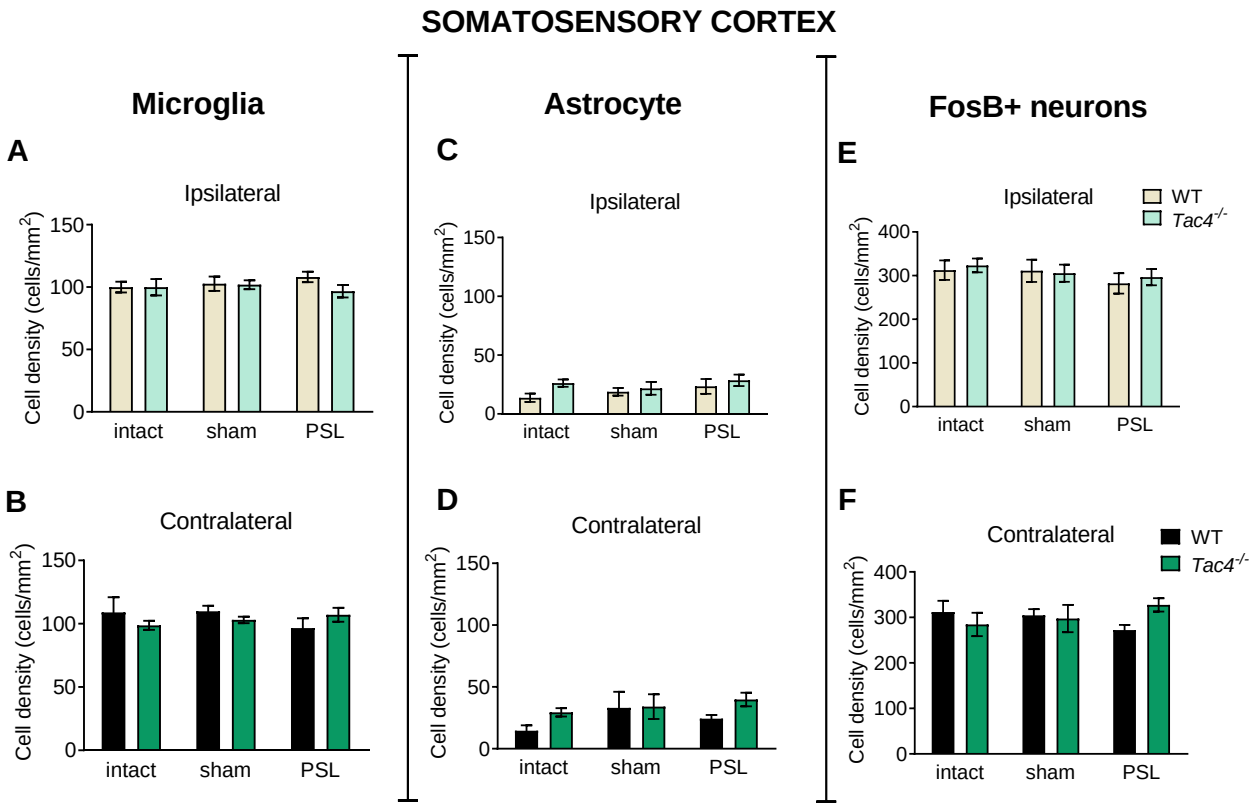

Figure 55. Iba1+ microglia (A, B), GFAP+ astrocytes (C, D) and FosB+ neurons (E, F) in the L4-L6 representation of the somatosensory cortex of intact, sham- and PSL-operated WT and HK-1-deficient (Tac4$^{-/-}$) mice (n = 5–8 per group; factorial ANOVA + Tukey's posttest). Color hues have been reversed compared to spinal cord figure to indicate the neuronal pathways crossing to the other side of the body.

6.4 Skin disease models

6.4.1 Oxazolone-induced allergic contact dermatitis

6.4.1.1 The absence of HK-1 markedly decreased ear swelling 24 hours after treatment

Results are shown as % of the ear thickness compared to respective control values of each ear of each individual mouse. The most pronounced ear swelling developed 24 hours after administering oxazolone solution to the ear in both WT (154.26 ± 4.41 %) and *Tac4*$^{-/-}$ mice (132.76 ± 3.27 %). At this timepoint *Tac4*$^{-/-}$ mice had significantly milder ear swelling compared to WTs. Contralateral ear treated with solvent (96% ethanol) did not show significant increase in thickness compared to control values (Figure 56).

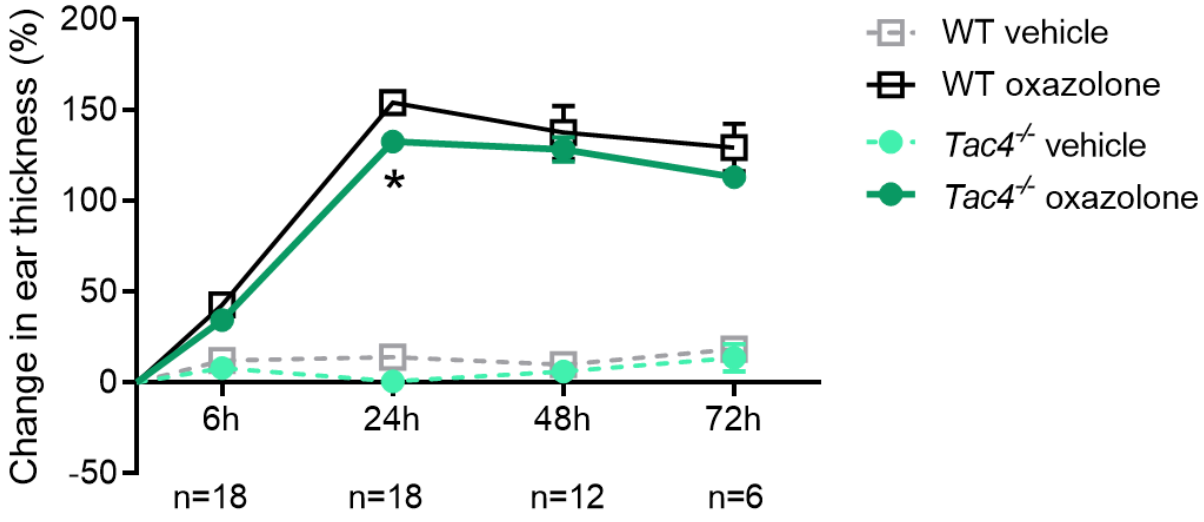

*Figure 56. Oxazolone-induced change in ear thickness in WT and HK-1-deficient (Tac4-/-) mice. Contralateral ear treated with 96% ethanol vehicle shown as control (n = 6-18 per group, *p < 0.05, vs. WT, repeated measures two-way ANOVA + Bonferroni's post hoc test).*

6.4.1.2 MPO-activity did not change in the absence of HK-1

MPO-activity increased significantly 24 hours after oxazolone treatment in both WT (6.55 x 10^5 ± 1.94 x 10^5 p/s) and *Tac4*$^{-/-}$ (5.67 x 10^5 ± 10^5 p/s) mice. Increased activity could still be detected after 48 hours, but this did not differ significantly from the respective control sides. There was no significant difference between WT and *Tac4*$^{-/-}$ groups (Figure 57).

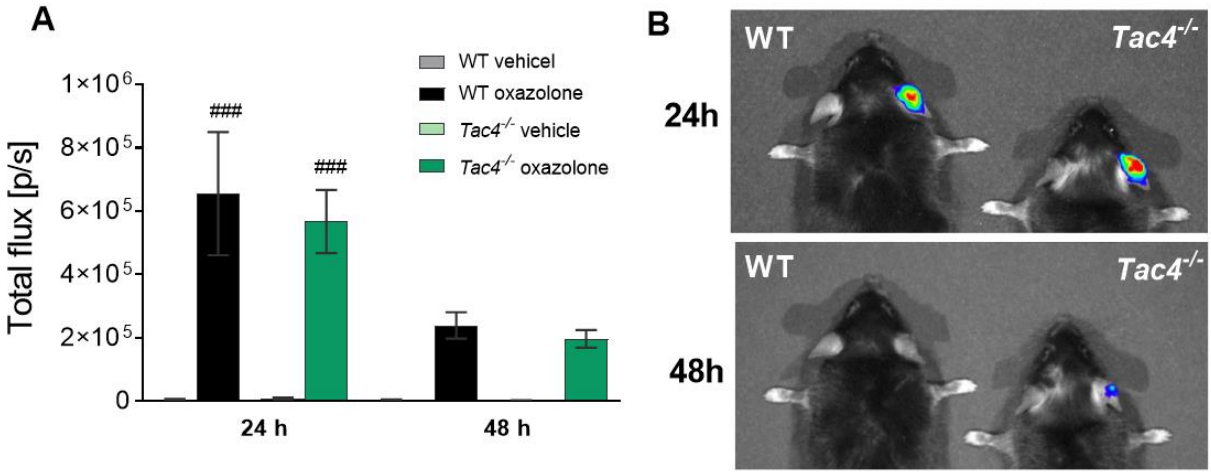

Figure 57. MPO-activity seen after oxazolone (right ear) and 96% ethanol (vehicle, left ear) treatment in WT and HK-1-deficient (Tac4-/-) mice (A) (n = 12-18 per group, #p < 0.001 vs. vehicle-treated side, repeated measures two-way ANOVA + Bonferroni's post hoc test). Representative photos visualizing MPO-activity (B).

6.4.1.3 Plasma extravasation did not change in the absence of HK-1

Plasma extravasation increased significantly 24 hours after oxazolone treatment in both WT (6.55 x 10^5 ± 1.94 x 10^5 p/s) and *Tac4*$^{-/-}$ (5.67 x 10^5 ± 10^5 p/s) mice with no significant difference between groups and remained significantly high at 48 hours as well (Figure 58).

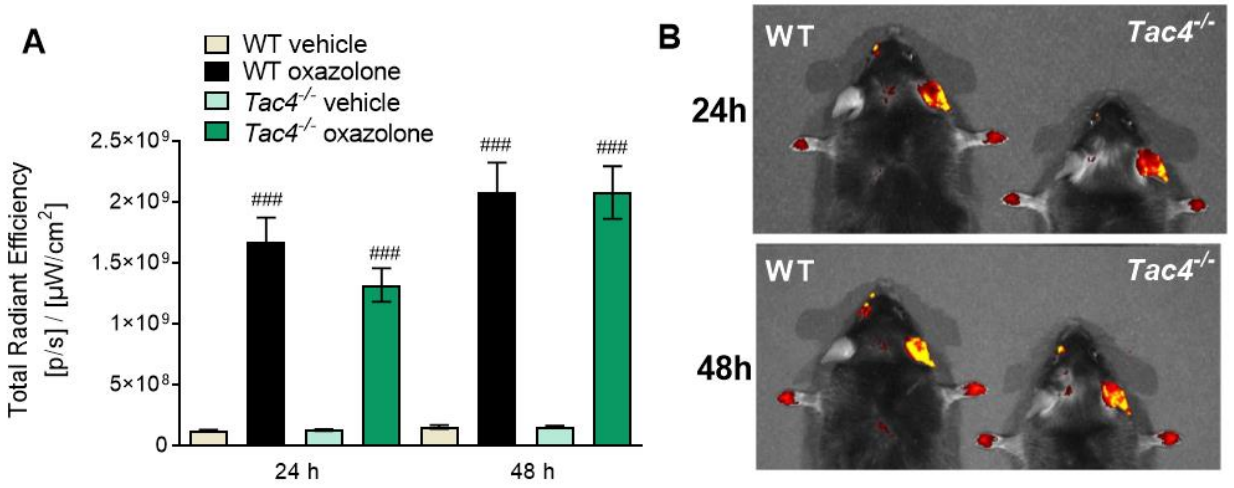

Figure 58. Plasma leakage seen after oxazolone (right ear) and 96% ethanol (vehicle, left ear) treatment in WT and HK-1-deficient (Tac4$^{-/-}$*) mice (A) (n = 12-18 per group, ###p < 0.001 vs. vehicle-treated side, repeated measures two-way ANOVA + Bonferroni's post hoc test). Representative photos visualizing plasma leakage (B).*

6.4.1.4 *Tac4* mRNA found in hair follicles of ear

Upregulation of *Tac4* could not be seen after treatment. In all samples *Tac4* specific signal was detected only in the hair follicle (Figure 59).

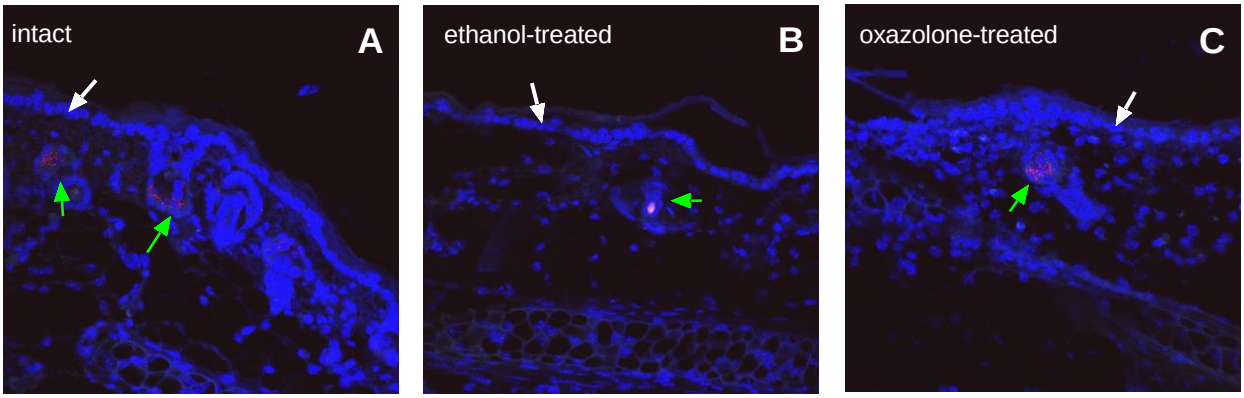

Figure 59. Representative Tac4 mRNA expression in the ear of intact (A), ethanol-treated (B) and oxazolone-treated (C) WT mice by RNAscope. Tac4 mRNA in red counterstained with DAPI. Autofluorescence of hair can be seen on panel B. green arrow – hair follicle; white arrow – epidermis.

6.4.1.5 *Tac4* mRNA expression in inguinal lymph node as a validation of the RNAscope method

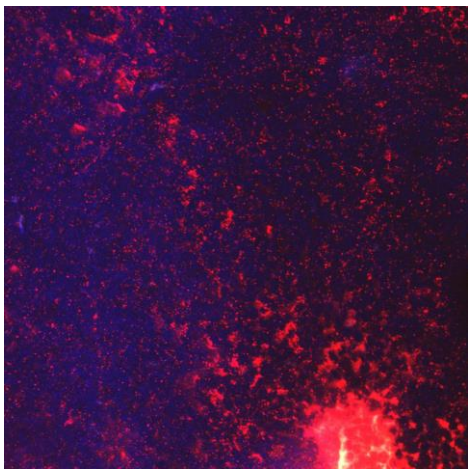

Tac4 specific signals could be seen in abundance in the inguinal lymph node. This preparation was used as a positive control of the technique (Figure 60).

Figure 60. Representative Tac4 mRNA expression in the inguinal lymph node of oxazolone treated WT mice. Tac4 mRNA in red counterstained with blue DAPI.

6.4.1.6 IFNγ was significantly higher at 24 h in the absence of HK-1

IL2 became elevated in both WT (124.64 ± 33.33 pg/g) and *Tac4*$^{-/-}$ (114.57 ± 25.99 pg/g) oxazolone treated groups 24 h after ear treatment and remained elevated until the end of the experiment with no significant difference between WT and Tac4$^{-/-}$ groups (Figure 61A). IFNγ-level increased 24 hours after treatment to 392.24 ± 103.21 pg/g in WT and a significantly higher 777.47 ± 236.52 pg/g in *Tac4*$^{-/-}$ mice. Beginning on the 2nd day IFNγ-levels returned to baseline in both groups (Figure 61B). TNFα-level began to elevate after 24 hours and reached its peak after 72 h (687.22 ± 79.61 pg/g in WT and 697.81 ± 107.25 pg/g in *Tac4*$^{-/-}$). There was no observed difference in the absence of HK-1 (Figure 61C).

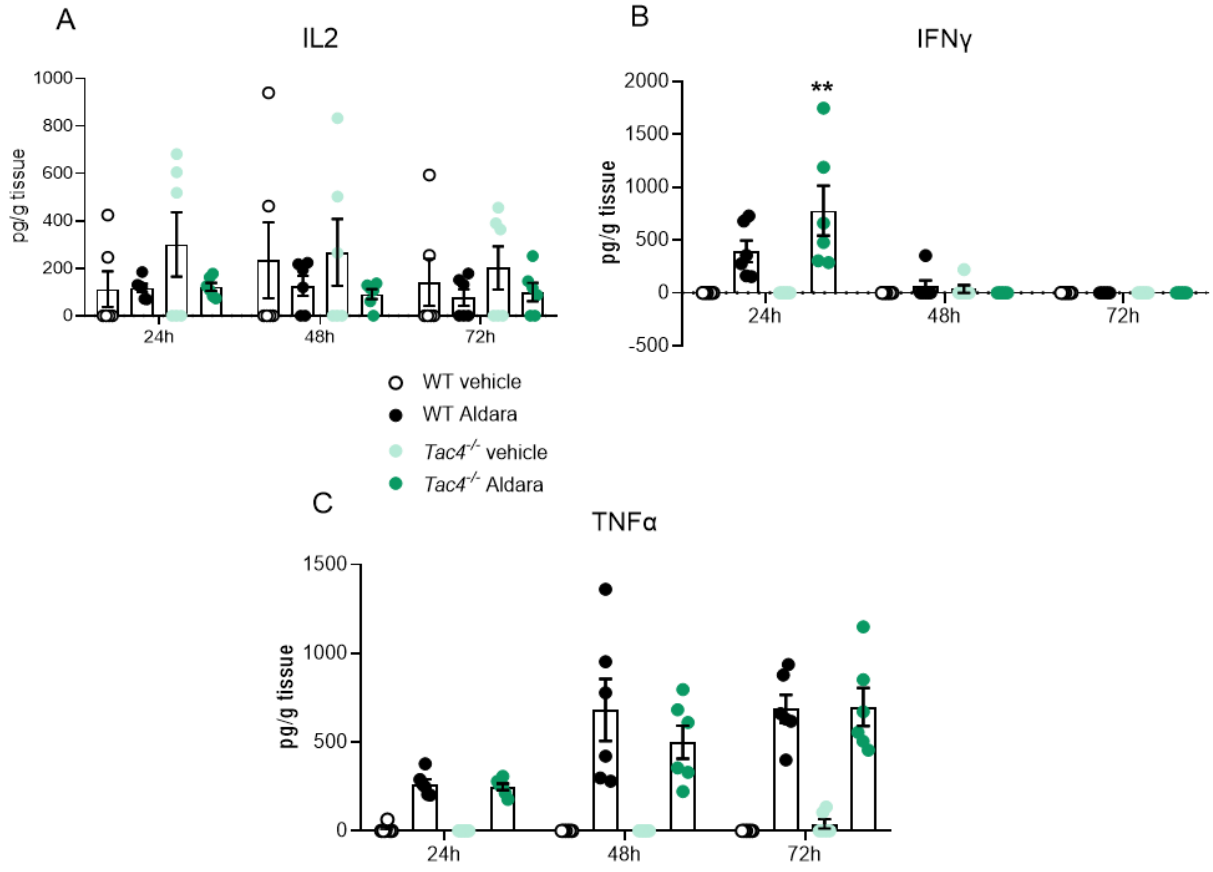

*Figure 61. IL2, IFNγ- and TNFα-levels in oxazolone- and 96% ethanol (vehicle)-treated ears of WT and HK-1-deficient (Tac4$^{-/-}$) mice (n = 6 per group; **p < 0.01 vs. WT, two-way ANOVA + Bonferroni's post hoc test).*

6.4.1.7 IL4 was significantly higher at 24 h in the absence of HK-1

IL4 reached its peak after 24 h in both groups with a significantly higher level in *Tac4*$^{-/-}$ (13097.82 ± 1579.92 pg/g) compared to WT (8492.77 ± 1616.49 pg/g) and began to return to near-baseline level by 48 h (Figure 62A). IL5 increased after 24 h with levels showing no difference in the absence of HK-1 (107.20 ± 37.53 pg/g in WT and 91.961 ± 30.09 in *Tac4*$^{-/-}$) and began to decrease in the following days (Figure 62B).

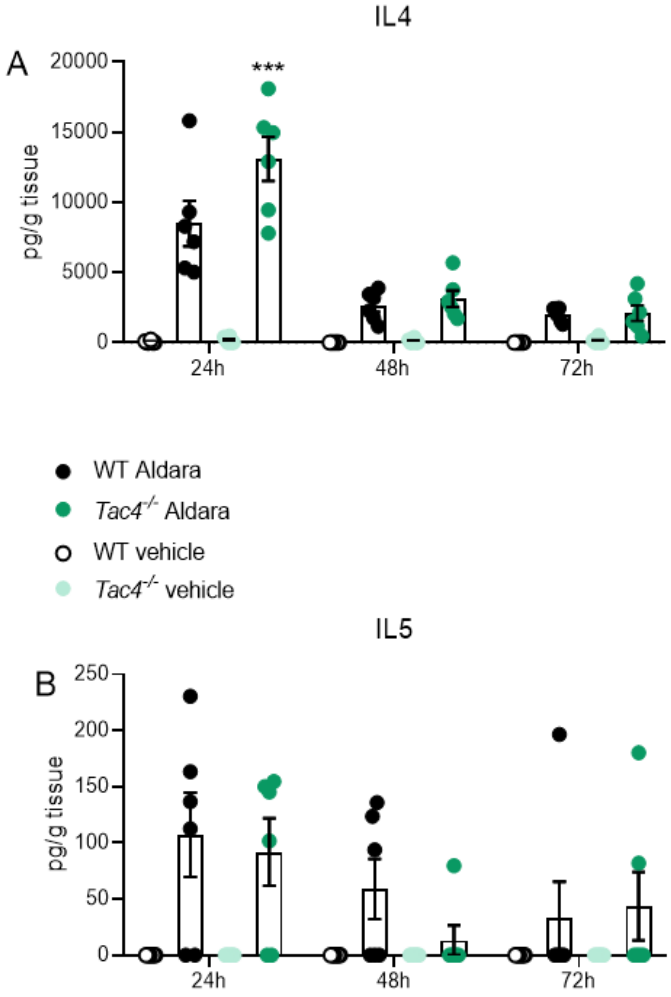

Figure 62. IL4- and IL5-levels in oxazolone- and 96% ethanol (vehicle)-treated ears of WT and HK-1-deficient (Tac4$^{-/-}$*) mice (n = 3-6 per group; ***p < 0.001 vs. WT, two-way ANOVA + Bonferroni's post hoc test).*

6.4.2 Aldara-induced psoriasiform dermatitis

6.4.2.1 Change in skinfold thickness was significantly smaller at 96 h in the absence of HK-1

Results are shown as % of the skinfold thickness compared to respective control values of each skin area. Thickening of skin was already detectable 24 h after first treatment. Though the results of both KO groups were below WT's curve, it only reached statistical significance at the 96 h timepoint in *Tac4*$^{-/-}$ mice (WT 56.48 ± 6.78; Tac4$^{-/-}$ 31.47 ± 5.13; *Tacr1*$^{-/-}$ 31.48 ± 8.84; Figure 63A). Representative pictures show the dorsal skin of mice before first treatment and at the end of experiment (Figure 63B)

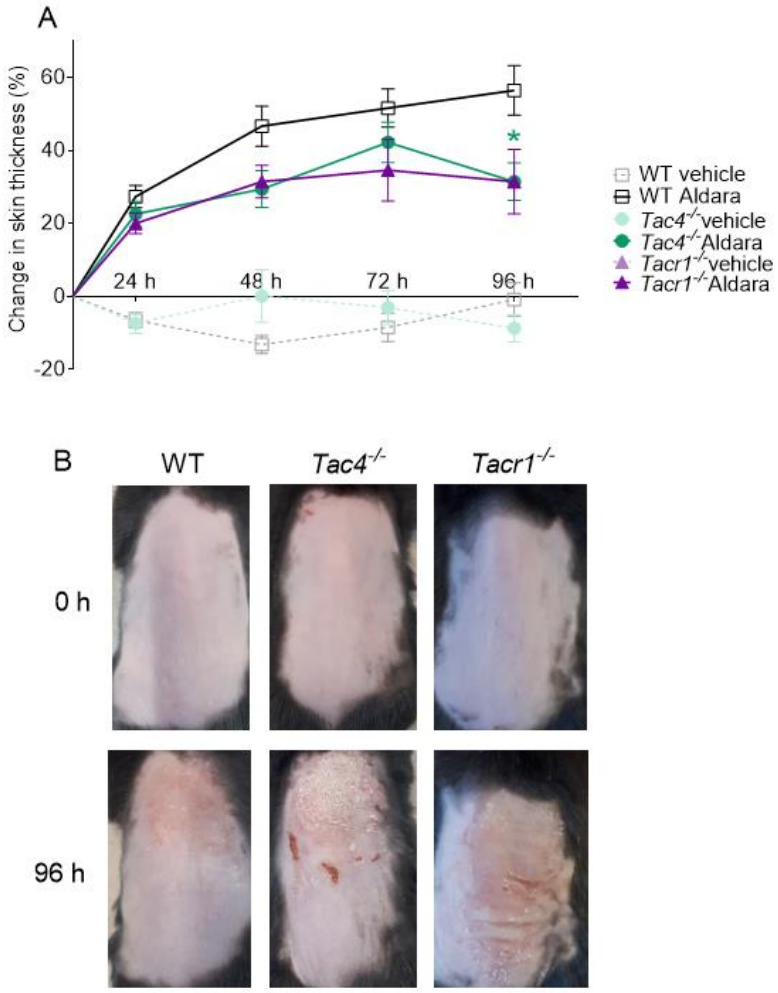

Figure 63. Aldara-induced change in skinfold thickness in WT, Tacr1$^{-/-}$ *and HK-1-deficient (Tac4*$^{-/-}$*) mice. Control skin area (lower left side of back) treated with vaseline vehicle shown as control (A) (n = 10-15 per group, *p < 0.05, vs. WT, repeated measures two-way ANOVA + Bonferroni's post hoc test). Representative pictures of dorsal skin before treatment (0 h) and after 96 h (B).*

6.4.2.2 Change in detectable blood flow was significantly smaller at 96 h in the absence of HK-1

Results are shown as % of the blood flow compared to respective control values of skin area. Increase of blood flow already detectable 24 h after first treatment. *Tac4*$^{-/-}$ mice had significantly lower levels of detectable blood perfusion at 96 h (WT 47.42 ± 6.65 %; *Tac4*$^{-/-}$ 15.19 ± 8.6 %; *Tacr1*$^{-/-}$ 42.01 ± 14.1 %; Figure 64A). Representative pictures show the heat map of dorsal skin before first treatment and at the end of the experiment (Figure 64B)

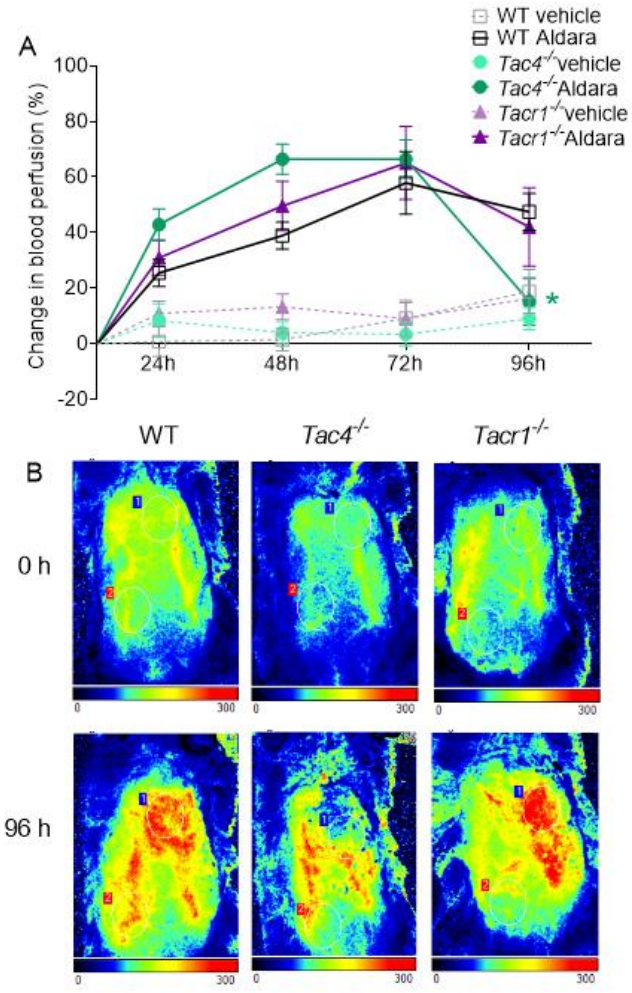

Figure 64. Aldara-induced change in skin blood flow in WT, HK-1-deficient (Tac4$^{-/-}$*) and Tacr1*$^{-/-}$ *mice. Control skin area (lower left side of back) treated with vaseline vehicle shown as control (A) (n = 10-15 per group, *p < 0.05, vs. WT, repeated measures two-way ANOVA + Bonferroni's post hoc test). Representative heat maps of dorsal skin before treatment (0 h) and after 96 h (B).*

6.4.2.3 *Tac4* mRNA found in hair follicles of skin

Accumulation of *Tac4* could not be seen after treatment. In all samples *Tac4* specific signal was detected only in the hair follicle (Figure 65). According to panel B the *Tac4* signal is located in the bulge area of the follicle.

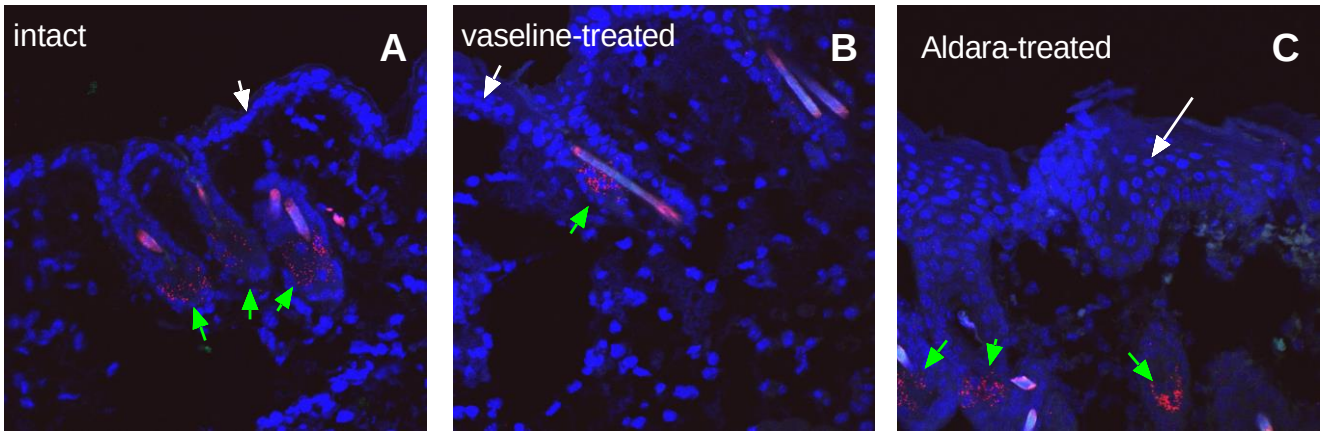

Figure 65. Representative Tac4 mRNA expression in the skin of intact (A), vaseline-treated (B) and Aldara-treated (C) WT mice by RNAscope. Tac4 mRNA in red counterstained with DAPI. Autofluorescence of hair can be seen on all panels. green arrow – hair follicle with Tac4 signal; white arrow – epidermis.

6.4.2.4 There was no significant difference in IL1β or TNFα levels in the absence of HK-1 or NK_1 receptor

Both IL1β or TNFα levels reached their peak 24 h after initial Aldara treatment in WT mice (35.83 ± 7.89 pg/g and 8.65 ± 4.19 pg/g respectively) and remained elevated until the end of the experiment. There was no significant difference in the absence of HK-1 of NK_1 receptor (Figure 66).

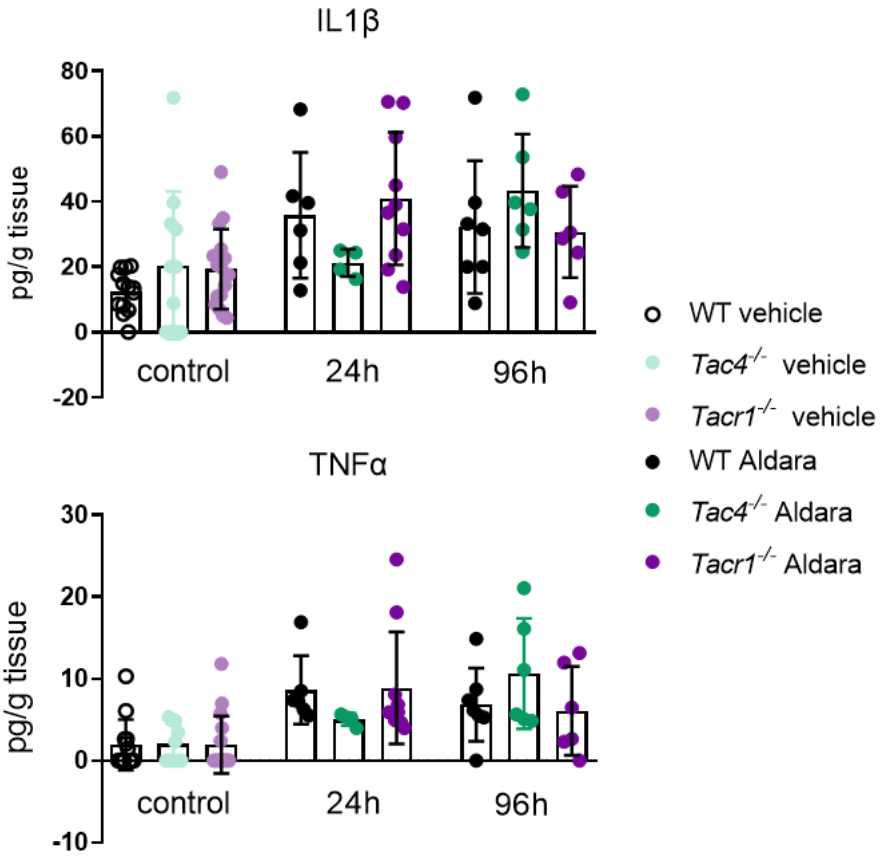

*Figure 66. IL1β- and TNFα-levels in Aldara- and vaseline (vehicle)-treated skin of WT, Tacr1-/- and HK-1-deficient (Tac4−/−) mice (n = 4-10 per group; **p < 0.01 vs. WT, two-way ANOVA + Bonferroni's post hoc test).*

7 Discussion

7.1 HK-1 mediates arthritic pain and inflammation independently of NK_1 receptor.

We showed that HK-1 is an important mediator of central- and peripheral sensitization during joint inflammation, which was independent of NK_1 receptor in the K/BxN and CFA models. HK-1 also contributes to edema formation, histopathological processes and prevents MPO increase.

model	method	*Tac4*$^{-/-}$ (lack of HK-1)	*Tacr1*$^{-/-}$ (lack of NK_1 rec.)
K/BxN	mechanical hyperalgesia	↓	N
	edema	↓	N
	heat sensitivity	↓	
	cold tolerance	N	N
	grid grasping	N	N
	weight	N	N
	visual arthritis score		N
	MPO activity	↑ on 2nd day	
	plasma leakage	N	
	histopathological score	↓	
	PCR (WT)	DRG: *Tac4* mRNA in did not change significantly	
		spinal cord: no *Tac4* mRNA was detected	
MCT	mechanical hyperalgesia	↓	↓*
	edema	↓	↓*
	increase in blood flow	N	N*
CFA	mechanical hyperalgesia	↓	N
	knee edema	↓	N
	MPO-activity	↑	

Table 3. Summary of arthritis experiment results

Using three different methods of inducing arthritis we were able to obtain a more detailed picture on the role of HK-1. K/BxN-induced arthritis is a widely accepted chronic passive disease transfer model[120] which can mimic several aspects of the human condition, including central sensitization. In our experiments we saw that edema (which correlates to inflammatory responses) resolved 14 days after serum administration, while mechanical hyperalgesia persisted for another week indicating central sensitization independent of inflammation on the periphery.

HK-1 contributes to both the early, dominantly peripheral pain as well as the late, central sensitization related pain, while NK_1 receptor did not contribute to arthritis related pain. Edema formation and pathohistological score were also milder in the absence of HK-1, this reinforces that HK-1 has a role in the peripheral inflammatory reaction. It is worth noting that on the 14th day when histological samples were taken even the WT scored only 4 out of 9 points, so at this point the joint inflammation was already receding.

On day 2 and 6 of K/BxN arthritis the absence of HK-1 did not affect dye extravasation in the fluorescent imaging study. Vascular leakage is not the only component of edema formation, so it cannot exclusively explain the differences in paw swelling. In a study using chronic CFA model we found that HK-1 contributed to histopathological changes in the joint while not contributing to edema formation[121], so the vascular effects of HK-1 do not seem to be pronounced.

Despite the detrimental effect of HK-1 in joint inflammation so far, MPO increase occurred earlier (on day 2) in the absence of HK-1. MPO is produced by neutrophils and macrophages and is known as a mediator of tissue damage and inflammation. One possible explanation is some sort of mechanism trying to compensate for the absence of HK-1 by increasing MPO production, however previous studies have found that in certain circumstances, when elevated in the early phase of the cascade, MPO can prevent inflammation[122]. The mechanism is not well understood, products of MPO can facilitate the switch to adaptive immunity and inhibit T-cell responses while downregulating the innate immunity. Since neutrophils can produce HK-1 as well, it is plausible for them to have interactions, however so far there is no corresponding data in the literature.

Acute CFA-induced arthritis[123] is initiated by macrophages and based on our findings HK-1 contributed to both pain and knee swelling, while NK_1 receptor did not. MCT as a local mediator of inflammation released from mast cells contributes to the development of arthritis[124] and elicits its effects through sensory neurons[125]. HK-1 played a role in related mechanical hyperalgesia and edema, but not in increasing blood flow. The effects of HK-1 are mediated through NK_1 receptor, as *Tacr1*$^{-/-}$ mice showed a similar response in a previous article[125]. Based on these findings we can see compelling evidence that HK-1 mediates its effects in arthritis not only through inflammatory cells, but also through the sensory neurons, in certain models independently of the NK_1 receptor.

7.2 HK-1 activates primary sensory neurons independently of NK_1 receptor and prevents capsaicin-induced desensitization.

	PTX-pretreatment	Tacr1$^{-/-}$ neurons	NK1 antagonist pretreatment	Ca^{++}-free media	TRPV1 antagonist pretreatment	TRPA1 antagonist pretreatment
HK-1 neuronal activating effect	n	n	n	↓	n	n
HK-1 diminished the desensitizing effect of capsaicin.						
SP diminished the desensitizing effect of capsaicin.						

Table 4. Summary of primary sensory neuron culture experiments

Our *in vitro* studies on cultured primary sensory neurons further explored the molecular mechanism of HK-1. HK-1 was able to directly activate the sensory neurons and elicit Ca^{2+} influx into the cells, while SP was not. The HK-1-induced Ca^{2+} influx was present in *Tacr1*$^{-/-}$ cells, as well as after pretreatment with NK_1 receptor antagonist or PTX, but not when the cells were cultured on Ca^{2+}-free media. This suggests an ion channel-coupled receptorial mechanism, but not TRPV1- or TRPA1-mediated mechanism, since the TRPV1 receptor antagonist AMG9810 and the TRPA1 receptor antagonist HC030031 did not influence the HK-1-induced Ca^{2+} influx response. Repeated administration of capsaicin to primary sensory neurons causes a decreasing intensity in Ca^{2+} influx as the TRPV1 receptors become desensitized from the repeated stimulus[126]. Both HK-1 and SP were able to neutralize this effect and elicit the full Ca^{2+}-influx response in the neurons. The neuronal activating ability of HK-1 has been shown in cholinergic hippocampal neurons, where it acted post-synaptically in a tetrodotoxin-resistant manner, however this response was not dependent on Ca^{2+} from the extracellular space[127]. These findings show the ability of HK-1 to act like classic tachykinin peptides and induce effects on neurons of sensory nerves.

7.3 HK-1 mediates certain acute nocifensive behaviors via NK_1 receptor activation.

	Tac4$^{-/-}$ (lack of HK-1)	*Tacr1*$^{-/-}$ (lack of NK_1 rec.)	*Tac1*$^{-/-}$ (lack of SP/NKA)
intraplantar formalin			
Phase 1:	N	N	N
Phase 2:	N	N	↓
intraperitoneal acetic-acid			
0-5 min	N	N	N
5-20 min	↓	↓	↓
20-30 min	N	↓	↓
intraplantar RTX			
heat pain	↓	↓ (20 min)	↓
mechanical hyperalgesia	↓	↓	↓ (6h)

Table 5. Summary of acute pain experiment results

When evoking acute neurogenic inflammation in the foot with the administration of the TRPV1 agonist RTX we saw that the heat threshold decrease and mechanical hyperalgesia were ameliorated in the absence of HK-1, NK_1 receptor and SP/NKA. This reinforces our in vitro findings where the presence of HK-1 and SP maintained the TRPV1 agonist sensitivity of the sensory neurons.

During the release of inflammatory mediators in the 2nd phase of formalin-induced nocifension only SP/NKA played a role, HK-1 and NK_1 receptor did not. None of the peptides or NK_1 receptor were involved in the 1st phase direct activation of sensory neurons in this model. SP/NKA and NK_1 receptor were the dominant mediators of visceral pain, HK-1 only had a weaker effect in the 2nd phase of the activation of visceral nociceptors.

7.4 HK-1 contributes to neuropathic pain and related neuroinflammation independently of NK_1 receptor activation, as well as motor coordination.

PSL	*Tac4*$^{-/-}$ (lack of HK-1)	*Tacr1*$^{-/-}$ (lack of NK_1 rec.)
mechanical hyperalgesia	↓	N*
cold sensitivity	↓	N*
motor coordination	baseline ↓ after operation N	N* N*
NGF	↑	
microglia	↓ dorsal spinal horn	
astrocyte	↓ dorsal spinal horn	
FosB+ neurons	N	

*Table 6. Summary of neuropathy experiment results. *Results published in Botz et al., 2013.*

In the PSL-induced neuropathic pain model HK-1 contributed to both mechanical hyperalgesia and decrease in cold threshold. This is unique to HK-1 among the tachykinins, as neither SP/NKA nor NK_1 receptor played a role in PSL-induced pain[113]. The level of NGF did not change in WT animals after PSL, in *Tac4*$^{-/-}$ animals it began from a significantly lower level and increased when neuropathy developed. While NGF is best known for contributing to pain, it is also an important trophic factor of neurons which could contribute to the regeneration of damaged nerves. It is also noteworthy that, as with the MPO in joint inflammation, we saw again that in the absence of HK-1 a seemingly detrimental factor increased when the disease developed. NGF has been shown to increase the level of SP in DRG neurons *in vitro*[128], but interaction between NGF and HK-1 has not been studied yet.

When examining different levels of the pain pathway with immunohistochemistry methods we saw relevant differences in the lamina I-II of the spinal dorsal horn, as HK-1 contributed to the increase of microglia cells after operation. HK-1 seems to be an important mediator of microglia activation: the production of HK-1 is upregulated when microglia[129] become activated; and

blocking microglia activation with minocyclin decreases HK-1 production, as well as pain related behavior in rats[130].

The PSL operation did not influence motor coordination, HK-1-deficient mice had worse motor coordination than WT mice. This correlates with previous reports of a paradoxically high HK-1 expression in the cerebellum: in most brain regions SP is the dominant tachykinin and HK-1 is present in small amounts, while in the cerebellum HK-1 is dominant[49]. The cerebellum has the lowest NK1 receptor expression among different regions of the brain[131]. With this finding we provided the first functional data in correlation with the high HK-1 expression in the cerebellum. Though the cerebellum is known for its role in motor coordination, it has a role in emotional processing as well[132], with a study even pinpointing its importance in reward anticipation[133]. Though NK_1 receptor antagonists have been suggested as antidepressants, their application has yielded mixed results[134]. It could be interesting to include the cerebellum in further studies of mood disorders alongside the conventional mood-related cerebral brain regions.

7.5 HK-1 mediates in skin swelling in an allergic contact dermatitis model via the NK_1 receptor.

Oxazolone-induced allergic contact dermatitis		
	Tac4$^{-/-}$ (lack of HK-1)	*Tacr1*$^{-/-}$ (lack of NK_1 rec.)
Skin swelling	↓ (24h)	↓*
Increased MPO-activity	N	N*
Increased plasma extravasation	N	
IFNγ-increase	↑ (24h)	↑ (48h)*
TNFα-increase	N	↓ (48h)*
IL2-increase	N	N*
IL4-increase	↑ (24h)	N*
IL5-increase	N	N*
RNAscope (WT)	No upregulation, *Tac4* mRNA found in hair follicle bulge region	

*Table 7. Summary of allergic contact dermatitis experiment results. *Results published in Bánvölgyi et al., 2005.*

The results of our experiments showed that HK-1 only has a minor role in oxazolone-induced allergic contact dermatitis, decreasing ear edema only at the 24h timepoint. At this timepoint the inflammatory cytokines IFNγ and IL4 increased despite the milder reaction in the ear. Though IL4 is known as a promoter of Th2-cell differentiation and allergic reaction[135], it can also down-regulate the inflammation in contact dermatitis which may explain the alleviated skin swelling at this timepoint[136]. Furthermore, neutralization of IL4 leads to the increased production of inflammatory mediators as IFN-γ, IL2, IL12 p40, and IL1β. In a previous study the absence of NK_1 receptor showed a more robust and persistent alleviation of symptoms of allergic contact dermatitis[55,89]. NK_1 receptor produced by the T-cells has a pivotal role in survival and developement of Th1 then Th17 type cells[55]. Resting and stimulated T cells can produce both HK-1 and SP, so based on our findings, the NK_1 receptor seems to be the crucial component of the process, and the presence of one of its agonists (SP) was enough to elicit its effects in T cells.

The HK-1 present in the bulge area of the hair follicle did not influence the outcome in this study and will be discussed later.

7.6 HK-1 mediates in skin swelling in the late phase of a psoriasis model.

Aldara-induced psoriasiform dermatitis		
	Tac4$^{-/-}$ (lack of HK-1)	*Tacr1*$^{-/-}$ (lack of NK_1 rec.)
Skin swelling	↓ (96h)	N
Increased blood flow	↓ (96h)	N
IL1β-increase	N	N
TNFα-increase	N	N
RNAscope (WT)	No upregulation, *Tac4* mRNA found in hair follicle bulge region	

Table 8. Summary of Aldara-induced psoriasiform dermatitis experiment results

While increase in skin thickness was markedly milder in both *Tac4*$^{-/-}$ and *Tacr1*$^{-/-}$ mice, this only reached statistical significance in case of *Tac4*$^{-/-}$ mice at the last measured timepoint. There was no difference in blood flow between WTs and KOs, which correlates with previous finding in our studies and others' that HK-1 does not have a robust effect on vascular changes. The significant decrease in blood flow at 96 hours in case of *Tac4*$^{-/-}$ mice can be contributed to the more intensive scaling of the skin in these animals, as the scaling skin influenced the laser speckle device's ability to detect the moving blood cells in the layers below. The process of T cell activation in psoriasis also includes Th17 cells, it is more dependent on IL23 than IL2. TCR signaling pathways are fully functional in NK_1 receptor-deficient cells, and T-cell apoptosis in NK_1 receptor-deficient cells could be prevented with IL2 supplementation in the study examining the mechanism of allergic contact dermatitis[55]. A study of skin biopsies of patients with plaque psoriasis with pruritus concluded that not just NK_1, but NK_2 receptor were upregulated in the lesions as well as NKA positive immune cells and nerve fibers[94]. Probably due to the complexity of the tachykinin system psoriasis was able to develop in mice even in the absence of HK-1 or NK_1 receptor. As in the ear hair follicles, *Tac4* mRNA was found in the bulge area of the hair follicles of the dorsal skin as well. Though it does not seem to play a role in psoriasiform dermatitis either, this was the first study to precisely locate HK-1 in the skin. The bulge is the area of the hair follicle at the insertion of the arrector pili muscle. It contains epidermal stem cells which can be progenitors of basal cell

carcinoma[137], and pluripotent stem cells which can differentiate, among others, into beating cardiac muscle cells and glial cells[138]. The expression of HK-1 in this bulge area proposes exciting new research prospects but goes beyond the scope of this study.

Our results provided evidence for the complex regulatory roles of HK-1 in pathologies related to sensory-immune interactions, whether in immune mechanism-triggered pain like arthritis, or nerve damage-induced neuroinflammation (gliosis). Although HK-1 did not exert a predominant role in the investigated dermatitis models, its presence in the stem cell rich bulge region is a particularly valuable novel information. The discovery of murine MrgprB2 and human MRGPRX2 receptors as novel targets of HK-1, as well as the dual antagonist of both NK_1 receptor and MRGPRX2 has reopened the possibility of novel analgesics targeting the tachykinin system.

8 Summary: conclusions from the novel results

The tachykinin HK-1 mediates

- arthritis-related pain and inflammation in acute and chronic models, including late central sensitization independently of NK_1 receptor activation, while it prevents neutrophil MPO activity increase;
- TRPV1 activation-induced acute neurogenic inflammation, somatic and visceral nocifensive behaviors via the NK_1 receptor;
- primary sensory neuronal activation in a pertussis toxin-insensitive, NK_1 receptor-independent, but extracellular Ca^{2+}-dependent manner, as well as the prevention of capsaicin-induced desensitization;
- neuropathic pain and related neuroinflammation (gliosis) in the lamina I-II of the spinal dorsal horn independently of the NK_1 receptor, while it prevents peripheral NGF increase;
- motor coordination independently of NK_1-receptor, which is supported by the high HK-1 and low NK_1 receptor expressions in the cerebellum;
- skin swelling in psoriasis and allergic contact dermatitis models, while it prevents IFNγ and IL4 level increase in allergic contact dermatitis. The HK-1 encoding *Tac4* mRNA is present in the bulge area of the hair follicles of the mouse skin.

The findings are summarized in Figure 67.

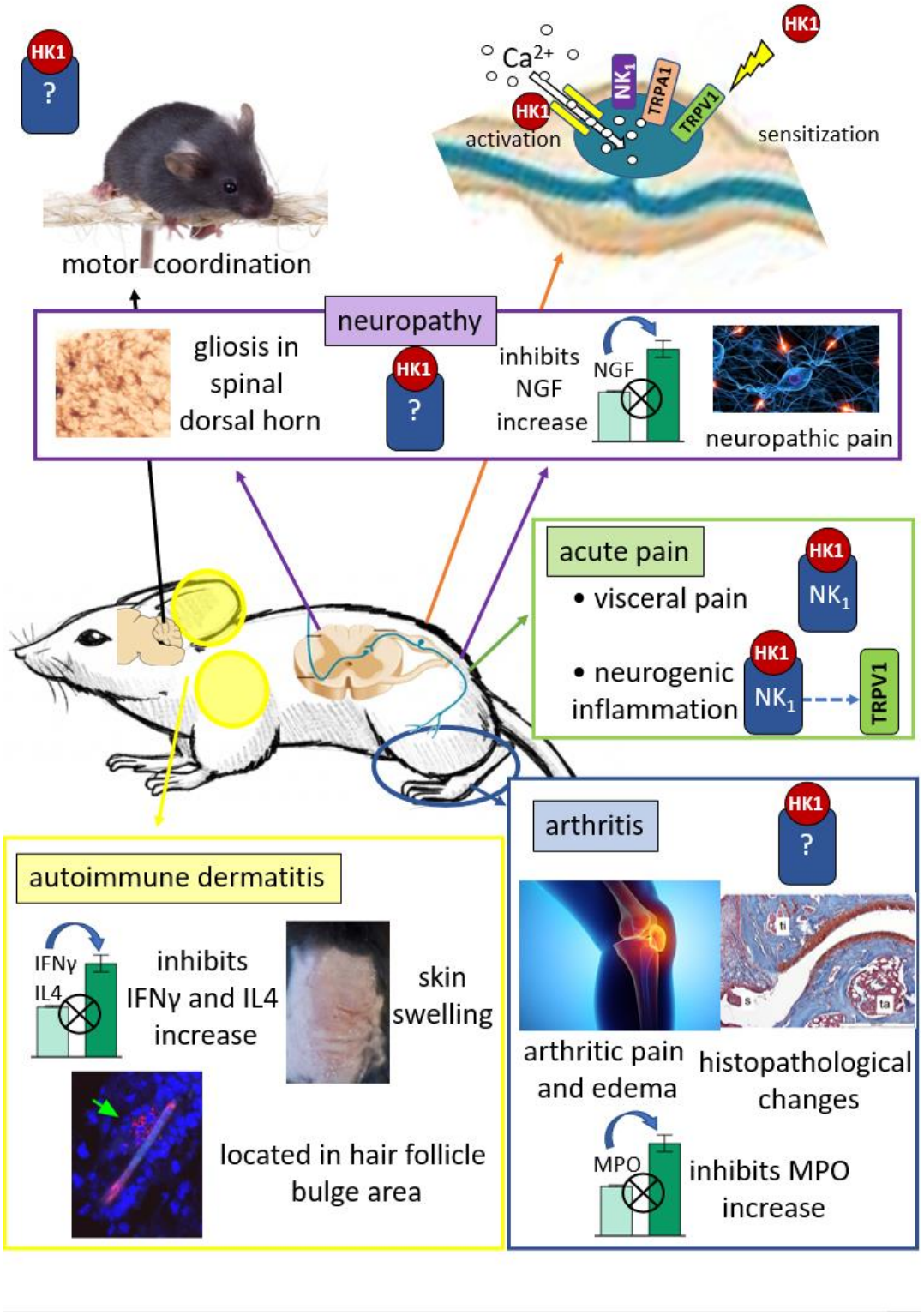

Figure 67. Summary of novel results

9 Literature

1. Murphy, K. R. *et al.* Prevalence of Specific Types of Pain Diagnoses in a Sample of United States Adults. *Pain Physician* **20**, E257–E268 (2017).

2. Domenichiello, A. F. & Ramsden, C. E. The silent epidemic of chronic pain in older adults. *Prog Neuropsychopharmacol Biol Psychiatry* **93**, 284–290 (2019).

3. Mansfield, K. E., Sim, J., Jordan, J. L. & Jordan, K. P. A systematic review and meta-analysis of the prevalence of chronic widespread pain in the general population. *Pain* **157**, 55–64 (2016).

4. Breivik, H., Collett, B., Ventafridda, V., Cohen, R. & Gallacher, D. Survey of chronic pain in Europe: prevalence, impact on daily life, and treatment. *Eur J Pain* **10**, 287–333 (2006).

5. Treede, R.-D. *et al.* Chronic pain as a symptom or a disease: the IASP Classification of Chronic Pain for the International Classification of Diseases (ICD-11). *Pain* **160**, 19–27 (2019).

6. Nalamachu, S. An overview of pain management: the clinical efficacy and value of treatment. *Am J Manag Care* **19**, s261-266 (2013).

7. Hylands-White, N., Duarte, R. V. & Raphael, J. H. An overview of treatment approaches for chronic pain management. *Rheumatol Int* **37**, 29–42 (2017).

8. Watson, J. C. & Sandroni, P. Central Neuropathic Pain Syndromes. *Mayo Clin Proc* **91**, 372–385 (2016).

9. Goebel, A. Immune activation and autoimmunity in chronic pain conditions and response to immunoglobulin G. *Clin Exp Immunol* **178**, 39–41 (2014).

10. Pinho-Ribeiro, F. A., Verri, W. A. & Chiu, I. M. Nociceptor Sensory Neuron-Immune Interactions in Pain and Inflammation. *Trends Immunol* **38**, 5–19 (2017).

11. Zengeler, K. E. & Lukens, J. R. Innate immunity at the crossroads of healthy brain maturation and neurodevelopmental disorders. *Nature Reviews Immunology* 1–15 (2021) doi:10.1038/s41577-020-00487-7.

12. Aspelund, A. *et al.* A dural lymphatic vascular system that drains brain interstitial fluid and macromolecules. *Journal of Experimental Medicine* **212**, 991–999 (2015).

13. Louveau, A. *et al.* Structural and functional features of central nervous system lymphatic vessels. *Nature* **523**, 337–341 (2015).

14. Al-Chalabi, M., Reddy, V. & Gupta, S. Neuroanatomy, Spinothalamic Tract. in *StatPearls* (StatPearls Publishing, 2021).

15. Martyn, J. A. J., Mao, J. & Bittner, E. A. Opioid Tolerance in Critical Illness. *N Engl J Med* **380**, 365–378 (2019).

16. Ossipov, M. H., Morimura, K. & Porreca, F. Descending pain modulation and chronification of pain. *Curr Opin Support Palliat Care* **8**, 143–151 (2014).

17. Szolcsányi, J. Capsaicin and sensory neurones: a historical perspective. *Prog Drug Res* **68**, 1–37 (2014).

18. Jancsó, N., Jancsó-Gábor, A. & Szolcsányi, J. Direct evidence for neurogenic inflammation and its prevention by denervation and by pretreatment with capsaicin. *Br J Pharmacol Chemother* **31**, 138–151 (1967).

19. Szolcsányi, J., Helyes, Z., Oroszi, G., Németh, J. & Pintér, E. Release of somatostatin and its role in the mediation of the anti-inflammatory effect induced by antidromic stimulation of sensory fibres of rat sciatic nerve. *Br J Pharmacol* **123**, 936–942 (1998).

20. Gangadharan, V. & Kuner, R. Pain hypersensitivity mechanisms at a glance. *Dis Model Mech* **6**, 889–895 (2013).

21. Hsieh, M.-T., Donaldson, L. F. & Lumb, B. M. Differential contributions of A- and C-nociceptors to primary and secondary inflammatory hypersensitivity in the rat. *Pain* **156**, 1074–1083 (2015).

22. Dubner, R. & Ren, K. Endogenous mechanisms of sensory modulation. *Pain* **Suppl 6**, S45–S53 (1999).

23. Porreca, F., Ossipov, M. H. & Gebhart, G. F. Chronic pain and medullary descending facilitation. *Trends Neurosci* **25**, 319–325 (2002).

24. D'Mello, R. & Dickenson, A. H. Spinal cord mechanisms of pain. *British Journal of Anaesthesia* **101**, 8–16 (2008).

25. Hill, R. NK1 (substance P) receptor antagonists--why are they not analgesic in humans? *Trends Pharmacol Sci* **21**, 244–246 (2000).

26. Werge, T. The tachykinin tale: molecular recognition in a historical perspective. *J Mol Recognit* **20**, 145–153 (2007).

27. Joos, G. F., Pauwels, R. A. & van der Straeten, M. E. The mechanism of tachykinin-induced bronchoconstriction in the rat. *Am Rev Respir Dis* **137**, 1038–1044 (1988).

28. Linnik, M. D. & Moskowitz, M. A. Identification of immunoreactive substance P in human and other mammalian endothelial cells. *Peptides* **10**, 957–962 (1989).

29. Mashaghi, A. *et al.* Neuropeptide Substance P and the Immune Response. *Cell Mol Life Sci* **73**, 4249–4264 (2016).

30. Page, N. M., Woods, R. J. & Lowry, P. J. A regulatory role for neurokinin B in placental physiology and pre-eclampsia. *Regul Pept* **98**, 97–104 (2001).

31. Zhang, Y., Lu, L., Furlonger, C., Wu, G. E. & Paige, C. J. Hemokinin is a hematopoietic-specific tachykinin that regulates B lymphopoiesis. *Nat Immunol* **1**, 392–397 (2000).

32. Feickert, M. & Burckhardt, B. B. Validated mass spectrometric assay for the quantification of substance P and human hemokinin-1 in plasma samples: A design of experiments concept for comprehensive method development. *J Pharm Biomed Anal* **191**, 113542 (2020).

33. Page, N. M. *et al.* Characterization of the endokinins: human tachykinins with cardiovascular activity. *Proc Natl Acad Sci U S A* **100**, 6245–6250 (2003).

34. Bellucci, F. *et al.* Pharmacological profile of the novel mammalian tachykinin, hemokinin 1. *Br J Pharmacol* **135**, 266–274 (2002).

35. Differences in the length of the carboxyl terminus mediate functional properties of neurokinin-1 receptor - PubMed. https://pubmed.ncbi.nlm.nih.gov/18713853/.

36. Fong, T. M., Anderson, S. A., Yu, H., Huang, R. R. & Strader, C. D. Differential activation of intracellular effector by two isoforms of human neurokinin-1 receptor. *Mol Pharmacol* **41**, 24–30 (1992).

37. Tansky, M. F., Pothoulakis, C. & Leeman, S. E. Functional consequences of alteration of N-linked glycosylation sites on the neurokinin 1 receptor. *Proc Natl Acad Sci U S A* **104**, 10691–10696 (2007).

38. Garcia-Recio, S. & Gascón, P. Biological and Pharmacological Aspects of the NK1-Receptor. *Biomed Res Int* **2015**, 495704 (2015).

39. Ganjiwale, A. & Cowsik, S. M. Membrane-induced structure of novel human tachykinin hemokinin-1 (hHK1). *Biopolymers* **103**, 702–710 (2015).

40. Mou, L. *et al.* The N-terminal domain of human hemokinin-1 influences functional selectivity property for tachykinin receptor neurokinin-1. *Biochem Pharmacol* **81**, 661–668 (2011).

41. Page, N. M. New challenges in the study of the mammalian tachykinins. *Peptides* **26**, 1356–1368 (2005).

42. Helyes, Z. *et al.* Involvement of preprotachykinin A gene-encoded peptides and the neurokinin 1 receptor in endotoxin-induced murine airway inflammation. *Neuropeptides* **44**, 399–406 (2010).

43. Lembo, P. M. C. *et al.* Proenkephalin A gene products activate a new family of sensory neuron--specific GPCRs. *Nat Neurosci* **5**, 201–209 (2002).

44. Dong, X., Han, S., Zylka, M. J., Simon, M. I. & Anderson, D. J. A diverse family of GPCRs expressed in specific subsets of nociceptive sensory neurons. *Cell* **106**, 619–632 (2001).

45. Solinski, H. J., Gudermann, T. & Breit, A. Pharmacology and signaling of MAS-related G protein-coupled receptors. *Pharmacol Rev* **66**, 570–597 (2014).

46. Azimi, E. *et al.* Dual action of neurokinin-1 antagonists on Mas-related GPCRs. *JCI Insight* **1**,.

47. Tiwari, V. *et al.* Mas-Related G Protein-Coupled Receptors Offer Potential New Targets for Pain Therapy. *Adv Exp Med Biol* **904**, 87–103 (2016).

48. Manorak, W. *et al.* Upregulation of Mas-related G Protein coupled receptor X2 in asthmatic lung mast cells and its activation by the novel neuropeptide hemokinin-1. *Respir Res* **19**, 1 (2018).

49. Duffy, R. A. *et al.* Centrally administered hemokinin-1 (HK-1), a neurokinin NK1 receptor agonist, produces substance P-like behavioral effects in mice and gerbils. *Neuropharmacology* **45**, 242–250 (2003).

50. Klassert, T. E. *et al.* Differential expression of neurokinin B and hemokinin-1 in human immune cells. *J Neuroimmunol* **196**, 27–34 (2008).

51. Nelson, D. A. & Bost, K. L. Non-neuronal mammalian tachykinin expression. *Front Biosci* **9**, 2166–2176 (2004).

52. Tran, A. H., Berger, A., Wu, G. E. & Paige, C. J. Regulatory mechanisms in the differential expression of Hemokinin-1. *Neuropeptides* **43**, 1–12 (2009).

53. Milne, C. D., Fleming, H. E., Zhang, Y. & Paige, C. J. Mechanisms of selection mediated by interleukin-7, the preBCR, and hemokinin-1 during B-cell development. *Immunol Rev* **197**, 75–88 (2004).

54. Wang, W. *et al.* Hemokinin-1 activates the MAPK pathway and enhances B cell proliferation and antibody production. *J Immunol* **184**, 3590–3597 (2010).

55. Morelli, A. E. *et al.* Neurokinin-1 Receptor Signaling Is Required for Efficient Ca2+ Flux in T-Cell-Receptor-Activated T Cells. *Cell Rep* **30**, 3448-3465.e8 (2020).

56. Cunin, P. *et al.* The tachykinins substance P and hemokinin-1 favor the generation of human memory Th17 cells by inducing IL-1β, IL-23, and TNF-like 1A expression by monocytes. *J Immunol* **186**, 4175–4182 (2011).

57. Fu, C.-Y. *et al.* Effects and mechanisms of supraspinal administration of rat/mouse hemokinin-1, a mammalian tachykinin peptide, on nociception in mice. *Brain Res* **1056**, 51–58 (2005).

58. Watanabe, C., Mizoguchi, H., Bagetta, G. & Sakurada, S. Involvement of spinal glutamate in nociceptive behavior induced by intrathecal administration of hemokinin-1 in mice. *Neurosci Lett* **617**, 236–239 (2016).

59. Watanabe, C., Mizoguchi, H., Yonezawa, A. & Sakurada, S. Characterization of intrathecally administered hemokinin-1-induced nociceptive behaviors in mice. *Peptides* **31**, 1613–1616 (2010).

60. Naono-Nakayama, R., Sunakawa, N., Ikeda, T. & Nishimori, T. Differential effects of substance P or hemokinin-1 on transient receptor potential channels, TRPV1, TRPA1 and TRPM8, in the rat. *Neuropeptides* **44**, 57–61 (2010).

61. Tsilioni, I., Russell, I. J., Stewart, J. M., Gleason, R. M. & Theoharides, T. C. Neuropeptides CRH, SP, HK-1, and Inflammatory Cytokines IL-6 and TNF Are Increased in Serum of Patients with Fibromyalgia Syndrome, Implicating Mast Cells. *J Pharmacol Exp Ther* **356**, 664–672 (2016).

62. Chinn, S., Caldwell, W. & Gritsenko, K. Fibromyalgia Pathogenesis and Treatment Options Update. *Curr Pain Headache Rep* **20**, 25 (2016).

63. Deliconstantinos, G., Barton, S., Soloviev, M. & Page, N. Mouse Hemokinin-1 Decapeptide Subjected to a Brain-specific Post-translational Modification. *In Vivo* **31**, 991–998 (2017).

64. Palma, C. Tachykinins and their receptors in human malignancies. *Curr Drug Targets* **7**, 1043–1052 (2006).

65. Lonergan, A., Theoharides, T., Tsilioni, E. & Rebeiz, E. Substance P and Hemokinin 1 in Nasal Lavage Fluid of Patients with Chronic Sinusitis and Nasal Polyposis. *OTO Open* **3**, 2473974X19875076 (2019).

66. González-Santana, A. *et al.* Altered expression of the tachykinins substance P/neurokinin A/hemokinin-1 and their preferred neurokinin 1/neurokinin 2 receptors in uterine leiomyomata. *Fertil Steril* **106**, 1521–1529 (2016).

67. Mou, L. *et al.* Neurokinin-1 receptor directly mediates glioma cell migration by up-regulation of matrix metalloproteinase-2 (MMP-2) and membrane type 1-matrix metalloproteinase (MT1-MMP). *J Biol Chem* **288**, 306–318 (2013).

68. Zhang, Y. *et al.* Human hemokinin-1 promotes migration of melanoma cells and increases MMP-2 and MT1-MMP expression by activating tumor cell NK1 receptors. *Peptides* **83**, 8–15 (2016).

69. Borbély, É. & Helyes, Z. Role of hemokinin-1 in health and disease. *Neuropeptides* **64**, 9–17 (2017).

70. Sparks, J. A. Rheumatoid Arthritis. *Ann Intern Med* **170**, ITC1–ITC16 (2019).

71. McWilliams, D. F. & Walsh, D. A. Pain mechanisms in rheumatoid arthritis. *Clin Exp Rheumatol* **35 Suppl 107**, 94–101 (2017).

72. Day, A. L. & Curtis, J. R. Opioid use in rheumatoid arthritis: trends, efficacy, safety, and best practices. *Curr Opin Rheumatol* **31**, 264–270 (2019).

73. Chancay, M. G., Guendsechadze, S. N. & Blanco, I. Types of pain and their psychosocial impact in women with rheumatoid arthritis. *Women's Midlife Health* **5**, 3 (2019).

74. Donaldson, L. F., McQueen, D. S. & Seckl, J. R. Neuropeptide gene expression and capsaicin-sensitive primary afferents: maintenance and spread of adjuvant arthritis in the rat. *J Physiol* **486 (Pt 2)**, 473–482 (1995).

75. Sun, W.-H. & Dai, S.-P. Tackling Pain Associated with Rheumatoid Arthritis: Proton-Sensing Receptors. *Adv Exp Med Biol* **1099**, 49–64 (2018).

76. Sommer, C. & Kress, M. Recent findings on how proinflammatory cytokines cause pain: peripheral mechanisms in inflammatory and neuropathic hyperalgesia. *Neuroscience Letters* **361**, 184–187 (2004).

77. Ebbinghaus, M. *et al.* Contribution of Inflammation and Bone Destruction to Pain in Arthritis: A Study in Murine Glucose-6-Phosphate Isomerase-Induced Arthritis. *Arthritis Rheumatol* **71**, 2016–2026 (2019).

78. Cao, Y., Fan, D. & Yin, Y. Pain Mechanism in Rheumatoid Arthritis: From Cytokines to Central Sensitization. *Mediators Inflamm* **2020**, 2076328 (2020).

79. Krock, E., Jurczak, A. & Svensson, C. I. Pain pathogenesis in rheumatoid arthritis-what have we learned from animal models? *Pain* **159 Suppl 1**, S98–S109 (2018).

80. Dineen, J. & Freeman, R. Autonomic Neuropathy. *Semin Neurol* **35**, 458–468 (2015).

81. Hammi, C. & Yeung, B. *Neuropathy*. *StatPearls [Internet]* (StatPearls Publishing, 2020).

82. Marcello, L. *et al.* Remodelling of supraspinal neuroglial network in neuropathic pain is featured by a reactive gliosis of the nociceptive amygdala. *Eur J Pain* **17**, 799–810 (2013).

83. Watson, J. C. & Dyck, P. J. B. Peripheral Neuropathy: A Practical Approach to Diagnosis and Symptom Management. *Mayo Clin Proc* **90**, 940–951 (2015).

84. Attal, N. *et al.* EFNS guidelines on the pharmacological treatment of neuropathic pain: 2010 revision. *Eur J Neurol* **17**, 1113-e88 (2010).

85. Calvo, M., Dawes, J. M. & Bennett, D. L. The role of the immune system in the generation of neuropathic pain. *The Lancet Neurology* **11**, 629–642 (2012).

86. Dhingra, N., Gulati, N. & Guttman-Yassky, E. Mechanisms of contact sensitization offer insights into the role of barrier defects vs. intrinsic immune abnormalities as drivers of atopic dermatitis. *J Invest Dermatol* **133**, 2311–2314 (2013).

87. Dearman, R. J., Basketter, D. A. & Kimber, I. Characterization of Chemical Allergens as a Function of Divergent Cytokine Secretion Profiles Induced in Mice. *Toxicology and Applied Pharmacology* **138**, 308–316 (1996).

88. Liu, B. *et al.* TRPA1 controls inflammation and pruritogen responses in allergic contact dermatitis. *FASEB J* **27**, 3549–3563 (2013).

89. Bánvölgyi, A. *et al.* Evidence for a novel protective role of the vanilloid TRPV1 receptor in a cutaneous contact allergic dermatitis model. *J Neuroimmunol* **169**, 86–96 (2005).

90. Boehncke, W.-H. & Schön, M. P. Psoriasis. *The Lancet* **386**, 983–994 (2015).

91. Conrad, C. & Gilliet, M. Psoriasis: from Pathogenesis to Targeted Therapies. *Clinic Rev Allerg Immunol* **54**, 102–113 (2018).

92. Riol-Blanco, L. *et al.* Nociceptive sensory neurons drive interleukin-23-mediated psoriasiform skin inflammation. *Nature* **510**, 157–161 (2014).

93. Zhu, T. H. *et al.* The Role of the Nervous System in the Pathophysiology of Psoriasis: A Review of Cases of Psoriasis Remission or Improvement Following Denervation Injury. *Am J Clin Dermatol* **17**, 257–263 (2016).

94. Amatya, B., El-Nour, H., Holst, M., Theodorsson, E. & Nordlind, K. Expression of tachykinins and their receptors in plaque psoriasis with pruritus. *Br J Dermatol* **164**, 1023–1029 (2011).

95. Zimmer, A. *et al.* Hypoalgesia in mice with a targeted deletion of the tachykinin 1 gene. *Proc Natl Acad Sci U S A* **95**, 2630–2635 (1998).

96. De Felipe, C. *et al.* Altered nociception, analgesia and aggression in mice lacking the receptor for substance P. *Nature* **392**, 394–397 (1998).

97. Berger, A. *et al.* Targeted deletion of the tachykinin 4 gene (TAC4-/-) influences the early stages of B lymphocyte development. *Blood* **116**, 3792–3801 (2010).

98. Kouskoff, V. *et al.* Organ-specific disease provoked by systemic autoimmunity. *Cell* **87**, 811–822 (1996).

99. Korganow, A.-S. *et al.* From Systemic T Cell Self-Reactivity to Organ-Specific Autoimmune Disease via Immunoglobulins. *Immunity* **10**, 451–461 (1999).

100. Christensen, A. D., Haase, C., Cook, A. D. & Hamilton, J. A. K/BxN Serum-Transfer Arthritis as a Model for Human Inflammatory Arthritis. *Front Immunol* **7**, (2016).

101. Tjølsen, A., Berge, O.-G., Hunskaar, S., Rosland, J. H. & Hole, K. The formalin test: an evaluation of the method. *Pain* **51**, 5–17 (1992).

102. Bölcskei, K. *et al.* Investigation of the role of TRPV1 receptors in acute and chronic nociceptive processes using gene-deficient mice. *Pain* **117**, 368–376 (2005).

103. Sándor, K. *et al.* Impaired nocifensive behaviours and mechanical hyperalgesia, but enhanced thermal allodynia in pituitary adenylate cyclase-activating polypeptide deficient mice. *Neuropeptides* **44**, 363–371 (2010).

104. Sándor, K., Helyes, Z., Gyires, K., Szolcsányi, J. & László, J. Static magnetic field-induced anti-nociceptive effect and the involvement of capsaicin-sensitive sensory nerves in this mechanism. *Life Sci* **81**, 97–102 (2007).

105. Meyer, R. A. & Campbell, J. N. Myelinated nociceptive afferents account for the hyperalgesia that follows a burn to the hand. *Science* **213**, 1527–1529 (1981).

106. Seltzer, Z., Dubner, R. & Shir, Y. A novel behavioral model of neuropathic pain disorders produced in rats by partial sciatic nerve injury. *Pain* **43**, 205–218 (1990).

107. Effect of lipid raft disruption on TRPV1 receptor activation of trigeminal sensory neurons and transfected cell line - PubMed. https://pubmed.ncbi.nlm.nih.gov/19958765/.

108. Horváth, S., Kemény, Á., Pintér, E. & Gyulai, R. A Localized Aldara (5% Imiquimod)-Induced Psoriasiform Dermatitis Model in Mice Using Finn Chambers. *Curr Protoc Pharmacol* **90**, e78 (2020).

109. Helyes, Z. *et al.* Antiinflammatory and analgesic effects of somatostatin released from capsaicin-sensitive sensory nerve terminals in a Freund's adjuvant-induced chronic arthritis model in the rat. *Arthritis Rheum* **50**, 1677–1685 (2004).

110. Tékus, V. *et al.* A CRPS-IgG-transfer-trauma model reproducing inflammatory and positive sensory signs associated with complex regional pain syndrome. *Pain* **155**, 299–308 (2014).

111. Horváth, Á. *et al.* Transient receptor potential ankyrin 1 (TRPA1) receptor is involved in chronic arthritis: in vivo study using TRPA1-deficient mice. *Arthritis Res Ther* **18**, 6 (2016).

112. Jakus, Z., Simon, E., Balázs, B. & Mócsai, A. Genetic deficiency of Syk protects mice from autoantibody-induced arthritis. *Arthritis Rheum* **62**, 1899–1910 (2010).

113. Botz, B. *et al.* Role of Pituitary Adenylate-Cyclase Activating Polypeptide and Tac1 gene derived tachykinins in sensory, motor and vascular functions under normal and neuropathic conditions. *Peptides* **43**, 105–112 (2013).

114. Schwab, W., Bilgiçyildirim, A. & Funk, R. H. W. Microtopography of the autonomic nerves in the rat knee: A fluorescence microscopic study. *The Anatomical Record* **247**, 109–118 (1997).

115. Gaszner, B. *et al.* The behavioral phenotype of pituitary adenylate-cyclase activating polypeptide-deficient mice in anxiety and depression tests is accompanied by blunted c-Fos expression in the bed nucleus of the stria terminalis, central projecting Edinger-Westphal nucleus, ventral lateral septum, and dorsal raphe nucleus. *Neuroscience* **202**, 283–299 (2012).

116. The Mouse Brain in Stereotaxic Coordinates, Compact - 3rd Edition. https://www.elsevier.com/books/the-mouse-brain-in-stereotaxic-coordinates-compact/franklin/978-0-12-374244-5.

117. Aczél, T. *et al.* Hemokinin-1 Gene Expression Is Upregulated in Trigeminal Ganglia in an Inflammatory Orofacial Pain Model: Potential Role in Peripheral Sensitization. *Int J Mol Sci* **21**, (2020).

118. Kecskés, A. *et al.* Characterization of Neurons Expressing the Novel Analgesic Drug Target Somatostatin Receptor 4 in Mouse and Human Brains. *Int J Mol Sci* **21**, (2020).

119. Pfaffl, M. W. A new mathematical model for relative quantification in real-time RT-PCR. *Nucleic Acids Res* **29**, e45 (2001).

120. Malcangio, M. Translational value of preclinical models for rheumatoid arthritis pain. *PAIN* **161**, 1399–1400 (2020).

121. Borbély, E. *et al.* Role of tachykinin 1 and 4 gene-derived neuropeptides and the neurokinin 1 receptor in adjuvant-induced chronic arthritis of the mouse. *PLoS One* **8**, e61684 (2013).

122. Arnhold, J. & Flemmig, J. Human myeloperoxidase in innate and acquired immunity. *Arch Biochem Biophys* **500**, 92–106 (2010).

123. Billiau, A. & Matthys, P. Modes of action of Freund's adjuvants in experimental models of autoimmune diseases. *J Leukoc Biol* **70**, 849–860 (2001).

124. Kobayashi, Y. & Okunishi, H. Mast cells as a target of rheumatoid arthritis treatment. *Jpn J Pharmacol* **90**, 7–11 (2002).

125. Borbély, É. *et al.* Role of capsaicin-sensitive nerves and tachykinins in mast cell tryptase-induced inflammation of murine knees. *Inflamm Res* **65**, 725–736 (2016).

126. Balla, Z., Szoke, E., Czéh, G. & Szolcsányi, J. Effect of capsaicin on voltage-gated currents of trigeminal neurones in cell culture and slice preparations. *Acta Physiol Hung* **88**, 173–196 (2001).

127. Morozova, E., Wu, M., Dumalska, I. & Alreja, M. Neurokinins robustly activate the majority of septohippocampal cholinergic neurons. *Eur J Neurosci* **27**, 114–122 (2008).

128. Pan, P., Huang, S. & Hu, C. Nerve growth factor induced expression of iNOS and substance P in dorsal root ganglion sensory neuron and interferon regulatory factor-1. *Zhong Nan Da Xue Xue Bao Yi Xue Ban* **36**, 386–391 (2011).

129. Sakai, A., Takasu, K., Sawada, M. & Suzuki, H. Hemokinin-1 gene expression is upregulated in microglia activated by lipopolysaccharide through NF-κB and p38 MAPK signaling pathways. *PLoS One* **7**, e32268 (2012).

130. Matsumura, T. *et al.* Increase in hemokinin-1 mRNA in the spinal cord during the early phase of a neuropathic pain state. *Br J Pharmacol* **155**, 767–774 (2008).

131. Okumura, M. *et al.* Quantitative analysis of NK1 receptor in the human brain using PET with 18F-FE-SPA-RQ. *J Nucl Med* **49**, 1749–1755 (2008).

132. Adamaszek, M. *et al.* Consensus Paper: Cerebellum and Emotion. *Cerebellum* **16**, 552–576 (2017).

133. Wagner, M. J., Kim, T. H., Savall, J., Schnitzer, M. J. & Luo, L. Cerebellar granule cells encode the expectation of reward. *Nature* **544**, 96–100 (2017).

134. McLean, S. Do substance P and the NK1 receptor have a role in depression and anxiety? *Curr Pharm Des* **11**, 1529–1547 (2005).

135. Schmidt-Weber, C. B. Anti-IL-4 as a new strategy in allergy. *Chem Immunol Allergy* **96**, 120–125 (2012).

136. Asada, H., Linton, J. & Katz, S. I. Cytokine Gene Expression during the Elicitation Phase of Contact Sensitivity: Regulation By Endogenous IL-4. *Journal of Investigative Dermatology* **108**, 406–411 (1997).

137. Pontén, F., Ren, Z., Nistér, M., Westermark, B. & Pontén, J. Epithelial-stromal interactions in basal cell cancer: the PDGF system. *J Invest Dermatol* **102**, 304–309 (1994).

138. Hoffman, R. M. & Amoh, Y. Hair Follicle-Associated Pluripotent(HAP) Stem Cells. *Prog Mol Biol Transl Sci* **160**, 23–28 (2018).

10 List of publications

10.1 Publications related to the thesis:

Ágnes Hunyady*, Zsófia Hajna*, Tímea Gubányi, Bálint Scheich, Ágnes Kemény, Balázs Gaszner, Éva Borbély, Zsuzsanna Helyes; Hemokinin-1 is an important mediator of pain in mouse models of neuropathic and inflammatory mechanisms. Brain Res Bull. 2019 Apr;147:165-173. PMID: 30664920 DOI: 10.1016/j.brainresbull.2019.01.015

Éva Borbély*, **Ágnes Hunyady***, Krisztina Pohóczky, Maja Payrits, Bálint Botz, Attila Mócsai, Alexandra Berger, Éva Szőke, Zsuzsanna Helyes; Hemokinin-1 as a Mediator of Arthritis-Related Pain via Direct Activation of Primary Sensory Neurons. Front Pharmacol. 2021 Jan 13;11:594479. PMID: 33519457 PMCID: PMC7839295 DOI: 10.3389/fphar.2020.594479

10.2 Publications not related to the thesis:

B Scheich, P Vincze, É Szőke, É Borbély, **Á Hunyady**, J Szolcsányi, Á Dénes, Zs Környei, B Gaszner, Zs Helyes; Chronic stress-induced mechanical hyperalgesia is controlled by capsaicin-sensitive neurones in the mouse. Eur J Pain. 2017 Sep;21(8):1417-1431. PMID: 28444833 DOI: 10.1002/ejp.1043

Éva Borbély, Maja Payrits, **Ágnes Hunyady**, Gréta Mező, Erika Pintér; Important regulatory function of transient receptor potential ankyrin 1 receptors in age-related learning and memory alterations of mice. Geroscience. 2019 Oct;41(5):643-654. PMID: 31327098 PMCID: PMC6885083 DOI: 10.1007/s11357-019-00083-1

Boglárka Kántás, Rita Börzsei, Éva Szőke, Péter Bánhegyi, Ádám Horváth, **Ágnes Hunyady**, Éva Borbély, Csaba Hetényi, Erika Pintér, Zsuzsanna Helyes; Novel Drug-Like Somatostatin Receptor 4 Agonists are Potential Analgesics for Neuropathic Pain. Int J Mol Sci. 2019 Dec 11;20(24):6245. PMID: 31835716 PMCID: PMC6940912 DOI: 10.3390/ijms20246245

Boglárka Kántás, Éva Szőke, Rita Börzsei, Péter Bánhegyi, Junaid Asghar, Lina Hudhud, Anita Steib, **Ágnes Hunyady**, Ádám Horváth, Angéla Kecskés, Éva Borbély, Csaba Hetényi, Gábor Pethő, Erika Pintér, Zsuzsanna Helyes; In Silico, In Vitro and In Vivo Pharmacodynamic Characterization of Novel Analgesic Drug Candidate Somatostatin SST 4 Receptor Agonists. Front Pharmacol. 2021 Jan 27;11:601887. PMID: 33815096 PMCID: PMC8015869 DOI: 10.3389/fphar.2020.601887

Cumulative impact factor of publications related to the thesis: 7.595

Impact factor of other publications: 11.772

Number of citations (MTMT): 36

Number of independent citations (MTMT): 21

Number of citations (Google Scholar): 41

11 List of conference presentations

11.1 International conferences

Hemokinin-1 mediates neuropathic pain in a mouse model of traumatic neuropathy: role in spinal glia activation and peripheral NGF production
AMSE Congress, Pécs, Hungary, 2018.10.4-6., poster
Agnes Hunyady, Eva Borbely, Balint Scheich, Agnes Kemeny, Balazs Gaszner, Zsuzsanna Helyes

Hemokinin-1 is an important mediator of arthritic and neuropathic pain in mouse models
11th FENS Forum of Neuroscience, Berlin, Germany 2018.07.7-11., poster
Agnes Hunyady, Eva Borbely, Balint Scheich, Agnes Kemeny, Balazs Gaszner, Zsuzsanna Helyes

Hemokinin-1 is an important mediator of arthritic and neuropathic pain in mouse models
14th International Medical Postgraduate Conference, Hradec Kralove, Czech Republic, 2017.11.23-24., oral presentation
Agnes Hunyady, Eva borbely, Zsuzsanna Helyes

The effect of somatostatin 4 receptor agonists in mouse models of neuropathic pain, anxiety and depression-like behavior
FENS Regional Meeting, Pécs, Hungary, 2017.09.20-23., poster
Agnes Hunyady, Eva Borbely, Boglarka Kantas, Erika Pinter, Janos Szolcsanyi, Éva Szőke, Zsuzsanna Helyes

11.2 Domestic (Hungarian) conferences

A hemokinin-1 gyulladáskeltő szerepe pszoriáziform bőrgyulladás és allergiás kontakt dermatitisz egérmodelljeiben
FAMÉ 2019 - Magyar Kísérletes és Klinikai Farmakológiai Társaság, Magyar Anatómus Társaság, Magyar Mikrocirkulációs és Vaszkuláris Biológiai Társaság, Magyar Élettani Társaság közös Vándorgyűlése Budapest, 2019.06.05-08., oral presentation, **Pharmacology section grand prize**
Hunyady Ágnes, Helyes Zsuzsanna, Kemény Ágnes, Horváth Szabina, Horváth Ádám

A hemokinin-1 szerepet játszik krónikus traumás neuropátia kialakulásában centrális és perifériás mechanizmusokkal
Idegtudomanyi Centrum PhD/TDK konferencia, Pécs, 2018.11.22-23., oral presentation,
3. place
Hunyady Ágnes, Borbély Éva, Helyes Zsuzsanna

Új típusú, szájon át adható szomatosztatin 4 receptor agonisták hatásának vizsgálata neuropátiás fájdalomra, szorongásra és depresszió-szerű viselkedésre egérmodellekben
Magyarországi Fájdalom Társaság kongresszusa, Szeged, 2018.11.9-10., poster
Hunyady Ágnes, Borbély Éva, Kántás Boglárka, Pintér Erika, Szolcsányi János, Helyes Zsuzsanna

Szomatosztatin 4 receptor agonisták vizsgálata neuropátiás fájdalom, szorongás és depresszió-szerű viselkedés egérmodelljeiben
Magyarországi Fájdalom Társaság konferenciája, Szeged, 2017.11.10-11., poster
Hunyady Ágnes, Borbély Éva, Kántás Boglárka, Pintér Erika, Szolcsányi János, Helyes Zsuzsanna

Szomatosztatin 4 receptor agonisták vizsgálata neuropátiás fájdalom, szorongás és depresszió-szerű viselkedés egérmodelljeiben
MÉT Konferenciája Debrecen 2017.06.13-16., poster
Hunyady Ágnes, Borbély Éva, Kántás Boglárka, Pintér Erika, Szolcsányi János, Helyes Zsuzsanna

12 Acknowledgements

I would like to thank my supervisors, Prof. Zsuzsanna Helyes and Dr Borbély Éva for their guidance throughout my PhD years and the student research years preceding it. I am most grateful to Prof. Erika Pintér, the head of the institute and leader of the Neuropharmacology doctoral program for the opportunity to conduct my research. I would also like to thank the members of the research group. Kata Bölcskei, Valéria Tékus for their guidance, Maja Payrits, Krisztina Pohóczky, Ádám István Horváth, Bálint Botz, Szabina Horváth, Angéla Kecskés, János Konkoly, Zsófia Hajna, Tímea Gubányi, Katinka Békefi and Nikolett Szentes for their contributions to the experimental work, Dóra Ömböli, Teréz Bagoly, Zsanett Szarka, Izabella Orbán and Anikó Perkecz for their professional technical assistance; as well as our collaborators Gaszner Balázs, Mócsai Attila for their contributions. I wish to thank all members of the Department of Pharmacology and Pharmacotherapy valuable help. Finally, I would like to thank my family and friends for the help and support they provided over the years.

Brain Research Bulletin 147 (2019) 165–173

Contents lists available at ScienceDirect

Brain Research Bulletin

journal homepage: www.elsevier.com/locate/brainresbull

Research report

Hemokinin-1 is an important mediator of pain in mouse models of neuropathic and inflammatory mechanisms

Ágnes Hunyady[a,b,1], Zsófia Hajna[a,b,1], Tímea Gubányi[a,b], Bálint Scheich[a,b], Ágnes Kemény[a,b,c], Balázs Gaszner[d], Éva Borbély[a,b,1], Zsuzsanna Helyes[a,b,*,1]

[a] Department of Pharmacology and Pharmacotherapy, Medical School, University of Pécs, Hungary
[b] János Szentágothai Research Centre, Centre for Neuroscience, University of Pécs, Hungary
[c] Department of Medical Biology, Medical School, University of Pécs, Hungary
[d] Department of Anatomy, Medical School, University of Pécs, Hungary

ARTICLE INFO

Keywords:
Tachykinins
Formalin test
Writhing test
Resiniferatoxin-induced hypersensitivity
Microglia
NK1 receptor
Partial sciatic nerve ligation
NGF

ABSTRACT

The Tac4 gene-derived hemokinin-1 (HK-1) is present in pain-related regions and activates the tachykinin NK1 receptor, but with binding site and signaling pathways different from Substance P (SP). NK1 receptor is involved in nociception, but our earlier data showed that it has no role in chronic neuropathic hyperalgesia, similarly to SP. Furthermore, NK1 antagonists failed in clinical trials as analgesics due to still unknown reasons. Therefore, we investigated the role of HK-1 in pain conditions of distinct mechanisms using genetically modified mice.

Chronic neuropathic mechanical and cold hyperalgesia after partial sciatic nerve ligation (PSL) were determined by dynamic plantar aesthesiometry and withdrawal latency from icy water, motor coordination on the accelerating Rotarod. Peripheral nerve growth factor (NGF) production was measured by ELISA, neuronal and glia cell activation by immunohistochemistry in pain-related regions. Acute somatic and visceral chemonocifensive behaviors were assessed after intraplantar formalin or intraperitoneal acetic-acid injection, respectively. Resiniferatoxin-induced inflammatory mechanical and thermal hyperalgesia by aesthesiometry and increasing temperature hot plate.

Chronic neuropathic mechanical and cold hypersensitivity were significantly decreased in HK-1 deficient mice. NGF level in the paw homogenates of intact mice were significantly lower in case of HK-1 deletion. However, it significantly increased under neuropathic condition in contrast to wildtype mice, where the higher basal concentration did not show any changes. Microglia, but not astrocyte activation was observed 14 days after PSL in the ipsilateral spinal dorsal horn of wildtype, but not HK-1-deficient mice. However, under neuropathic conditions, the number of GFAP-positive astrocytes was significantly smaller in case of HK-1 deletion. Acute visceral, but not somatic nocifensive behavior, as well as neurogenic inflammatory mechanical and thermal hypersensitivity were significantly reduced by HK-1 deficiency similarly to NK1, but not to SP deletion.

We provide evidence for pro-nociceptive role of HK-1, via NK1 receptor activation in acute inflammation models, but differently from SP-mediated actions. Identification of its targets and signaling can open new directions in pain research.

1. Introduction

Pain is one of the most common medical and socio-economical problems world-wide. It can originate from several sources e.g. trauma, inflammation, cancer, metabolic diseases. The most debilitating and therapeutically challenging form is neuropathic pain, which is a very typical symptom of diabetes, genetic diseases and nerve injury (Dineen and Freeman, 2015). In many cases the presently available pharmacotherapy is not satisfactory, there are several therapy-resistant patients and the adjuvant analgesics currently in use (tricyclic antidepressants,

Abbreviations: HK-1, hemokinin-1; EKA/B/C/D, endokinin A/B/C/D; SP, substance P; Tac1/2/3, preprotachykinin1/2/3 gene; NK1/2/3, tachykinin NK1/2/3 receptor; Tacr1, tachykinin NK1 receptor encoding gene; PSL, partial sciatic nerve ligation

* Corresponding author at: Department of Pharmacology and Pharmacotherapy, Medical School, University of Pécs, H-7624, Pécs, Szigeti u. 12, Hungary.
E-mail address: zsuzsanna.helyes@aok.pte.hu (Z. Helyes).

[1] Ágnes Hunyady and Zsófia Hajna made equal contributions to the present work and similarly, Éva Borbély and Zsuzsanna Helyes contributed equally to this paper.

https://doi.org/10.1016/j.brainresbull.2019.01.015
Received 23 November 2018; Received in revised form 11 January 2019; Accepted 14 January 2019
Available online 18 January 2019

antiepileptics) have common and severe side effects (Watson and Dyck, 2015). Therefore, neuropathic pain is still an unmet medical need; understanding the underlying mechanisms and finding new key molecules is essential in determining new therapeutic targets.

Tachykinins are one of the oldest and most investigated group of neuropeptides. There are several data available about their location and broad range of functions, the drug developmental potential of Substance P (SP) and its tachykinin NK1 receptor have been studied for decades. The discovery of the newest member of the tachykinin family, hemokinin-1 (HK-1) changed our knowledge about these neuropeptides (Zhang et al., 2000). There is no doubt that tachykinins and their receptors are present and play a pivotal regulatory role in many functions of the airways, GI and urinary tracts, as well as central and peripheral nervous systems (CNS, PNS; Steinhoff et al., 2014). Furthermore, not only the neurons, but also glia cells express the NK1 receptor with discrepancies between spinal cord and brain, as well as between rodents and humans (Marriott, 2004). Clinical data also suggest the importance of SP and NK1 in pain states: elevated SP level was measured in patients with trigeminal neuralgia (Qin et al., 2016) or fibromyalgia (Tsilioni et al., 2016). Although agents that block the effect of SP on the NK1 receptor were very promising analgesic drug candidates based on animal models, they failed in clinical trials (Hill, 2000). There are several theories about their ineffectiveness including species-specific NK1 pharmacology, problems with the clinical trials, broad spectrum of transmitters involved in pain (Herbert and Holzer, 2002), but the answer still remains unclear. Another explanation might be the presence and modulatory function of HK-1 that can bind to different regions of the NK1 receptor, induce different signaling pathways as compared to SP, and can also act at other targets. Comparison of SP and HK-1 to reevaluate the previous results is particularly important to provide a better overview about the function of the tachykinin family.

The Tac4 gene-derived HK-1 is different from the other members of the tachykinin family, its predominant expression on the periphery, and lower but characteristic distribution in the brain (Duffy et al., 2003) have proposed a unique function for this peptide. Besides the immune system, its role in the nociceptive pathway and pain states is the most intensively investigated issue. However, based on present knowledge it is not clear whether HK-1 is pro- or anti-nociceptive (Borbély and Helyes, 2017), and whether it acts via its preferred NK1 receptor.

Therefore, we aimed to investigate the role of HK-1 in the pathophysiology of neuropathic and inflammatory pain to unravel its function and mechanisms.

2. Materials and methods

2.1. Animals

Experiments were carried out on Tac1 ($Tac1^{-/-}$), Tac4 ($Tac4^{-/-}$) gene-deficient, NK1 receptor knockout ($Tacr1^{-/-}$) mice and C57Bl/6 wildtypes (WT) of both sexes (8–12 weeks, 20–30 g). The original breeding pairs of the $Tac1^{-/-}$ and $Tacr1^{-/-}$ mice were obtained from the University of Liverpool, UK (Zimmer et al., 1998; De Felipe et al., 1998), while those of the $Tac4^{-/-}$ mice were donated by Berger et al. (2010). Transgenic mice with deletion of Tac1, Tac4 or Tacr1 were generated on a C57Bl/6 background and backcrossed to homozygosity for > 5 generations prior to using C57Bl/6 mice as controls, purchased from Charles-River Ltd. (Hungary). Germline transmission of the mutated allele and excision of the selection cassette were verified by PCR analysis. Animals were bred and kept in conventional animal house of the Department of Pharmacology and Pharmacotherapy, University of Pécs at 24–25 °C, 12 h light/dark cycles. Animals were provided standard diet and water ad libitum. Mice were housed in groups of 5–10 in polycarbonate cages (330 cm^2 floor space, 12 cm height) on wood shaving bedding. Behavioral tests and perfusion were carried out in the laboratory of the Department in the morning. The animals had a 60-min period prior each experiment for acclimatization. The investigator was always blinded to the treatments and the genotypes of the mice.

2.2. Ethics

All experiments were carried out according to the European Communities Council Directive of 2010/63/EU and Consideration Decree of Scientific Procedures of Animal Experiments (243/1988). The studies were approved by the Ethics Committee on Animal Research of Pécs University according to the Ethical Codex of Animal Experiments (BA 02/2000-9/2011).

2.3. Investigation of neuropathic pain (partial sciatic nerve ligation, PSL)

Traumatic mononeuropathy was induced by the 1/3–1/2 ligation of the right sciatic nerve, or partial sciatic nerve ligation (Seltzer et al., 1990.) under ketamine (100 mg/kg, i.p) and xylazine (10 mg/kg, i.p.)-induced anesthesia. In sham-operated group sciatic nerve was located, but not ligated. Mechanonociceptive threshold was characterized by the force exerted by a straight metal filament – when the animal removed its hindpaw, and it was assessed with a dynamic plantar aesthesiometer (Ugo Basile 37000, Comerio, Italy). Measurements were performed 3, 5, 7, 10, 14, 19 days after operation, and mechanical hyperalgesia was expressed as percentage change of mechanonociceptive threshold in comparison to the initial, control value (Helyes et al., 2004). Cold tolerance was examined with the latency of paw-withdrawal from 0 °C water, and the change was compared to the pre-operative control measurements of each mice (Tékus et al., 2014). Motor coordination was examined with the accelerating Rotarod 7, 10 and 19 days after operation (Ugo Basile, Comerio, Italy; Botz et al., 2013) (Fig. 1).

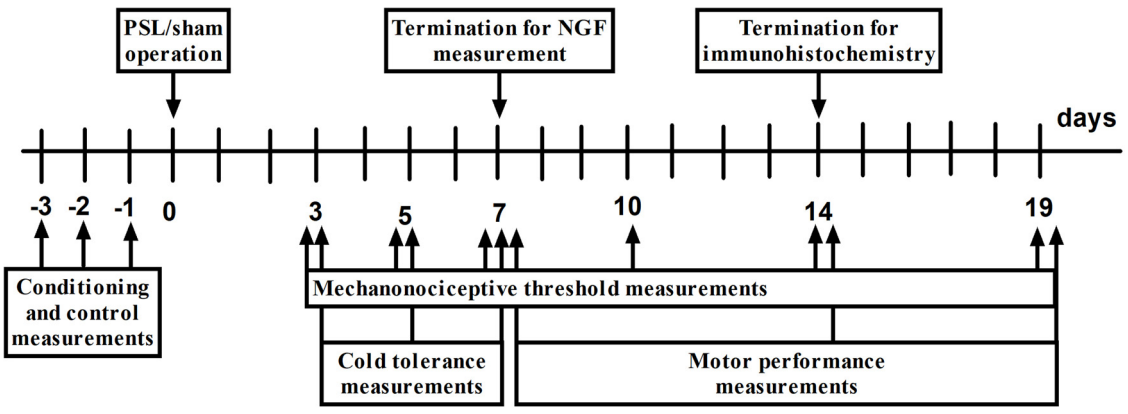

Fig. 1. Study design in the partial sciatic nerve-ligation (PSL)-induced neuropathy model.

2.4. Measurement of nerve growth factor (NGF) concentration in the paw

Nerve growth factor (NGF) is a member of a family of growth and survival factors known as neurotrophins. Enzyme-linked immunosorbent assay (ELISA) was applied in order to determine NGF expression at the level of protein using ChemiKine Nerve Growth Factor Sandwich ELISA Kit (Chemicon International, catalog nr: CYT304). Measurement was performed according to the manufacturer's instructions. Shortly, sheep polyclonal antibodies generated against mouse NGF were coated on a 96-well plate. Samples and standards were incubated overnight on the plate to let any NGF present in the sample bound to the immobilized antibodies. After removal of unbound biological components by washing, indirect labelling was performed using mouse anti-mouse NGF monoclonal primary antibody and peroxidase conjugated donkey anti-mouse IgG polyclonal antibodies. The formed immunocomplex was incubated with TMB/E Substrate. Enzyme reaction was stopped with HCl solution and color intensity was detected immediately using Labsystem Multiscan RC plate reader. Results were calculated after plotting of a standard curve and are given in pg/g tissue homogenate.

2.5. Examination of glial and neuronal activation with immunohistochemistry

The mice had their last pain threshold measurement on the 7th postoperative day, and returned to the animal house for 7 days of rest to allow the increase in FosB protein caused by handling to subside. On the 14th day after operation, the mice were perfused with 4% paraformaldehyde, and their spinal cord and brain were removed. Immunohistochemistry of the brains of C57Bl/6 and Tac4$^{-/-}$ animals was performed as it was previously described in detail (Gaszner et al., 2012). In brief, sections were cut for free-floating diaminobenzidine (Sigma-Aldrich Ltd, Missouri, USA) immunohistochemistry after marking the operated (right) side of the tissues with alcian blue stain (Merck, Darmstadt, Germany). Polyclonal rabbit antiserum against Iba1 (Wako Biochemicals, Osaka, Japan) and FosB (Santa Cruz Biotechnology Inc., Dallas, USA), monoclonal mouse antibody against GFAP protein (Leica Biosystems, Wetzlar, Germany). Goat anti-rabbit IgG were used for the detection of activated neurons and microglia, horse anti-mouse IgG for the detection of astrocytes. Photographs were taken with a digital camera (Spot RT; Nikon, Tokyo, Japan). Immunopositive cells were quantified in pain-related brain regions with microscope (Nikon Microphot FXA) and Inform software (Massachusetts, USA). The locations of the investigated areas were determined on the basis of the Paxinos and Franklin brain atlas (2003).

2.6. Examination of formalin-induced acute somatic nocifensive behavior

Acute somatic chemonociception was elicited by formalin (Formaldehydum solutum 37%; Ph.Hg. VII.; 50 µl, 2.5%) injected subcutaneously (s.c.) into the plantar surface of the right hindpaw. Nocifensive behavior – including the lifting, licking and shaking movement of the treated hindpaw - developed in two phases. The evolvement of the first phase (0–5 min, early phase) is thought to occur due to a direct activation of sensory nerve terminals, while the second one (20–45 min, late phase) develops mainly as a result of the release of acute inflammatory mediators (Tjølsen et al., 1992). Quantitative evaluation of the nocifensive reaction was performed in both examination periods: the duration of paw liftings and lickings was determined (Bölcskei et al., 2005; Sándor et al., 2010).

2.7. Investigation of acetic acid-evoked acute visceral nocifensive reaction (writhing test)

In order to investigate acute visceral chemonociception, intraperitoneal (i.p.) administration of acetic acid (0.2 ml per mouse, 0.6%) was carried out. As a result of chemical irritation of the peritoneum, abdominal contractions (writhing movements) occurred, regarded as typical sign of visceral nocifensive behavior. For quantitative assessment of this reaction, animals were placed in a transparent plastic box immediately after the injection and the amount of writhing movements was counted during the 0–5, 5–20 and 20–30 min time intervals (Sándor et al., 2007).

2.8. Investigation of resiniferatoxin (RTX)-induced acute thermal allodynia and mechanical hyperalgesia

Acute neurogenic inflammation of the right hindpaw was evoked by intraplantar injection of the ultrapotent Transient Receptor Potential Vanilloid 1 (TRPV1) receptor agonist resiniferatoxin (RTX; 20 µl, 0.03 µg/ml i.pl.). RTX evokes an acute neurogenic inflammatory reaction including the evolvement of a rapid thermal allodynia, and a subsequent mechanical hyperalgesia (Meyer and Campbell, 1981). Thermal allodynia was expressed as the drop of noxious heat threshold compared to the pre-injection control value. Noxious heat threshold was defined as the temperature where the animal first showed nocifensive behavior (lifting, licking or shaking of the hindpaw), and it was determined with an increasing temperature hot plate (IITC Life Science, Woodland Hills, CA, USA) prior to RTX-injection and 5, 10, 15 and 20 min following the treatment. Mechanical hyperalgesia was assessed by dynamic plantar aesthesiometry as described for the neuropathy model (see above) before the induction of inflammation and 2, 4, 6 and 24 h afterwards (Sándor et al., 2010).

2.9. Statistical analysis

Results are expressed as mean ± SEM of n = 4–16 mice per group in case of in vivo functional tests. Data obtained in these experiments were analysed with repeated measures two-way ANOVA followed by Bonferroni's posttest with GraphPad Prism 5 software (La Jolla, USA). The data of the immunohistological staining, due to the larger number of groups, was analysed with factorial ANOVA and Tukey's posttest with Statistica software (TIBCO Inc., Palo Alto, USA). In all cases $p < 0.05$ was accepted as statistically significant.

3. Results

3.1. Decreased neuropathic hyperalgesia and worse motor performance in HK-1 deficient mice

Compared to the pre-operation control values (9.29 ± 0.07 g in the WT and 9.10 ± 0.09 g in the gene-deleted group), significant mechanical hyperalgesia developed by day 5 after the sciatic nerve ligation in the WT group, reaching its maximum of −48.46 ± 4.01% on day 10, which was maintained until the end of the study. In the Tac4$^{-/-}$ group neuropathic mechanical hyperalgesia was significantly smaller throughout the whole experiment with the maximum of −29.03 ± 2.30% on day 10 (Fig. 2A).

The basal withdrawal latency from 0 °C water was 158.60 ± 4.09 and 147.41 ± 3.49 s in the WT and Tac4 gene-deleted groups, respectively. Withdrawal latency decreased earlier than the mechanonociceptive threshold, cold hyperalgesia developed on the 3rd postoperative day in the WT group, which was significantly smaller in the HK-1 deficient one until day 7, when the difference was not statistically significant any more (Fig. 2B).

The basal motor performance on the accelerating Rotarod was 56.64 ± 5.28 s in the WT and 38.13 ± 8.38 s in the HK-1-deficient group. This statistically not significant basal difference was also observed later, when repeating this measurement, and reached statistical significance on day 10. Despite the sensory changes, nerve ligation did not significantly alter the motor performance (Fig. 2C).

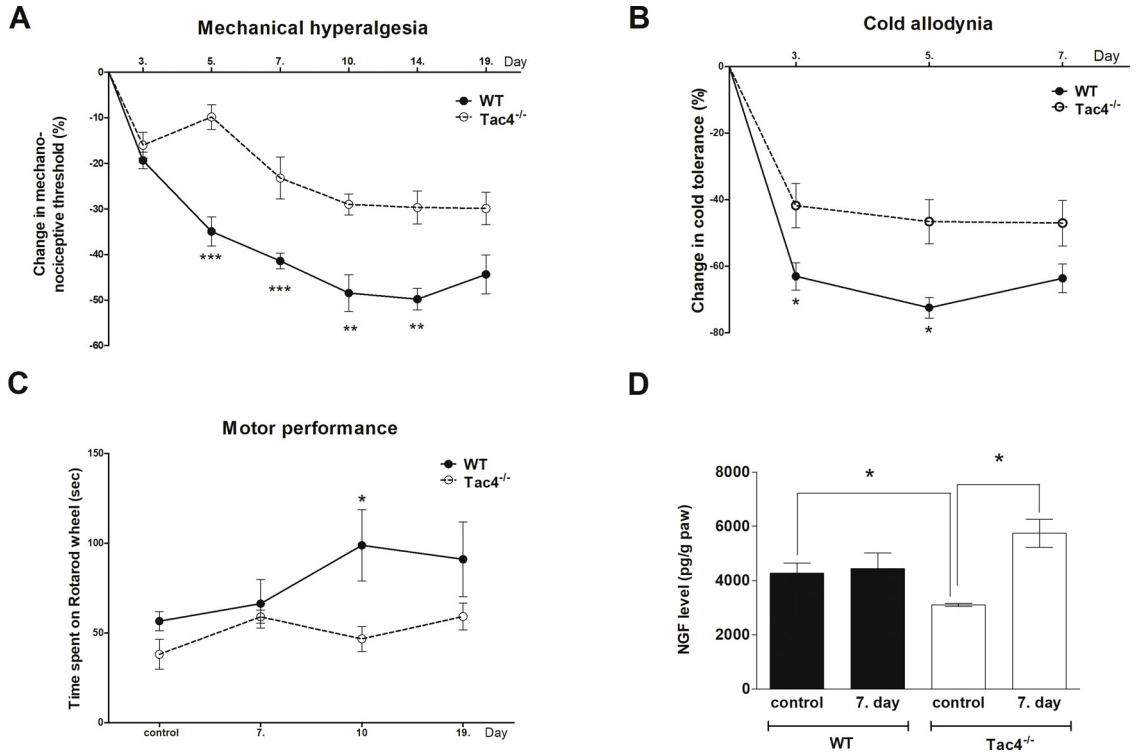

Fig. 2. Evaluation of neuropathic hyperalgesia and motor performance as well as peripheral NGF level in HK-1 deficient mice. PSL-induced mechanical hyperalgesia (A), cold allodynia (B) and motor performance (C). Paw NGF levels of control and PSL-operated mice (D). (n = 6–12 per group; *p < 0.05, **p < 0.01, ***p < 0.001 vs. WT, repeated measures two-way ANOVA + Bonferroni's post test, for NGF level measurement: two-way ANOVA + Bonferroni's post test).

3.2. Lower peripheral NGF concentration in HK-1-deficient mice increases after nerve injury

The NGF concentration of the paw homogenates was significantly lower in intact Tac4$^{-/-}$ mice compared to WTs. Under neuropathic condition, 7 days after PSL – when the postoperative pain component is not relevant anymore, and both mechanical and cold hyperalgesia are stable – NGF level was not altered in the WT group, but showed an almost 2-fold elevation in the HK-1-deficient one (Fig. 2D).

3.3. HK-1 mediates microglia activation in the spinal dorsal horn after PSL-induced neuropathy

In the spinal dorsal horn, the number of Iba1-immunopositive microglia did not differ under intact conditions in the WT and Tac4 gene-deficient groups (Figs. 3, E, 4 AA). In response to PSL microglia density significantly increased ipsilaterally in WT mice but not in the Tac4 gene-deleted mice (Figs. 3C, G, 4 A). There was no change on the contralateral side, resulting in significantly smaller cells numbers compared to the ipsilateral side in both groups (Figs. 3B, D, F, H, 4 B).

The number of GFAP-positive astrocytes were very similar in the spinal dorsal horn of both WT and HK-1-deficient mice under intact conditions. Despite the PSL-induced microgliosis described above, astrocyte numbers did not increase significantly in the WT group either ipsi- or contralaterally but interestingly even decreased in the Tac4$^{-/-}$ one on both sides (Fig. 4C, D).

The chronic neuronal activation marker FosB-immunopositivity did not show any changes in relation to genotype, PSL or side (Fig. 4E, F).

In pain-related brain regions, such as the PAG, amygdala and somatosensory cortex the number of Iba1-positive microglia was very similar in both groups, both under intact and neuropathic conditions. The GFAP-positive astrocyte counts were very low (below 40–50 cells/mm^2) in these regions, and therefore statistically significant changes were not detectable except for the lateral PAG, where significantly lower GFAP-immunopositivity was measured in intact HK-1-deficient mice. The FosB-immunopositivity was very stable and not affected by genetic modification or nerve injury either ipsi- or contralaterally (Suppl. Figs. 1–3).

In sham-operated mice significant changes of microglia, astrocyte or activated neuron counts were not observed compared to intact mice in any regions.

3.4. HK-1 mediates acute visceral nociception, inflammatory thermal allodynia and mechanical hyperalgesia

In WT mice, the total duration of formalin-induced paw lickings, liftings and shakings was 128.54 ± 16.80 s in the early phase referring to acute somatic chemonociception and 440.69 ± 35.74 s in the late phase evoked by neurogenic inflammatory mechanisms. There was no significant difference between Tac4 gene-deleted mice and WT mice in either phase (Fig. 5A).

The number of acetic acid-induced abdominal contractions were 0.75 ± 0.48, 19.25 ± 0.85 and 5.75 ± 0.63 in WT mice in the 0–5, 5–20 and 20–30 min time periods, respectively. However, in Tac4$^{-/-}$ mice writhing movements were significantly decreased in the second observational period, indicating a less intensive visceral nocifensive reaction (Fig. 5B).

The basal thermonociceptive thresholds of WT and Tac4$^{-/-}$ mice were 45.38 ± 0.86 °C and 46.03 ± 0.82 °C, respectively, showing no significant difference. Intraplantar RTX injection induced an 8.79 ± 1.48 °C decrease of the thermonociceptive threshold showing the development of an early thermal allodynia, which was maintained at a stable level throughout the 20-min investigation period. In contrast, in Tac4$^{-/-}$ mice this thermal allodynia was significantly attenuated compared to the WTs (Fig. 5C).

The basal mechanonociceptive thresholds of WT and Tac4$^{-/-}$ mice were 7.26 ± 0.16 g and 8.13 ± 0.17 g, respectively. There was a 34.05 ± 2.47% drop of the mechanonociceptive threshold

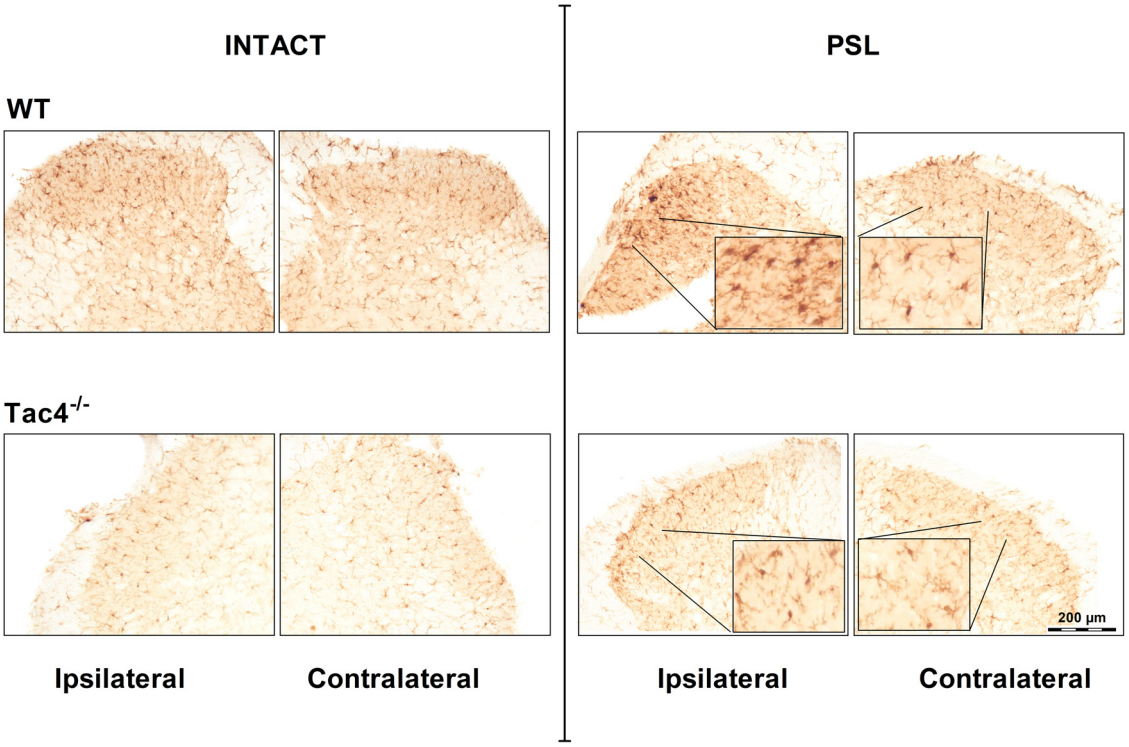

Fig. 3. Representative pictures of the Iba1-positive microglia in the I-III Rexed laminae of the spinal dorsal horn. Activated microglia cells of the spinal dorsal horn in intact (A, B) and PSL-operated (C, D) WT mice, as well as in intact (E, F) and PSL-operated (G, H) Tac4$^{-/-}$ animals. Scale bar = 200 µm; magnification: 10×; insert magnification: 20×.

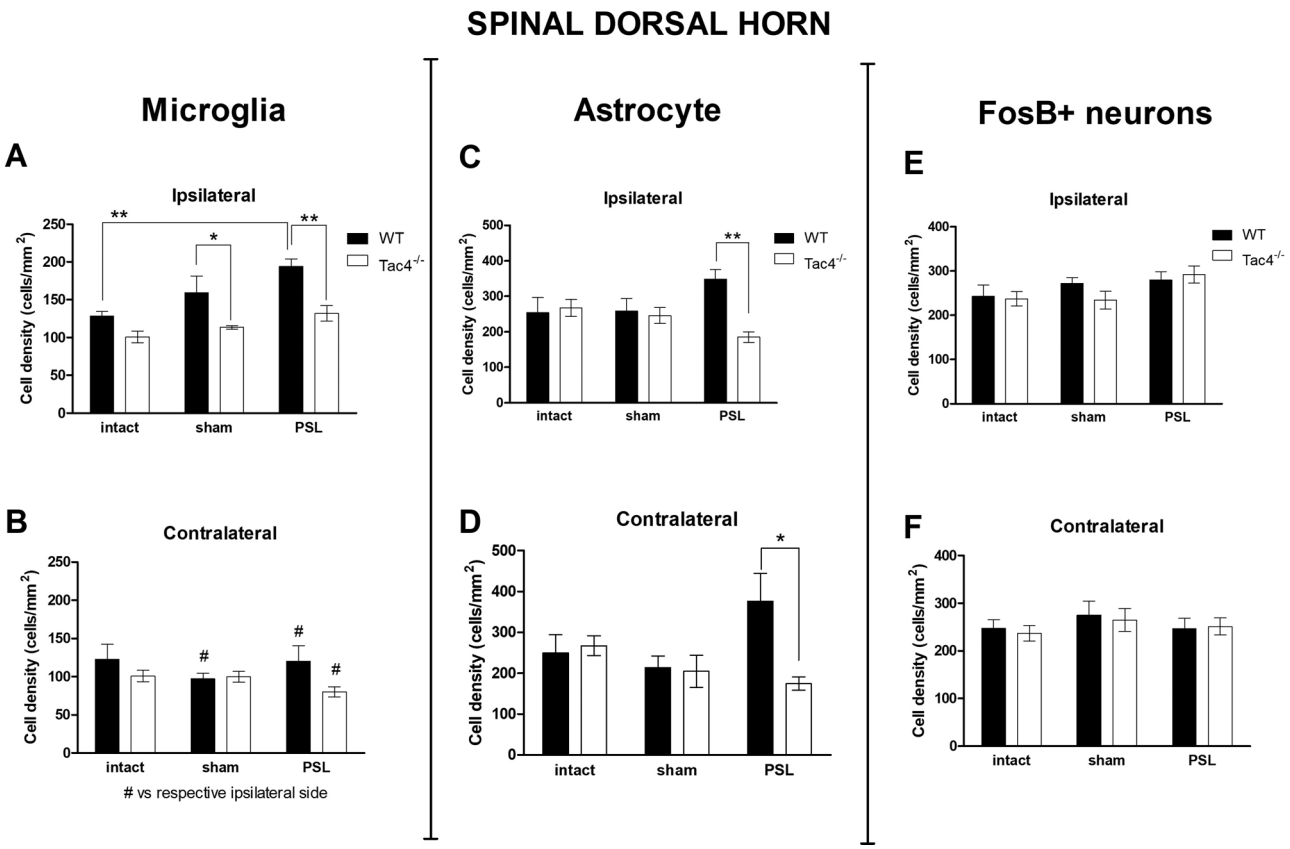

Fig. 4. Activation of the microglia, astrocytes and neurons in the I-III Rexed laminae of the spinal dorsal horn after PSL. Number of the Iba1-positive microglia in the ipsilateral (A) and contralateral (B) dorsal horn, GFAP-positive astrocytes in the ipsilateral (C) and contralateral (D) dorsal horn and FosB-positive neurons in the ipsilateral (E) and contralateral (F) dorsal horn of the spinal cord in intact, sham- and PSL-operated WT and HK-1 deficient mice. (n = 3–8 per group, *p < 0.05, **p < 0.01 vs. WT, #p < 0.05 vs. respective ipsilateral side, factorial ANOVA and Tukey's post test).

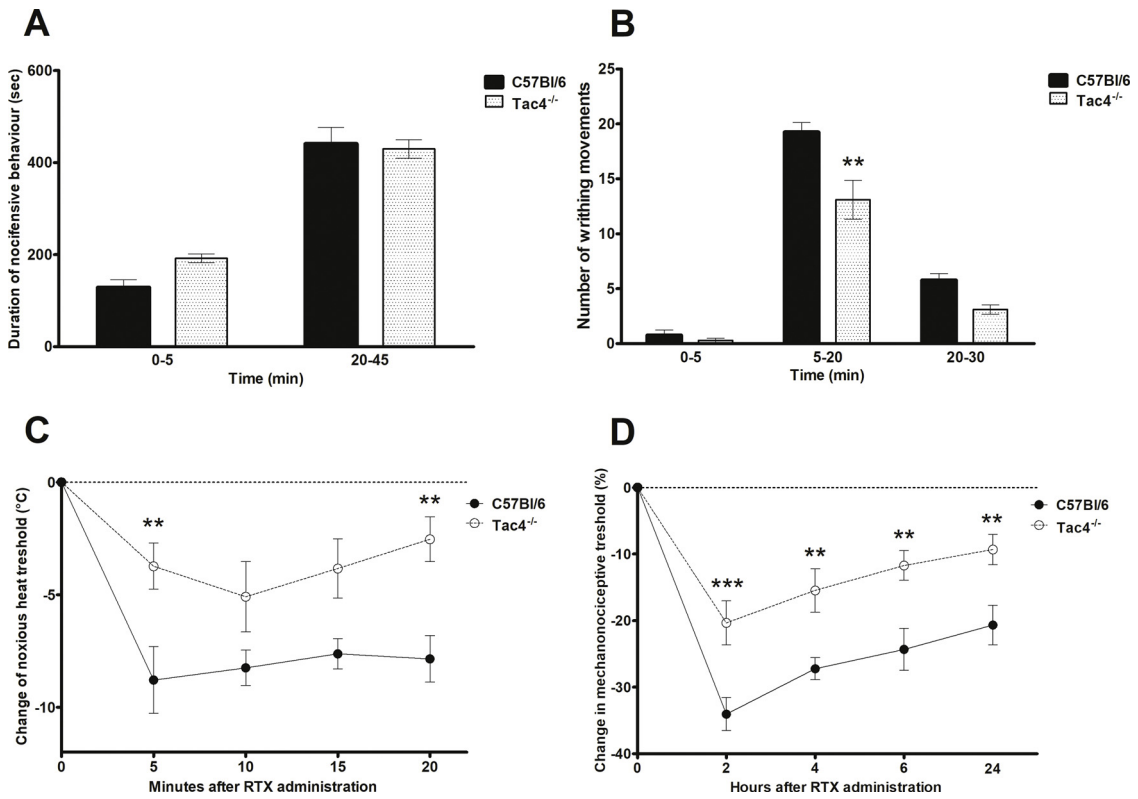

Fig. 5. Assessment of acute nocifensive behaviors as well as inflammatory thermal allodynia and mechanical hyperalgesia in mice lacking HK-1. (A) Formalin-induced nocifensive behavior did not alter in the Tac4 gene-deficient mice in comparison to the WT animals. (B) The number of acetic acid-evoked abdominal contractions (writhing movements) was significantly decreased in the Tac4$^{-/-}$ mice compared to the wildtypes. (C) RTX-induced thermal allodynia – demonstrated as a decrease of noxious heat threshold – was significantly reduced in the Tac4$^{-/-}$ animals in comparison to the WTs. (D) RTX-evoked mechanical hyperalgesia – calculated as a percentage drop of the mechanonociceptive threshold – was significantly attenuated in the Tac4$^{-/-}$ mice compared to the WT group (n = 4–16 per group, *p < 0.05, **p < 0.01, ***p < 0.001 vs. WT, repeated measures two-way ANOVA + Bonferroni's post test).

(mechanical hyperalgesia) in WT mice 2 h after RTX injection that decreased to -20.67 ± 2.97% by the 24 h time point. However, in Tac4$^{-/-}$ mice this later developing mechanical hyperalgesia was also significantly reduced in comparison to the WTs during the whole investigation period (Fig. 5D).

In order to investigate whether the effects of HK-1 are similar to SP and mediated by NK1 receptors, we also included Tac1$^{-/-}$ and Tacr1$^{-/-}$ mice in our studies. Formalin-induced somatic nocifensive behavior was significantly reduced in the late phase in Tac1$^{-/-}$ mice, but not in Tacr1$^{-/-}$ ones (Fig. 6A). Acetic acid-evoked writhing movements were significantly decreased both in the Tac1$^{-/-}$ and Tacr1$^{-/-}$ mice in the second and third phases (Fig. 6B). RTX-induced thermal hyperalgesia was abolished in the Tac1$^{-/-}$ mice but in the Tacr1$^{-/-}$ group significant decrease was only detected at the last, 20-min time point (Fig. 6C). However, mechanical hyperalgesia in this model was significantly attenuated in the Tacr1$^{-/-}$ mice, but not in the Tac1$^{-/-}$ group (Fig. 6D).

4. Discussion

With the help of gene-deleted mice we provided clear evidence that the Tac4 gene-encoded HK-1 is an important mediator of chronic neuropathic mechanical and cold hyperalgesia, microglia- and astrocyte activation in the spinal dorsal horn, and peripheral NGF-production. Furthermore, HK-1 is also involved in acute inflammatory thermal allodynia involving mainly peripheral mechanisms, as well as mechanical hyperalgesia including both central and peripheral sensitization. HK-1 participates in acute visceral chemonociception as well. We provided the first functional data for a role of HK-1 in motor coordination, which is supported by very high Tac4 mRNA expression in the cerebellum (Duffy et al., 2003).

Data about the role of HK-1 and related peptides in humans such as hHK-1, hHK-1(4–11) and endokinins in pain after their central administration are controversial. Intracerebroventricular injection of HK-1 induced pain responses like foot-tapping in gerbils and scratching in mice (Duffy et al., 2003), intrathecal administration caused scratching in rats (Endo et al., 2006). HK-1-induced pain reactions were suggested to be mediated by the interaction with the glutamate system in the spinal cord (Watanabe et al., 2016). Intrathecally administered endokinin A/B (EKA/B)-evoked scratching behavior and thermal hyperalgesia, while EKC/D did not (Yoshioka et al., 2006). In contrast, several data reported analgesic effects of HK-1, and suggested potential interactions with the opioid system (Fu et al., 2005, 2008; Yang and Dong, 2010). The virtually contradictory actions of hemokinins and endokinins in pain might be explained by its divergent actions in the CNS and in the periphery, as well as by the different doses applied. HK-1 was established to contribute to immune activation (Naono-Nakayama et al., 2010a; Sumpter et al., 2015, for review see Borbély and Helyes, 2017), which can be a factor in inflammatory pain. Microglia - the resident macrophages of the central nervous system - are known to increase HK-1 production when activated (Sakai et al., 2012), and HK-1-production could be decreased by blocking glia activation in neuropathic rats, as well as their pain-related behavior (Matsumura et al., 2008). There is no information regarding direct interactions of NGF and HK-1 in inflammation and pain, but it is known that NGF is an important factor of nociceptor development and the activation of peptidergic C-fibers releasing proinflammatory neuropeptides, including SP via its tyrosin kinase-linked receptors (Woolf and Ma, 2007). We describe the first results, that in the absence of HK-1, peripheral NGF level increases during neuropathic conditions, which might contribute to the

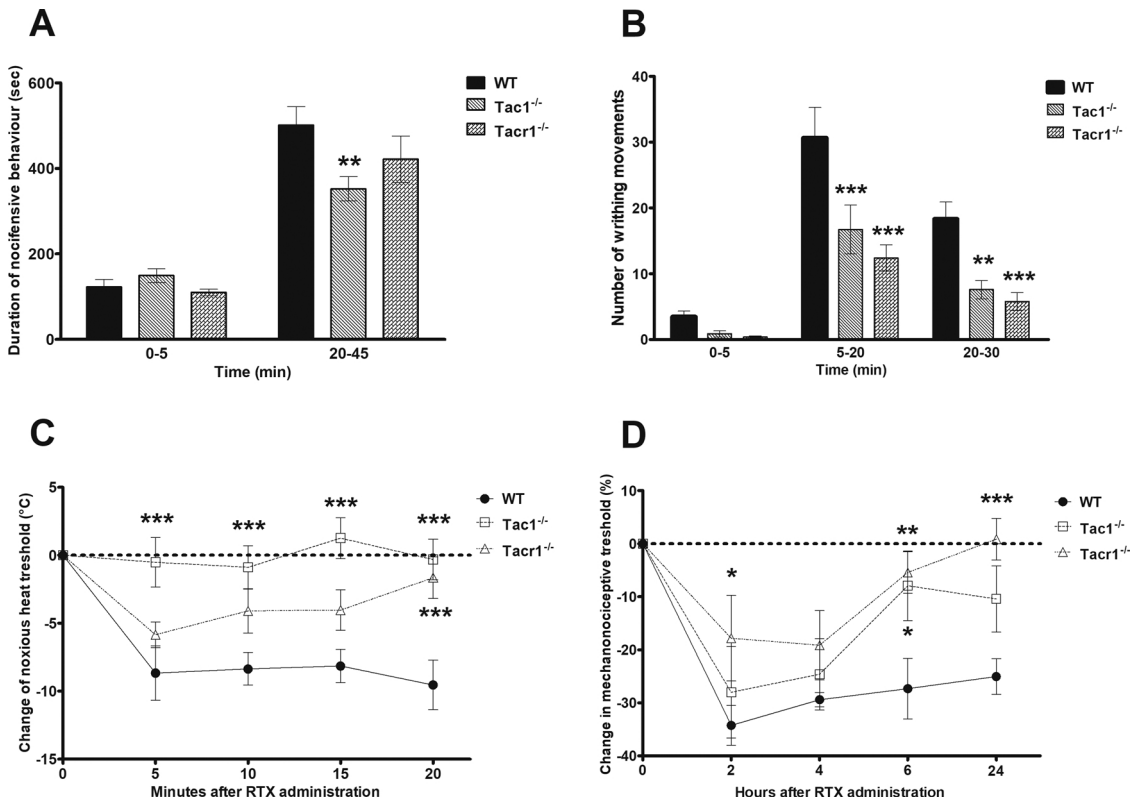

Fig. 6. Assessment of acute nocifensive behaviors as well as inflammatory thermal allodynia and mechanical hyperalgesia in mice lacking SP/NKA or the NK1 receptor. (A) Formalin-evoked paw liftings and lickings in the second phase were significantly attenuated in Tac1 gene-deleted mice compared to the wildtypes. (B) The amount of acetic acid-induced writhing movements was significantly decreased both in the Tac1$^{-/-}$ and in the Tacr1$^{-/-}$ mice in comparison to the WTs. (C) RTX-induced drop of the thermonociceptive threshold was completely abolished in Tac1$^{-/-}$ mice compared to the WT group, and tendentiously reduced in the Tacr1$^{-/-}$ mice. (D) RTX-elicited decrease of mechanonociceptive threshold was significantly attenuated in Tacr1$^{-/-}$ mice compared to the WT group (n = 6–9 per group, **p < 0.01, ***p < 0.001 vs. WT, repeated measures two-way ANOVA + Bonferroni's post test).

heeling of the damaged peripheral nerve fibres resulting in decreased hyperalgesia (Siniscalco et al., 2011).

Aside from NGF, other mediators are also released at the site of nerve injury, such as somatostatin, cytokines, and neurotransmitters like noradrenaline. The impairment of the noradrenergic transmission plays a role in neuropathic pain mechanisms: adrenergic α_2 agonists can be used as analgesics in post-ischemic allodynia (Yeo and Park, 2018), local anaesthetics – frequently given in neuropathic pain therapy – release noradrenaline from the sympathetic terminals of the spinal cord (Sircuta et al., 2016; Végh et al., 2017). The released noradrenaline may be responsible for pain killing effect by inhibiting the sensory nerves via α_2-adrenoceptor stimulation (Borbély et al., 2017b).

Concerning the target and mechanism of action, our present data in comparison with previously published results clearly demonstrate that in chronic neuropathic hyperalgesia HK-1 does not mediate its pronociceptive effect via the NK1 receptor (Botz et al., 2013) despite inflammatory hyperalgesia in the adjuvant-induced chronic arthritis model (Borbély et al., 2013). Several data suggest that some of the HK-1 effects are mediated by other targets, presumably its own receptor and/or through an NK1 receptor binding pocket different from SP (Endo et al., 2006; Watanabe et al., 2010; Borbély et al., 2013; Hajna et al., 2015; Borbély et al., 2017a). The complexity of HK action is also illustrated by the analgesic effects of hHK-1, but not its shorter fragment hHK-1(4–11) through NK1 receptor (Fu et al., 2008).

While we again showed that PSL does not cause impairment in the Rotarod test (Botz et al., 2013), we demonstrated that HK-1 deficient mice have worse motor performance. This can be explained by particularly high expression of Tac4 mRNA in the cerebellum (Duffy et al., 2003). This function is likely not mediated via the NK1 receptor, as similar results were found in mice lacking SP, but not NK1 receptor (Botz et al., 2013.).

The present results revealed that in contrast to chronic neuropathy SP and NKA, but not HK-1 and NK1 receptor mediate acute somatic nocifensive behaviors. SP/NKA might exert these actions by the NK2 receptor in this process. However, HK-1 is involved in the development of acute visceral chemonociception and inflammatory thermal hyperalgesia due to peripheral sensitization of the nociceptors similarly to SP/NKA, mainly via NK1 receptor activation.

However, under inflammatory conditions, where central sensitization in the spinal dorsal horn plays an important role besides peripheral mechanisms at the nerve terminals, NK1 receptor seems to be activated primarily by HK-1 and not by SP/NKA.

Interestingly, our investigations also revealed that in SP-deficient mice the acetic-acid-evoked nocifensive behavior was significantly less intensive, although previous reports only described a tendentious difference (Zimmer et al., 1998). The fact that we performed a longer and more detailed set of analysis is likely to explain these findings.

Our conclusion that HK-1 is differently involved in pain processing compared to SP/NKA is strongly supported by the literature. Although centrally administered HK-1 induced scratching response similarly to SP (Duffy et al., 2003; Endo et al., 2006), it did not influence the withdrawal latency to noxious thermal stimulation unlike SP (Endo et al., 2006). Moreover, HK-1 and SP differently modulated the nocifensive behavior in response to activation of several TRP channels (Naono-Nakayama et al., 2010b). Aside from these differences in the effects of HK-1 and SP, the release of proinflammatory/pronociceptive peptides from capsaicin-sensitive nerve terminals is modulated by several factors, i.e. activation of noradrenergic receptors. Dexmedetomidin, an α_2-adrenergic agonist, failed to change the baseline release of SP, but significantly decreased its capsaicin-evoked release (Takano

et al., 1993). The effect of α_2-adrenergic agonists can be blocked by α_2-receptor antagonists (Yamamoto and Nozaki-Taguchi, 1996). The expression pattern of HK-1 differs from that of SP: HK-1 is present in a much broader range of peripheral tissues, but at a lower level in the CNS compared to SP (Duffy et al., 2003). Furthermore, baseline Tac1 mRNA expression was higher than Tac4 in the dorsal spinal cord, but under neuropathic conditions only Tac4 expression increased significantly in rats (Matsumura et al., 2008). These can also provide an explanation for our findings that HK-1 differently contributes to neuropathic and inflammatory pain as compared to SP.

Our present study also revealed that HK-1 plays a predominant role in mechanical hyperalgesia not only under chronic traumatic neuropathic, but also under acute inflammatory conditions. These results are in accordance with our previous data in the adjuvant-induced arthritis model, where HK-1 was shown to mediate chronic inflammatory mechanical hyperalgesia (Borbély et al., 2013). Despite its considerably lower expression in the CNS compared to SP, HK-1 does contribute to the development of mechanical hyperalgesia involving both peripheral and central sensitization, while these tachykinins do not play a role in thermal hyperalgesia mediated by peripheral sensitization (Meyer et al., 2006). This is a very important result in the characterization of the neurobiology of HK-1.

5. Conclusion

HK-1 is an important mediator of chronic neuropathic pain via a non-NK1 receptor-mediated pathway. It activates microglia in the spinal dorsal horn and suppresses nerve damage-induced peripheral NGF production. Moreover, it also participates in acute inflammatory thermal allodynia and mechanical hyperalgesia, as well as acute visceral chemonociception, presumably through NK1 receptor activation. These findings help to better understand the pathophysiology of pain and might contribute to the development of novel analgesics.

Conflict of interest

None.

Acknowledgements

This study was sponsored by National Brain Research Program 2017-1.2.1-NKP-2017-00002, GINOP-2.3.2-15-2016-00050 (“PEPSYS: Complexity of peptidergic signalization and its role in systemic diseases”), EFOP-3.6.2-16-2017-00008 (“The role of neuro-inflammation in neurodegeneration: from molecules to clinics”), EFOP-3.6.1-16-2016-00004 and EFOP-3.6.3-VEKOP-16-2017-00009.

The authors are grateful to Alexandra Berger and John P. Quinn for providing the breeding pairs of the gene-deleted animals and to Dóra Ömböli and Izabella Orbán for their expert technical assistance.

Appendix A. Supplementary data

Supplementary material related to this article can be found, in the online version, at doi:https://doi.org/10.1016/j.brainresbull.2019.01.015.

References

Berger, A., Benveniste, P., Corfe, S.A., Tran, A.H., Barbara, M., Wakeham, A., Mak, T.W., Iscove, N.N., Paige, C.J., 2010. Targeted deletion of the tachykinin 4 gene (TAC4-/-) influences the early stages of B lymphocyte development. Blood 116, 3792–3801.

Bölcskei, K., Helyes, Z., Szabó, A., Sándor, K., Elekes, K., Németh, J., Almási, R., Pintér, E., Petho, G., Szolcsányi, J., 2005. Investigation of the role of TRPV1 receptors in acute and chronic nociceptive processes using gene-deficient mice. Pain 117, 368–376.

Borbély, É., Helyes, Z., 2017. Role of hemokinin-1 in health and disease. Neuropeptides 64, 9–17. https://doi.org/10.1016/j.npep.2016.12.003.

Borbély, E., Hajna, Z., Sándor, K., Kereskai, L., Tóth, I., Pintér, E., Nagy, P., Szolcsányi, J., Quinn, J., Zimmer, A., Stewart, J., Paige, C., Berger, A., Helyes, Z., 2013. Role of tachykinin 1 and 4 gene-derived neuropeptides and the neurokinin 1 receptor in adjuvant-induced chronic arthritis of the mouse. PLoS One 8, e61684. https://doi.org/10.1371/journal.pone.0061684.

Borbély, É., Hajna, Z., Nabi, L., Scheich, B., Tékus, V., László, K., Ollmann, T., Kormos, V., Gaszner, B., Karádi, Z., Lénárd, L., Paige, C.J., Quinn, J.P., Szolcsányi, J., Pintér, E., Keeble, J., Berger, A., Helyes, Z., 2017a. Hemokinin-1 mediates anxiolytic and antidepressant-like actions in mice. Brain Behav. Immun. 59, 219–232. https://doi.org/10.1016/j.bbi.2016.09.004.

Borbély, Z., Csomó, B.K., Kittel, Á., Gerber, G., Varga, G., Vizi, E.S., 2017b. Effect of rat spinal cord injury (hemisection) on the ex vivo uptake and release of [3H]noradrenaline from a slice preparation. Brain Res. Bull. 131, 150–155. https://doi.org/10.1016/j.brainresbull.2017.04.007.

Botz, B., Imreh, A., Sándor, K., Elekes, K., Szolcsányi, J., Reglődi, D., Quinn, J.P., Stewart, J., Zimmer, A., Hashimoto, H., Helyes, Z., 2013. Role of pituitary adenylate-cyclase activating polypeptide and Tac1 gene derived tachykinins in sensory, motor and vascular functions under normal and neuropathic conditions. Peptides 43, 105–112.

De Felipe, C., Herrero, J.F., O’Brien, J.A., Palmer, J.A., Doyle, C.A., Smith, A.J., Laird, J.M., Belmonte, C., Cervero, F., Hunt, S.P., 1998. Altered nociception, analgesia and aggression in mice lacking the receptor for substance P. Nature 392, 394–397.

Dineen, J., Freeman, R., 2015. Autonomic neuropathy. Semin. Neurol. 35, 458–468. https://doi.org/10.1055/s-0035-1558983.

Duffy, R.A., Hedrick, J.A., Randolph, G., Morgan, C.A., Cohen-Williams, M.E., Vassileva, G., Lachowicz, J.E., Laverty, M., Maguire, M., Shan, L.S., Gustafson, E., Varty, G.B., 2003. Centrally administered hemokinin-1 (HK-1), a neurokinin NK1 receptor agonist, produces substance P-like behavioral effects in mice and gerbils. Neuropharmacology 45 (August (2)), 242–250.

Endo, D., Ikeda, T., Ishida, Y., Yoshioka, D., Nishimori, T., 2006. Effect of intrathecal administration of hemokinin-1 on the withdrawal response to noxious thermal stimulation of the rat hind paw. Neurosci. Lett. 392, 114–117.

Fu, C.Y., Kong, Z.Q., Wang, K.R., Yang, Q., Zhai, K., Chen, Q., Wang, R., 2005. Effects and mechanisms of supraspinal administration of rat/mouse hemokinin-1, a mammalian tachykinin peptide, on nociception in mice. Brain Res. 1056, 51–58.

Fu, C.Y., Zhao, Y.L., Dong, L., Chen, Q., Ni, J.M., Wang, R., 2008. In vivo characterization of the effects of human hemokinin-1 and human hemokinin-1(4-11), mammalian tachykinin peptides, on the modulation of pain in mice. Brain Behav. Immun. 22, 850–860. https://doi.org/10.1016/j.bbi.2007.12.010.

Gaszner, B., Kormos, V., Kozicz, T., Hashimoto, H., Reglodi, D., Helyes, Z., 2012. The behavioral phenotype of pituitary adenylate-cyclase activating polypeptide-deficient mice in anxiety and depression tests is accompanied by blunted c-Fos expression in the bed nucleus of the stria terminalis, central projecting Edinger-Westphal nucleus, ventral lateral septum, and dorsal raphe nucleus. Neuroscience 202, 283–299. https://doi.org/10.1016/j.neuroscience.2011.11.046.

Hajna, Z., Borbély, É., Kemény, Á., Botz, B., Kereskai, L., Szolcsányi, J., Pintér, E., Paige, C.J., Berger, A., Helyes, Z., 2015. Hemokinin-1 is an important mediator of endotoxin-induced acute airway inflammation in the mouse. Peptides 64, 1–7. https://doi.org/10.1016/j.peptides.2014.12.002.

Helyes, Z., Szabó, A., Németh, J., Jakab, B., Pintér, E., Bánvölgyi, A., Kereskai, L., Kéri, G., Szolcsányi, J., 2004. Antiinflammatory and analgesic effects of somatostatin released from capsaicin-sensitive sensory nerve terminals in a Freund’s adjuvant-induced chronic arthritis model in the rat. Arthritis Rheum. 50, 1677–1685.

Herbert, M.K., Holzer, P., 2002. Why are substance P(NK1)-receptor antagonists ineffective in pain treatment? Anaesthesist 51, 308–319.

Hill, R., 2000. NK1 (substance P) receptor antagonists—why are they not analgesic in humans? Trends Pharmacol. Sci. 21, 244–246.

Marriott, I., 2004. The role of tachykinins in central nervous system inflammatory responses. Front. Biosci. 9, 2153–2165.

Matsumura, T., Sakai, A., Nagano, M., Sawada, M., Suzuki, H., Umino, M., Suzuki, H., 2008. Increase in hemokinin-1 mRNA in the spinal cord during the early phase of a neuropathic pain state. Br. J. Pharmacol. 155, 767–774. https://doi.org/10.1038/bjp.2008.301.

Meyer, R.A., Campbell, J.N., 1981. Myelinated nociceptive afferents account for the hyperalgesia that follows a burn to the hand. Science 213, 1527–1529.

Meyer, R.A., Ringkamp, M., Campbell, J.N., Raja, S.N., 2006. Peripheral mechanisms of cutaneous nociception. In: McMahon, S.B., Koltzenburg, M. (Eds.), Textbook of Pain. Elsevier, Amsterdam, pp. 3–33.

Naono-Nakayama, R., Sunakawa, N., Ikeda, T., Matsushima, O., Nishimori, T., 2010a. Subcutaneous injection of endokinin C/D attenuates carrageenan-induced inflammation. Peptides 31, 1767–1771. https://doi.org/10.1016/j.peptides.2010.05.019.

Naono-Nakayama, R., Sunakawa, N., Ikeda, T., Nishimori, T., 2010b. Differential effects of substance P or hemokinin-1 on transient receptor potential channels, TRPV1, TRPA1 and TRPM8, in the rat. Neuropeptides 44, 57–61. https://doi.org/10.1016/j.npep.2009.10.002.

Paxinos, G., Franklin, K., 2003. The Mouse Brain in Stereotaxic Coordinates, third ed. Elsevier Academic Press, San Diego.

Qin, Z.L., Yang, L.Q., Li, N., Yue, J.N., Wu, B.S., Tang, Y.Z., Guo, Y.N., Lai, G.H., Ni, J.X., 2016. Clinical study of cerebrospinal fluid neuropeptides in patients with primary trigeminal neuralgia. Clin. Neurol. Neurosurg. 143, 111–115. https://doi.org/10.1016/j.clineuro.2016.02.012.

Sakai, A., Takasu, K., Sawada, M., Suzuki, H., 2012. Hemokinin-1 gene expression is upregulated in microglia activated by lipopolysaccharide through NF-κB and p38 MAPK signaling pathways. PLoS One 7, e32268. https://doi.org/10.1371/journal.pone.0032268.

Sándor, K., Helyes, Z., Gyires, K., Szolcsányi, J., László, J., 2007. Static magnetic field-induced anti-nociceptive effect and the involvement of capsaicin-sensitive sensory nerves in this mechanism. Life Sci. 81, 97–102.

Sándor, K., Kormos, V., Botz, B., Imreh, A., Bölcskei, K., Gaszner, B., Markovics, A., Szolcsányi, J., Shintani, N., Hashimoto, H., Baba, A., Reglodi, D., Helyes, Z., 2010. Impaired nocifensive behaviours and mechanical hyperalgesia, but enhanced thermal allodynia in pituitary adenylate cyclase-activating polypeptide deficient mice. Neuropeptides 44, 363–371. https://doi.org/10.1016/j.npep.2010.06.004.

Seltzer, Z., Dubner, R., Shir, Y., 1990. A novel behavioral model of neuropathic pain disorders produced in rats by partial sciatic nerve injury. Pain 43, 205–218.

Siniscalco, D., Giordano, C., Rossi, F., Maione, S., de Novellis, V., 2011. Role of neurotrophins in neuropathic pain. Curr. Neuropharmacol. 9, 523–529. https://doi.org/10.2174/157015911798376208.

Sircuta, C., Lazar, A., Azamfirei, L., Baranyi, M., Vizi, E.S., Borbély, Z., 2016. Correlation between the increased release of catecholamines evoked by local anesthetics and their analgesic and adverse effects: role of K(+) channel inhibition. Brain Res. Bull. 124, 21–26. https://doi.org/10.1016/j.brainresbull.2016.03.009.

Steinhoff, M.S., von Mentzer, B., Geppetti, P., Pothoulakis, C., Bunnett, N.W., 2014. Tachykinins and their receptors: contributions to physiological control and the mechanisms of disease. Physiol. Rev. 94, 265–301. https://doi.org/10.1152/physrev.00031.2013.

Sumpter, T.L., Ho, C.H., Pleet, A.R., Tkacheva, O.A., Shufesky, W.J., Rojas-Canales, D.M., Morelli, A.E., Larregina, A.T., 2015. Autocrine hemokinin-1 functions as an endogenous adjuvant for IgE-mediated mast cell inflammatory responses. J. Allergy Clin. Immunol. 135https://doi.org/10.1016/j.jaci.2014.07.036. 1019–1030.e8.

Takano, M., Takano, Y., Yaksh, T.L., 1993. Release of calcitonin gene-related peptide (CGRP), substance P (SP), and vasoactive intestinal polypeptide (VIP) from rat spinal cord: modulation by alpha 2 agonists. Peptides 14, 371–378.

Tékus, V., Hajna, Z., Borbély, É., Markovics, A., Bagoly, T., Szolcsányi, J., Thompson, V., Kemény, Á., Helyes, Z., Goebel, A., 2014. A CRPS-IgG-transfer-trauma model reproducing inflammatory and positive sensory signs associated with complex regional pain syndrome. A CRPS-IgG-transfer-trauma model reproducing inflammatory and positive sensory signs associated with complex regional pain syndrome. Pain 155, 299–308.

Tjølsen, A., Berge, O.G., Hunskaar, S., Rosland, J.H., Hole, K., 1992. The formalin test: an evaluation of the method. Pain 51, 5–17.

Tsilioni, I., Russell, I.J., Stewart, J.M., Gleason, R.M., Theoharides, T.C., 2016. Neuropeptides CRH, SP, HK-1, and inflammatory cytokines IL-6 and TNF are increased in serum of patients with fibromyalgia syndrome, implicating mast cells. J. Pharmacol. Exp. Ther. 356, 664–672. https://doi.org/10.1124/jpet.115.230060.

Végh, D., Somogyi, A., Bányai, D., Lakatos, M., Balogh, M., Al-Khrasani, M., Fürst, S., Vizi, E.S., Hermann, P., 2017. Effects of articaine on [3H]noradrenaline release from cortical and spinal cord slices prepared from normal and streptozotocin-induced diabetic rats and compared to lidocaine. Brain Res. Bull. 135, 157–162. https://doi.org/10.1016/j.brainresbull.2017.10.011.

Watanabe, C., Mizoguchi, H., Yonezawa, A., Sakurada, S., 2010. Characterization of intrathecally administered hemokinin-1-induced nociceptive behaviors in mice. Peptides 31, 1613–1616. https://doi.org/10.1016/j.peptides.2010.04.025.

Watanabe, C., Mizoguchi, H., Bagetta, G., Sakurada, S., 2016. Involvement of spinal glutamate in nociceptive behavior induced by intrathecal administration of hemokinin-1 in mice. Neurosci. Lett. 617, 236–239. https://doi.org/10.1016/j.neulet.2016.02.027.

Watson, J.C., Dyck, P.J., 2015. Peripheral neuropathy: a practical approach to diagnosis and symptom management. Mayo Clin. Proc. 90, 940–951. https://doi.org/10.1016/j.mayocp.2015.05.004.

Woolf, C.J., Ma, Q., 2007. Nociceptors—noxious stimulus detectors. Neuron 55, 353–364.

Yamamoto, T., Nozaki-Taguchi, N., 1996. Clonidine, but not morphine, delays the development of thermal hyperesthesia induced by sciatic nerve constriction injury in the rat. Anesthesiology 85, 835–845.

Yang, Y., Dong, S., 2010. Effects of Endokinin A/B and Endokinin C/D on the modulation of pain in mice. Peptides 31, 94–100. https://doi.org/10.1016/j.peptides.2009.10.013.

Yeo, J., Park, S., 2018. Effect of dexmedetomidine on the development of mechanical allodynia and central sensitization in chronic post-ischemia pain rats. J. Pain Res. 11, 3025–3030. https://doi.org/10.2147/JPR.S184621.

Yoshioka, D., Takebuchi, F., Nishimori, T., Naono, R., Ikeda, T., Nakayama, T., 2006. Intrathecal administration of the common carboxyl-terminal decapeptide in endokinin A and endokinin B evokes scratching behavior and thermal hyperalgesia in the rat. Neurosci. Lett. 410, 193–197.

Zhang, Y., Lu, L., Furlonger, C., Wu, G.E., Paige, C.J., 2000. Hemokinin is a hematopoietic-specific tachykinin that regulates B lymphopoiesis. Nat. Immunol. 1, 392–397.

Zimmer, A., Zimmer, A.M., Baffi, J., Usdin, T., Reynolds, K., König, M., Palkovits, M., Mezey, E., 1998. Hypoalgesia in mice with a targeted deletion of the tachykinin 1 gene. Proc. Natl. Acad. Sci. U. S. A. 95, 2630–2635.

frontiers in Pharmacology

ORIGINAL RESEARCH
published: 13 January 2021
doi: 10.3389/fphar.2020.594479

Hemokinin-1 as a Mediator of *Arthritis*-Related Pain via Direct Activation of Primary Sensory Neurons

Éva Borbély[1,2†], Ágnes Hunyady[1,2†], Krisztina Pohóczky[1,2,3], Maja Payrits[1,2], Bálint Botz[1,4], Attila Mócsai[5], Alexandra Berger[6], Éva Szőke[1,2†] and Zsuzsanna Helyes[1,2,7†]*

[1]*János Szentágothai Research Centre and Centre for Neuroscience, University of Pécs, Pécs, Hungary,* [2]*Department of Pharmacology and Pharmacotherapy, Medical School, University of Pécs, Pécs, Hungary,* [3]*Department of Pharmacology, Faculty of Pharmacy, University of Pécs, Pécs, Hungary,* [4]*Department of Medical Imaging, Medical School, University of Pécs, Pécs, Hungary,* [5]*Department of Physiology, Semmelweis University, Budapest, Hungary,* [6]*Princess Margaret Cancer Centre, University Health Network, Toronto, ON, Canada,* [7]*PharmInVivo Ltd., Pécs, Hungary*

The tachykinin hemokinin-1 (HK-1) is involved in immune cell development and inflammation, but little is known about its function in pain. It acts through the NK1 tachykinin receptor, but several effects are mediated by a yet unidentified target. Therefore, we investigated the role and mechanism of action of HK-1 in arthritis models of distinct mechanisms with special emphasis on pain. Arthritis was induced by i.p. K/BxN serum (passive transfer of inflammatory cytokines, autoantibodies), intra-articular mast cell tryptase or Complete Freund's Adjuvant (CFA, active immunization) in wild type, HK-1- and NK1-deficient mice. Mechanical- and heat hyperalgesia determined by dynamic plantar esthesiometry and increasing temperature hot plate, respectively, swelling measured by plethysmometry or micrometry were significantly reduced in HK-1-deleted, but not NK1-deficient mice in all models. K/BxN serum-induced histopathological changes (day 14) were also decreased, but early myeloperoxidase activity detected by luminescent *in vivo* imaging increased in HK-1-deleted mice similarly to the CFA model. However, vasodilation and plasma protein extravasation determined by laser Speckle and fluorescent imaging, respectively, were not altered by HK-1 deficiency in any models. HK-1 induced Ca^{2+}-influx in primary sensory neurons, which was also seen in NK1-deficient cells and after pertussis toxin-pretreatment, but not in extracellular Ca^{2+}-free medium. These are the first results showing that HK-1 mediates arthritic pain and cellular, but not vascular inflammatory mechanisms, independently of NK1 activation. HK-1 activates primary sensory neurons presumably via Ca^{2+} channel-linked receptor. Identifying its target opens new directions to understand joint pain leading to novel therapeutic opportunities.

Keywords: experimental arthritis, arthritic pain, primary sensory neuron, neuroinflammation, tachykinin, *in vivo* optical imaging

OPEN ACCESS

Edited by:
Francesco De Logu,
University of Florence, Italy

Reviewed by:
Marco Sisignano,
Institut für Klinische Pharmakologie Universitätsklinikum Frankfurt, Germany
Raquel Tonello,
New York University, United States

****Correspondence:***
Agnes Hunyady
agnes.hunyady@gmail.com

†These authors have contributed equally to this work

Specialty section:
This article was submitted to Inflammation Pharmacology, a section of the journal Frontiers in Pharmacology

Received: *13 August 2020*
Accepted: *09 December 2020*
Published: *13 January 2021*

Citation:
Borbély É, Hunyady Á, Pohóczky K, Payrits M, Botz B, Mócsai A, Berger A, Szőke É and Helyes Z (2021) Hemokinin-1 as a Mediator of Arthritis-Related Pain via Direct Activation of Primary Sensory Neurons. Front. Pharmacol. 11:594479. doi: 10.3389/fphar.2020.594479

INTRODUCTION

Rheumatoid arthritis (RA) is the most common autoimmune disorder of the joints characterized by chronic inflammation and severe pain. Although the inflammation can be effectively controlled by nonsteroidal anti-inflammatory drugs (NSAIDs), steroids, disease-modifying antirheumatic drugs (DMARDs) and biologic agents (Sparks, 2019), pain is often resistant to these drugs

(McWilliams and Walsh, 2019). Persistent pain has resulted in an increased use of opioids among RA patients (Day and Curtis, 2019), though opioids are not effective in all cases (Chancay et al., 2019) suggesting more complex pain pathomechanisms in RA and making pain management an unmet medical need.

The joints are densely innervated by capsaicin-sensitive peptidergic sensory nerves (Donaldson et al., 1995) expressing, among others, the transient receptor potential vanilloid 1 (TRPV1) and ankyrin 1 (TRPA1) ion channels activated by a broad range of inflammatory mediators (Pinho-Ribeiro et al., 2017). These nerves play an important role in complex neuro-vascular-immune interactions resulting in chronic pain (Sun and Dai, 2018). Recently, intensive investigations have been initiated to reveal sensitization processes at molecular (Sommer and Kress, 2004) and histological levels alike (Ebbinghaus et al., 2019) that convert inflammatory to neuropathic pain and contribute to persistent arthritic pain. Exploration of its pathophysiological processes is hindered by the fact that no single animal model can mimic every aspect of RA, conclusions drawn using different models might not necessarily apply to the human disease (Krock et al., 2018). Studying the role of endogenous molecules of the sensory-vascular-immune interactions is essential to identify key mediators and potential novel drug targets.

Tachykinins are a family of neuropeptides that have been shown to play important roles in immune mechanisms, inflammatory vascular changes and pain (Onaga, 2014). Their best-known member, substance *p* (SP) acts mainly through the tachykinin neurokinin-1 receptor (NK1R), but can also bind to the other two tachykinin receptors, NK2R and NK3R, with much lower affinities. NK1R plays a key role in the wind-up mechanism in the spinal dorsal horn (Herrero et al., 2000), which is a crucial element in central sensitization leading to chronic pain. SP through NK1R also sensitizes the peripheral terminals of nociceptors (Nakamura-Craig and Smith, 1989). NK1R antagonists were developed as analgesic drug candidates, but despite promising preclinical results, they did not prove to be effective in human pain conditions. Therefore, tachykinins fell outside the focus of pain research until the discovery of hemokinin-1 (HK-1) in 2000 (Zhang et al., 2000) beginning a new era in this field. HK-1, encoded by the preprotachykinin-4 gene (*Tac4*), was first isolated from bone marrow B-cells (Zhang et al., 2000), and plays a role in T-lymphopoesis as well (Zhang and Paige, 2003). HK-1 consists of 11 amino acids, it has a close structural resemblance to SP, with seven matching aminoacids. HK-1 has the highest affinity to the NK1R similarly to SP (Morteau et al., 2001), but it has been proven that HK-1 can exert effects through other, so far unidentified target(s) (Borbély and Helyes, 2017). Our research group was the first to describe the mediator role of HK-1 in the chronic adjuvant-induced mouse model of inflammation and related nociception (Borbély et al., 2013). Recently, we proved that HK-1 is involved not only in inflammatory, but also nerve ligation-induced neuropathic pain, which develops independently of inflammation with prominent central sensitization mechanisms (Hunyady et al., 2019). The present work focused on investigating the involvement of HK-1 in arthritis models of distinct mechanisms with special emphasis on pain, nociceptive sensory neurons and the molecular mechanism of action.

MATERIALS AND METHODS

Animals and Ethics

Experiments were performed on inbred 12–18-week-old (25–30 g) male *Tac4* gene-deficient (*Tac4*$^{-/-}$) knockout (KO) and NK1 receptor-deleted (*Tacr1*$^{-/-}$) mice and their C57BL/6J wild type controls (WT) purchased from Charles-River Ltd. (Hungary). The original *Tacr1*$^{-/-}$ breeding pairs (De Felipe et al., 1998) were obtained from the University of Liverpool, United Kingdom, The *Tac4*$^{-/-}$ strain was donated by A. Berger (Berger et al., 2010). Both KO strains were generated on C57BL/6J background and backcrossed to homozygosity for over five generations. The mutated allele's germline transmission and excision of the selection cassette were verified by PCR analysis. The experimenters were blinded from the genotype and treatments in all cases. Animals were bred and kept in the conventional Laboratory Animal House of the Department of Pharmacology and Pharmacotherapy, University of Pécs at 24–25°C, 12 h light/dark cycles on wood shaving bedding in a standard polycarbonate cage with two to six mice per cage and provided with standard rodent diet and water ad libitum.

All experiments were carried out according to the European Communities Council Directive of 2010/63/EU, Consideration Decree of Scientific Procedures of Animal Experiments (243/1988) and Ethical Codex of Animal Experiments and to the NIH guidelines (Guide for the Care and Use of Laboratory Animals, NIH Publication 86–23). The project was approved by the Ethics Committee on Animal Research of the University of Pécs and license was provided (BA 02/2000–2/2012).

Serum Transfer Arthritis

K/BxN arthritogenic and BxN non-arthritogenic sera were harvested as described earlier (Jakus et al., 2010). Arthritis was induced by intraperitoneally (i.p.) injecting 150–150 μL of the arthritogenic serum on the 0 and 3 day of the experiment. The control groups received the same amount of non-arthritogenic serum. The mechanonociceptive threshold, heat threshold and cold tolerance were measured (methods described below). Paw edema was quantified using plethysmometry (Ugo Basile 7140), bodyweight was monitored after the first serum administration as a parameter of general well-being. Weight loss was given as the percentage of lost weight compared to pretreatment control values. Arthritis severity was scored using a semiquantitative visual scale where 0–0.5 was no change and 10 was maximal inflammation (Jakus et al., 2010). Swelling and redness of all four feet were considered for the score. To assess joint function mice were placed on a horizontal grid, the grid was turned upside-down and the latency to fall was measured. The grasping ability needed in this test correlates with the joint function. *In vivo* imaging was performed with IVIS Lumina II (PerkinElmer; 60 s acquisition, F/Stop = 1, Binning = 8) before treatment and 2 and 6 days after to quantify plasma extravasation and

myeloperoxidase (MPO) activity, as described below. We chose these time points to collect data from the acute phase on day 2 when the vascular inflammatory components are predominant, and from the chronic phase on day 6, when the cellular inflammatory mechanisms are more remarkable (Horváth et al., 2016). On the 14th day after serum administration tibiotarsal joints were removed for histological staining with Safranin stain. Fibroblast proliferation, leukocyte invasion and thickness of synovium were evaluated with 0–3 score depending on severity, the maximum possible score being 9.

Mast Cell Tryptase (MCT)-Induced Acute Knee Monoarthritis

MCT can be found in abundance in synovial fluid contributing to the inflammation in different types of arthritis (RA, osteoarthritis, spondyloarthritis) by activating the protease-activated receptor 2 (PAR2) on the sensory nerves and inflammatory cells. To investigate acute inflammatory synovial microcirculatory changes, 1 h after guanethidine (12 mg/kg i. p., Sigma) pretreatment, MCT (Merck Millipore) was applied topically to the synovial membrane of the knee joint (12 μg/ml, 20 μL), after removing the skin under ketamine- and xylazine-induced (100 mg/kg and 10 mg/kg i. p, respectively) anesthesia. Contralateral knee joint was treated with 0.9% saline. Blood flow was continuously monitored by laser Speckle imaging for 40 min after the treatment, and the differences compared to the baseline values of the respective area were calculated. To measure acute inflammatory hyperalgesia and edema, MCT was injected intra-articularly (20 μL, 12 μg/ml) into the right knee joint. The paw mechanonociceptive threshold and knee diameter were measured at 2, 4, and 6 h post-injection.

Complete Freund's Adjuvant (CFA)-Induced Subacute Knee Monoarthritis

CFA is heat-killed *Mycobacterium tuberculosis* suspended in paraffin oil (1 mg/ml; Sigma-Aldrich) which is taken up by macrophages, activate their reactive oxygen species, cytokine and enzyme generation within a few hours causing localized arthritis of the injected joint without severe systemic symptoms.

CFA (20 μL) was injected into the right mouse knee joint under ketamin-xylazine anesthesia as described above. Contralateral knee joint was treated with 20 μL 0.9% saline. Paw mechanonociceptive threshold and antero-posterior knee diameter were measured 2, 6, and 24 h after CFA administration, changes were expressed as percentage of change compared to the pre-injection values. MPO activity was measured 24 h after treatment.

Measurement of the Mechanonociceptive and Heat Thresholds

The mechanonociceptive threshold was measured with the dynamic plantar esthesiometer (DPE; Ugo Basile 37000) before (to determine baseline nociceptive threshold) and after treatment. The post-treatment values are shown as the percentage of threshold-decrease of the individual mouse compared to its baseline thresholds. Heat threshold was determined as the temperature where the animal showed nocifensive behavior (shaking, licking, lifting of the hind paw) on increasing temperature hot plate (IITC Life Sciences), the cut-off value was set at 53 °C. Cold hyperalgesia was given as the latency to paw-withdrawal from 0°C water.

In vivo Optical Imaging

Mice were anesthetized with ketamine-xylazine anesthesia for *in vivo* imaging with IVIS Lumina II (PerkinElmer; 120s acquisition, F/stop = 1, Binning = 8) instrument and Living Image® software (PerkinElmer). Luminol sodium salt (5-amino-2,3-dihydro-1,4-phthalazine-dione; 150 mg/kg) injection was given i. p. in sterile PBS solution for MPO imaging. MPO from neutrophil granulocytes produces reactive oxygen species which interact with luminol and result in luminescent signals which we measured 10 min after administration. Luminescence was expressed as total radiance (total photon flux/s) in identical Regions of Interests (ROIs) around the joints.

Inflammatory vascular leakage was evaluated by fluorescence imaging with the Fluorescent Molecular Tomography (FMT) 2000 system (PerkinElmer Ltd.) using the 680 nm laser of the equipment. A micellar formulation of the fluorescent IR-676 dye (Spectrum-Info) dissolved in a 5 w/v% aqueous solution of Kolliphor HS 15 (polyethylene-glycol-15-hydroxystearate; Sigma-Aldrich) was given i. v. in a 0.5 mg/kg dose under ketamine-xylazine anesthesia. The measurement was carried out 20 min afterward dye administration with fluorescence expressed as the calculated amount of fluorophore (pmol) (Botz et al., 2015) in identical Regions of Interests (ROIs) around the ankle joints.

Tissue Preparation and Protocol for qPCR

L3-L5 lumbar spinal cord and the respective dorsal root ganglia (DRG; total of six DRGs pooled per mouse) were obtained from WT mice 6 days after treatment when behavioral results showed the greatest difference between WT and *Tac4*$^{-/-}$ animals. Mice were divided into three groups: K/BxN treated arthritic (n = 8), BxN serum treated control (n = 5) and intact control (n = 7). Spinal cord samples of *Tac4*$^{-/-}$ mice served as negative (n = 3), while inguinal lymph nodes from WT mice served as positive controls (n = 2).

Tissue samples were harvested after cervical dislocation and placed immediately into 500 μL TRI reagent (Molecular Research Center, Inc.), snap-frozen on dry ice, then stored on -80°C until processing.

Tissue samples were thawed out on ice and homogenized in TRI reagent. After homegenization, total RNA was extracted using Direct-zol RNA MicroPrep (Zymo Research) according to the manufacturer's instructions (Aczél et al., 2020). The quantity of the extracted RNA was examined using Nanodrop ND-1000 Spectrophotometer V3.5 (Nano-Drop Technologies, Inc.). RNA samples were treated with dnase I in order to remove contamining genomic DNA, and 500 ng of RNA was reverse transcribed into cDNA using High Capacity cDNA

Reverse Transcription Kit (Thermo Fisher Scientific). SensiFAST™ Probe Lo-ROX Kit (Meridiane Bioscience, Memphis, United States) was used according to the manual in the QuantStudio five Real-Time PCR System (Thermo Fisher Scientific). Transcripts of the reference gene *glucuronidase beta* (*Gusb*, Kecskés et al., 2020) and the target gene *Tac4* were evaluated using FAM-conjugated specific probes (Mm01197698_m1, and Mm00474083_m1 respectively, Thermo Fisher Scientific). The gene expression was calculated using ΔΔCt method (Pfaffl, 2001).

Primary Cultures of Trigeminal Ganglion (TG) Neurons

TG cultures were prepared from neonatal NMRI mice. Ganglia were excised in ice-cold phosphate-buffered saline (PBS), incubated in PBS containing collagenase Type XI (1 mg/ml) and then in PBS with deoxyribonuclease I (1,000 units/ml) for 8 min. Cells were plated on poly-D-lysin-coated glass coverslips in a medium containing Dulbecco's-Modified Eagle Medium-low glucose (D-MEM), 5% horse serum, 5% newborn calf serum, 5% fetal bovine serum, 0.1% penicillin-streptomycin, 200 ng/ml nerve growth factor (NGF). Cells were maintained at 37°C in a humidified atmosphere with 5% CO2 (Szoke et al., 2010).

Ratiometric Technique of Intracellular Free Calcium Concentration ([Ca^{2+}]i) Measurement with the Fluorescent Indicator Fura-2 AM.

One-two-day-old neurons were incubated for 30 min at 37°C with 1 μM of fluorescent Ca^{2+} indicator dye, fura-2-AM. Cells were washed with extracellular solution (ECS). Calcium transients were detected with microfluorimetry as described elsewhere (Szoke et al., 2010). Fluorescent imaging was performed with an Olympus LUMPLAN FI/x20 0.5 W water immersion objective and a digital camera (CCD, SensiCam PCO) and a Monochromator (Polychrome II., Till Photonics) (generated light: 340 and 380 nm, emitted light: 510 nm). Axon Imaging Workbench 2.1 (AIW, Axon Instruments) software was used, R = F340/F380 was monitored, data were subsequently processed by the Origin software version 7.0 (Originlab Corp.). Ratiometric response peak magnitude was measured. Capsaicin (330 nM), AITC (100 μM), HK-1 (500 nM, 1 μM) and SP (500 nM, 1 μM) were administered during the experiments. CP99994, AMG 9810 and HC 030031 were administered in 10 μM concentration.

Drugs and Chemicals

AITC (Sigma) was dissolved in dimethyl sulfoxide (DMSO) (Sigma) to obtain 10 mM stock solution. Further dilutions were made with ECS solution to reach final concentrations of 100 μM. Capsaicin (Sigma) was dissolved in DMSO to obtain a 10 mM stock solution. Further dilutions were made with ECS or Hank's solution to reach final concentrations of 330 or 100 nM, respectively. Penicillin-streptomycin was purchased from Gibco. D-MEM-low glucose, collagenase type XI, deoxyribonuclease I, horse serum, newborn calf serum, fetal bovine serum, poly-D-lysine, glycine, NGF, pertussis toxin (PTX), SP, HK-1 were purchased from Sigma. CP99994, AMG 9810 and HC 030031 were purchased from Tocris.

Statistical Analysis

The treatments were not randomized within cages to prevent control animals from harming the arthritic animals. Results are expressed as the means ± SEM of n = 6–10 mice per group in case of *in vivo* functional tests. Data obtained in these experiments were analyzed with repeated measures two-way ANOVA followed by Bonferroni's post-test with GraphPad Prism 5 software. In all cases $p < 0.05$ was accepted as statistically significant.

RESULTS

HK-1 Mediates Mechanical Hyperalgesia, Paw Edema and Decrease in Heat Threshold in Chronic Immune Arthritis

Compared to pre-treatment control values, a significant decrease in pain threshold developed in WT mice by the 5th day of the experiment (-33.5 ± 4.1%). This spontaneously resolved by the end of the 3rd week. *Tac4*$^{-/-}$ mice showed significantly milder decrease in the pain threshold (-19.4 ± 3.8% on day 5) throughout the entire experiment (**Figure 1A**). The decrease in heat threshold began in WT mice at the 4th day (47.6 ± 1.3°C) and was significantly less severe in *Tac4*$^{-/-}$ mice (50.6 ± 0.8°C) (**Figure 1B**).

Paw edema developed by the 3rd day of the experiment (43.8 ± 7.2% in WT), and spontaneously resolved by 2 weeks after serum administration with significantly milder edema seen in *Tac4*$^{-/-}$ mice (**Figure 1C**). Decrease in cold tolerance, body weight and time spent on grid occurred in the experiment, but gene deletion resulted in no difference (**Figures 1D–F**). Change in mechanonociceptive threshold, arthritis score, paw volume, cold tolerance, body weight and time spent on grid in NK1R deficient mice showed no difference compared to WT mice (**Supplementary Figure S1**).

HK-1 Decreases MPO-Activity in K/BxN Serum-Transfer Arthritis

Tac4$^{-/-}$ mice showed a marked increase in MPO-activity 2 days after serum administration (6,16 × 105 ± 6,83 × 104 p/s), whereas in WT mice it became significant on the 4th day (409,917 ± 56729) (**Figure 2A**). An increase in plasma extravasation was detectable in both groups on the 2nd and 6th day, but no effect of the gene-deletion could be observed (**Figure 2B**). Representative pictures of MPO-activity can be seen on **Figure 2C**.

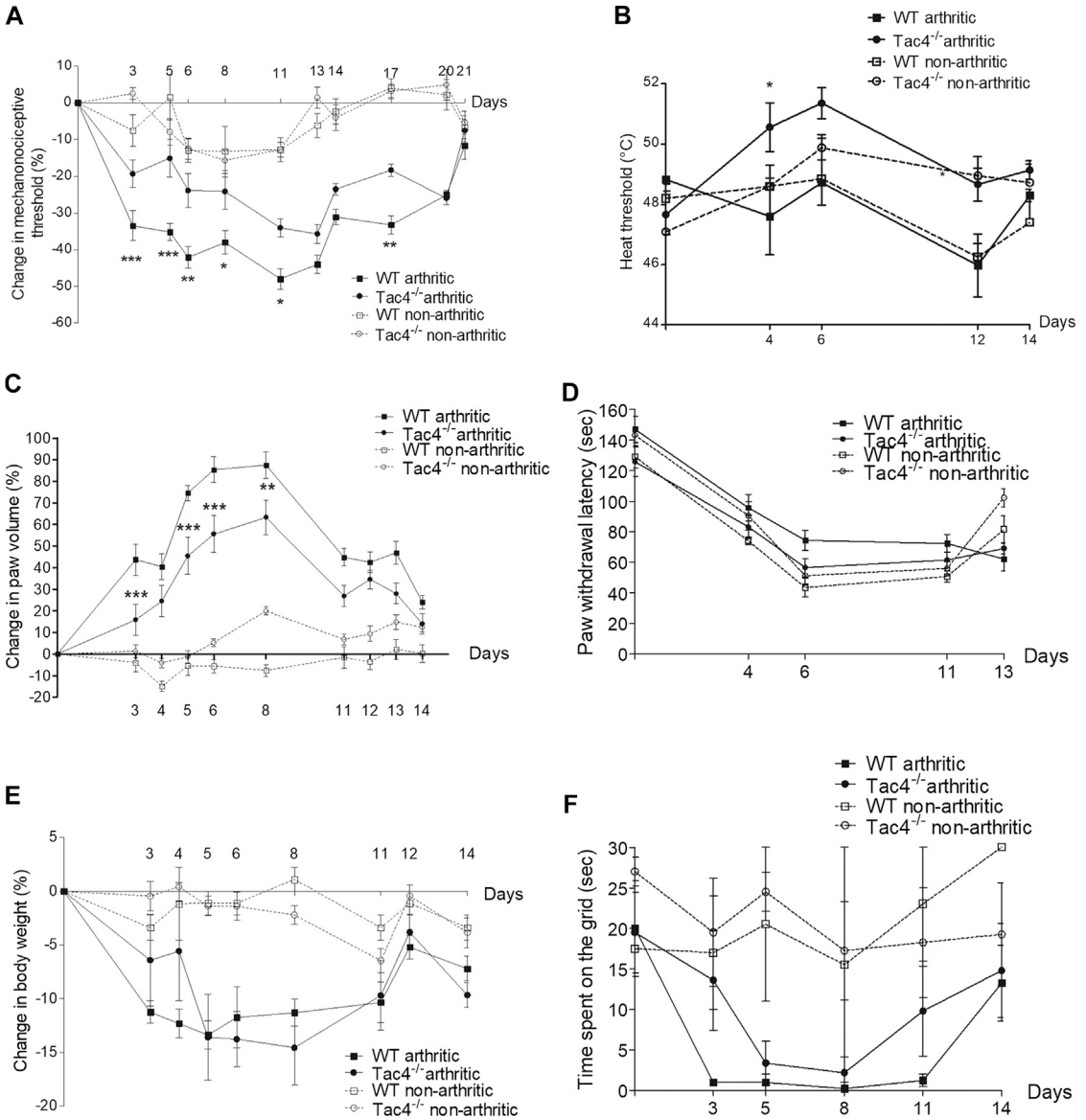

FIGURE 1 | Change in mechanonociceptive threshold **(A)**, heat threshold **(B)**, paw volume **(C)**, cold tolerance **(D)**, body weight **(E)** and time spent on grid **(F)** in K/BxN serum-induced arthritis of wild type (WT) and hemokinin-1-deficient (*Tac4*$^{-/-}$) mice in comparison with BxN serum-treated non-arthritic groups (n = 4–10 per group; $^{*}p < 0.05$, $^{**}p < 0.01$, $^{***}p < 0.001$ vs. arthritic WT, repeated measures two-way ANOVA + Bonferroni's post test).

HK-1 Increases Histopathological Arthritis Severity

On the 14th day of the experiment WT mice had a severity score of 4.0 ± 0.5 out of a maximum of nine points, while *Tac4*$^{-/-}$ mice had a significantly lower score of 2.5 ± 0.5 (**Figure 3**).

Tac4 mRNA Expression in DRG and Spinal Cord

Tac4 mRNA showed a stable expression in the DRG throughout the experiment, with a slight, non-significant decrease on day 6 (**Supplementary Figure S3**). In dorsal spinal cord samples, *Tac4* specific signals were not detectable. The specificity of the reaction was proved by using inguinal lymph nodes as positive control. RNA samples of *Tac4*$^{-/-}$ mice served as negative controls, in which samples we did not observe any amplification products with the applied probes.

HK-1 Mediates Mechanical Hyperalgesia and Knee Edema in MCT-Induced Acute Monoarthritis

Mechanical hyperalgesia developed in WT mice 2 days after MCT administration (-11.8 ± 4.0%), while knee edema developed on the 4th day (13.3 ± 1.6). Both parameters were significantly less

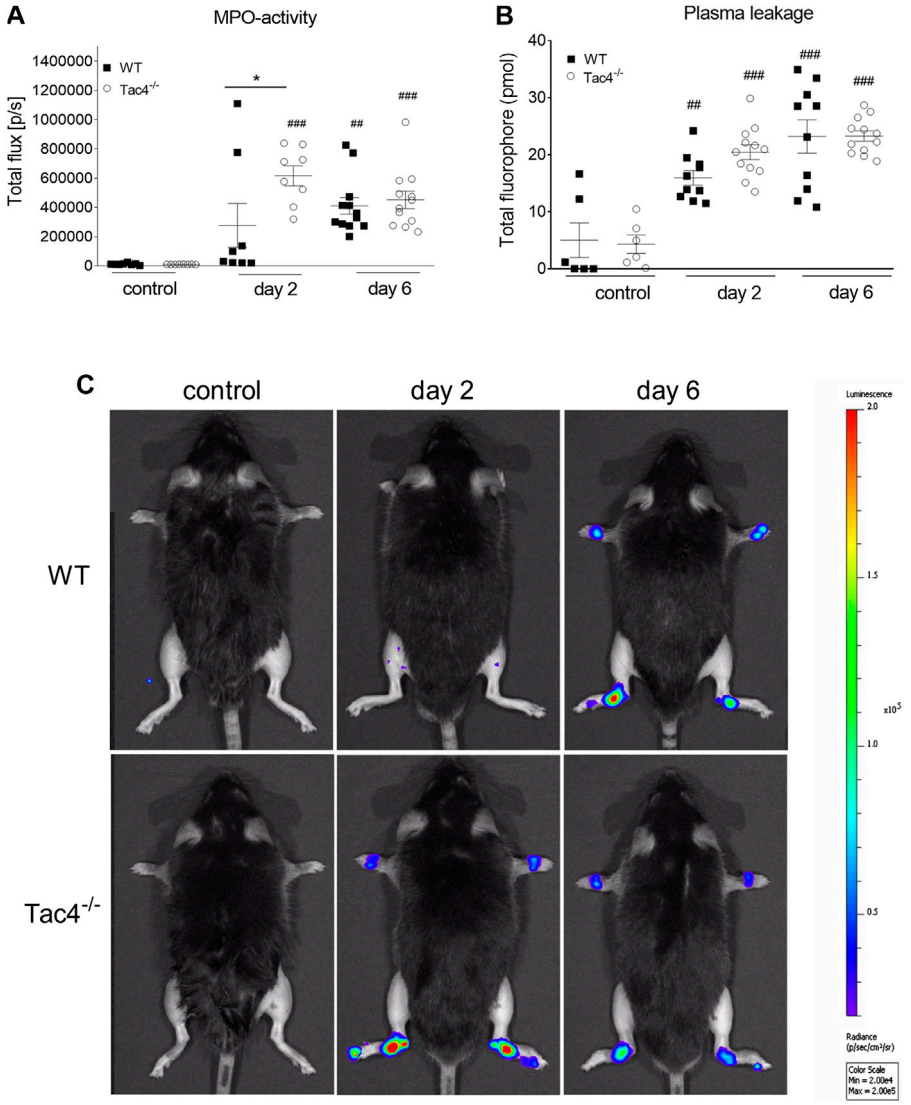

FIGURE 2 | Quantitative evaluation of MPO-activity **(A)** and IR-676 dye extravasation **(B)** in K/BxN arthritogenic serum-treated wild type (WT) and hemokinin-1-deficient (*Tac4*$^{-/-}$) mice. Representative images of MPO-activity **(C)**. Box plots demonstrate medians with the upper and lower quartiles and all individual data points; *n* = 6–12 per group; **p* < 0.05 vs. WT, ##*p* < 0.01, ###*p* < 0.001 vs. control (one-way ANOVA + Bonferroni's post test).

severe in *Tac4*$^{-/-}$ mice. Increase in blood flow was detectable in the first 40 min after treatment but showed no significant difference between the groups (**Figure 4**).

HK-1 Mediates Mechanical Hyperalgesia and Knee Edema, but Decreases MPO Activity in CFA-Induced Subacute Knee Inflammation

Mechanical hyperalgesia and knee edema were detectable 2, 6 and 24 h after the CFA administration. *Tac4*$^{-/-}$ mice had a significantly milder mechanical hyperalgesia at every time point and less severe knee edema at 24 h. *Tac4*$^{-/-}$ mice showed a significant increase in MPO-activity (457,125 ± 94397) (**Figure 5**). Changes in mechanonociceptive threshold and knee volume did not show significant difference to WT mice in NK1R deficient mice (**Supplementary Figure S2**).

HK-1 Directly Activates Primary Nociceptive Sensory Neurons

First, the effects of HK-1 and SP were investigated. Both peptides in 500 nM (**Figures 6A–E**) and SP in 1 μM concentration (data not shown) had no effect on Ca^{2+}-influx, but 1 μM HK-1 caused remarkable Ca^{2+}-influx (R = 0.67 ± 0.07) in 26.39 ± 4.5% of the neurons (19 out of 72). In the next step, we investigated the mechanism of HK-1 action and the characteristics of the Ca^{2+}-signal. The NK1 receptor antagonist CP99994 did not influence the HK-1 response, 20.93 ± 3.8% of the cells (9 out of 43) responded with Ca^{2+}-influx (R = 0.62 ± 0.08). This was

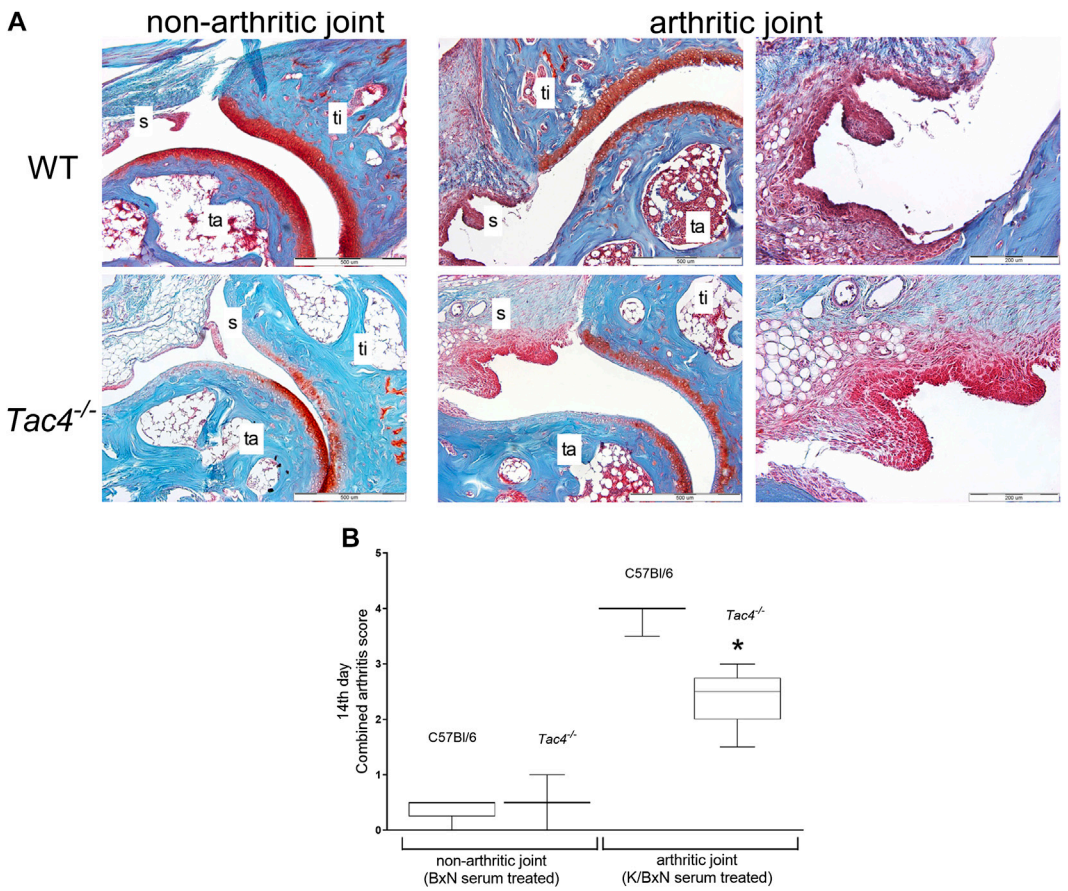

FIGURE 3 | Representative histopathological pictures of safranin O-stained tibiotarsal joint showing ×100 and ×200 magnifications with 500 and 200 μm scale bars, respectively. ti = tibia, ta = tarsus, s = synovium **(A)**. Semiquantitative histopathological score of K/BxN serum treated wild type (WT) and hemokinin-deficient (*Tac4*$^{-/-}$) arthritic mice in comparison with non-arthritic controls. Box plots demonstrate the medians with upper and lower quartiles of n = three to five per group (*p < 0.05 vs. WT, Mann-Whitney test) **(B)**.

similar in neurons of NK1R gene-deleted mice (21.4 ± 3.5%, nine out of 42 responsive cells, R = 0.49 ± 0.04). The G-protein-coupled receptor (GPCR) blocker PTX influenced neither the ratio of the responding neurons (24.49 ± 3.6%; 12 out of 49) nor the extent of the response (R = 0.74 ± 0.03) to HK-1. In order to investigate potential HK-1-induced Ca^{2+}-release from intracellular stores as a consequence of PTX-insensitive GPCR mechanism, we did measurements using Ca^{2+} free ECS. No Ca^{2+}-signal was detected in this condition indicating that HK-1 evokes Ca^{2+}-influx from the extracellular space. The response to HK-1 was detected in the presence of the TRPV1 antagonist AMG8910, 22.7 ± 4% of the cells (5 out of 22) responded with Ca^{2+}-influx (R = 0.7 ± 0.28) and the TRPA1 antagonist HC 030031, 19.2 ± 4.7% of the cells (5 out of 26) responded with Ca^{2+}-influx (R = 0.32 ± 0.26).

In the next experiment four or five repeated treatments of capsaicin on the same cultured sensory neurons were performed, and the effect of 500 nM HK-1 and SP was investigated on capsaicin-evoked Ca^{2+}-influx. The first application of 330 nM capsaicin induced transient Ca^{2+}-accumulation which gradually decreased in response to the second capsaicin stimulus due to TRPV1 (transient receptor potential cation channel subfamily V member 1) desensitization. Meanwhile, both HK-1 and SP administered in separate cultures after the second capsaicin stimulus diminished the desensitization as shown by the third and fourth capsaicin-evoked responses (**Figures 6F–I**).

DISCUSSION

Here we provide the first evidence for an important role of HK-1 in pain transmission using different arthritis models. This is likely to be mediated by direct activation of primary sensory neurons via NK1R-independent, PTX-insensitive, but extracellular Ca^{2+}-dependent mechanism. Besides its key importance in pain development, HK-1 has a complex regulatory function in joint inflammatory processes: it mediates edema formation and histopathological alterations including inflammatory cell accumulation, but inhibits early neutrophil/macrophage-dependent MPO-activity increase in the chronic model.

K/BxN induced arthritis is a widely accepted chronic passive transfer disease model (Malcangio, 2020), MCT is an important

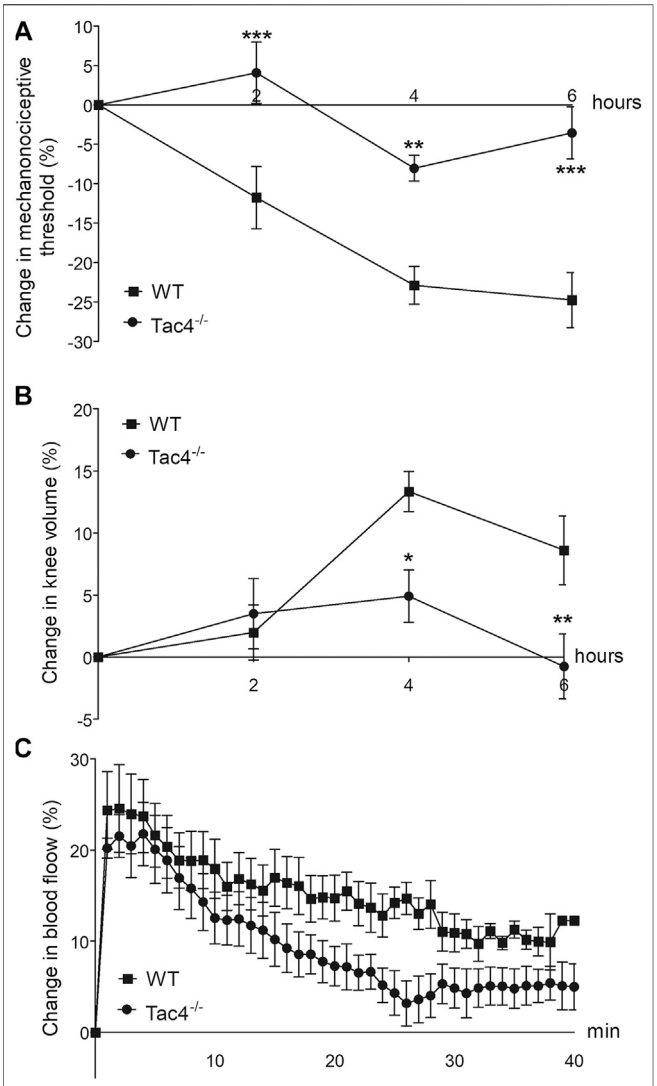

FIGURE 4 | Changes in mechanonociceptive threshold **(A)**, knee diameter **(B)** and blood flow **(C)** in mast cell tryptase-induced acute arthritis of wild type (WT) and hemokinin-1-deficient (*Tac4*$^{-/-}$) mice. Data points demonstrate the means ± SEM of n = 5–10 per group; $^{*}p < 0.05$, $^{**}p < 0.01$, $^{***}p < 0.001$ vs. WT (repeated measures two-way ANOVA + Bonferroni's post test).

local mediator of inflammation (Kobayashi and Okunishi, 2002), mediating its effects through sensory neurons (Borbély et al., 2016), and acute CFA (Billiau and Matthys, 2001) induced arthritis is initiated by macrophages. Using these three methods we could obtain a more detailed picture on how HK-1 influences the development of joint inflammation and related pain.

The deficiency of HK-1, but not the NK1R resulted in significantly decreased swelling in the acute models and also in the early phase of the chronic experiment. Plasma leakage was not altered by HK-1 on days 2 and 6, but only venular fenestration and dye extravasation at the timepoints of the examination can be detected with the applied *in vivo* fluorescent imaging technique (Botz et al., 2015). This is one component of the edema formation, but it does not exclusively explain paw swelling differences at the respective observation timepoints mainly due to different kinetics of the different components of the vascular changes (vasodilation and leakage). We found no difference in edema formation in the chronic adjuvant-induced active immunization-based model in HK-1 or NK1R deficient mice (Borbély et al., 2013), therefore, the edemogenic action of HK-1 seems to develop in a much earlier phase of the inflammatory process. The arteriolar vasodilation and microcirculation-increase was not affected either by HK-1-deletion in the MCT-model, which suggests that HK-1 is not a predominant regulator of the vascular (Borbély et al., 2013) functions.

Cellular inflammatory response in the chronic arthritis model, as shown by the histopathological arthritis score, was significantly reduced in HK-1-deficient mice. These results are supported by the well-established immunoregulatory role of HK-1. B-cells play an important role in RA, restricting their function has been shown to ameliorate autoimmune arthritis (Tóth et al., 2019), and HK-1 plays a critical role in the development of these cells (Zhang et al., 2000). It also influences monocyte/macrophage development (Berger et al., 2007) and neutrophils *in vitro* (Klassert et al., 2008), which play a role in arthritis development (Smith and Haynes, 2002). We found that despite reduced functional and morphological inflammatory alterations, MPO increase related to neutrophil and macrophage activation occurred earlier (on day 2) in the absence of HK-1. This virtual contradiction can be explained by data showing that although MPO is generally known as a mediator of tissue damage and inflammation, it has been shown to prevent inflammation as well (Arnhold and Flemmig, 2010). The elevation of MPO especially in the early phase of the inflammatory cascade is considered to be protective, though the mechanism is not well understood. MPO products have been suggested to downregulate innate immunity, facilitate the switch to adaptive immunity and inhibit T-cell reponses (Prokopowicz et al., 2012). We have seen similar relation between elevated MPO and decreased inflammatory parameters in a previous study (Horváth et al., 2016). Since HK-1 and MPO are both produced by neutrophils, they might have direct interactions, but these have not yet been studied. There is limited evidence about the involvement of HK-1 in pain which, in agreement with our present results, found it to be pro-nociceptive. Intracerebroventricular administration of low dose (1–10 pmol) HK-1 caused nocifensive behavior, while high dose (≥0.1 nmol) caused analgesia, all of which could be counteracted by an NK1R antagonist, as well as opioid antagonists (Fu et al., 2005). Other studies have shown that lumbar intrathecal administration of 0.1 nmol HK-1 caused pain reaction in mice which could be inhibited by an NMDA receptor antagonist (Watanabe et al., 2016), but not an NK1R antagonist (Watanabe et al., 2010). These results suggest that high doses of HK-1 might have non-specific actions resulting in divergent outcomes. Our earlier paper provided evidence that HK-1 has an important role in neuropathic pain and microglia activation (Hunyady et al., 2019). Other studies found that HK-1 mRNA expression increases in the dorsal spinal cord of neuropathic rats which could be blocked by inhibiting microglia activation and

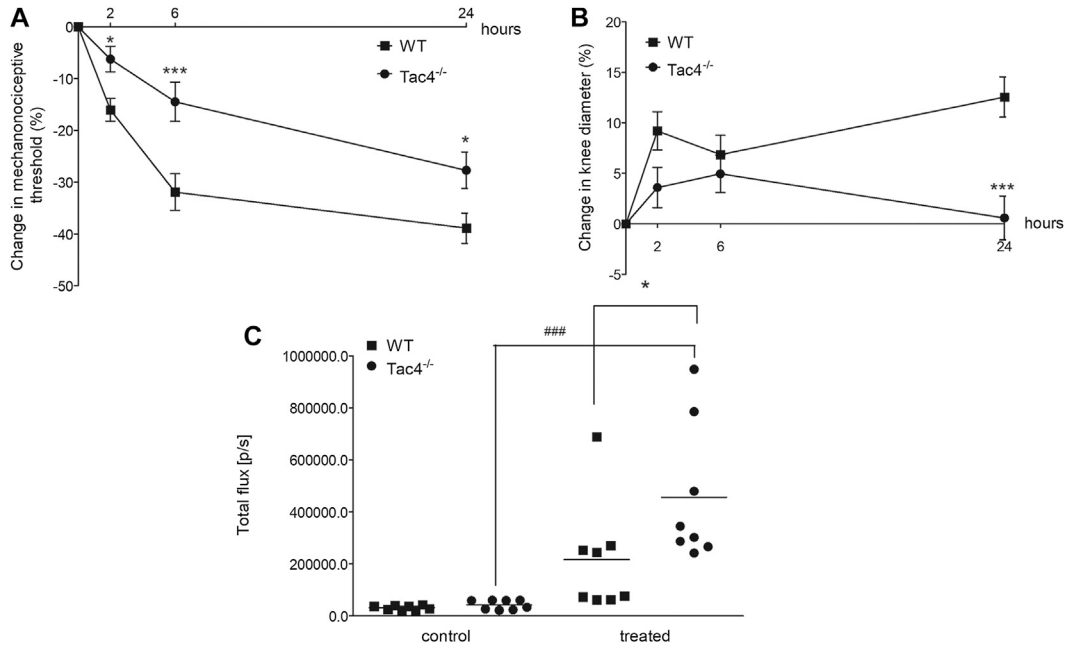

FIGURE 5 | Changes in mechanonociceptive threshold **(A)**, AP knee diameter **(B)**, and MPO-activity **(C)** in CFA-induced acute arthritis of WT and HK-1-deficient (*Tac4*$^{-/-}$) mice. Data points demonstrate the means ± SEM **(A)**, **(B)** or medians with upper and lower quartiles of $n = 8–15$ per group; $^{*}p < 0.05$, $^{**}p < 0.01$, $^{***}p < 0.001$ vs. WT, $^{###}p < 0.001$ vs. control (repeated measures two-way ANOVA + Bonferroni's post test; for MPO activity: one-way ANOVA + Bonferroni's post test).

alleviating pain (Matsumura et al., 2008). Our current results show that HK-1 mediates both the early inflammatory pain, and the late neuropathic-type pain in arthritis observed during the 3rd week of the K/BxN experiment (Christianson et al., 2010), while other studies showed the activation of spinal microglia in experimental arthritis (Agalave et al., 2014). Earlier findings showed significantly decreased HK-1 mRNA in the DRG in the collagen antibody induced arthritis (CAIA) mouse model (Makino et al., 2012), which is in agreement with the tendency we demonstrated in the present paper, although the decrease was not statistically significant due to individual variations. Joint inflammation was alleviated by NK1R antagonists in the CAIA model, while the pain could only be inhibited by indomethacin. In agreement with these findings we have also showed that the NK1 receptor does not play a role in arthritic pain, however, we conclude that HK-1 might be an important mediator in an NK1R-independent manner by directly activating primary sensory neurons.

Despite little information about HK-1 in pain and arthritis, the best-known member of the tachykinin family, SP, and the NK1R have been thoroughly investigated in these conditions (Zieglgänsberger, 2019). It is well established that SP via NK1R activation is involved in pain, which initiated considerable pharmacological research in this field. Despite the proof-of-concept of SP as a pain mediator, unfortunately, NK1R-antagonists have failed as analgesics in clinical trials (Botz et al., 2017), suggesting a yet unknown mechanism that can circumvent NK1R-targeted approaches. SP mediates chondrocyte differentiation in cell cultures (Millward-Sadler et al., 2003) and vasodilation in arthritic mice (Keeble et al., 2005) through the NK1 receptor. SP-like immunoreactivity was shown to increase in the primary sensory neurons of dorsal root ganglia (DRG) of arthritic mice (Willcockson et al., 2010), but the number of sensory nerve fibers of the arthritic joint capsule, that are the main sources of SP, decreased (Buma et al., 2000). Since SP and HK-1 cannot be differentiated by immunological methods, it is possible that these immunohistochemistry data referred (at least partially) to HK-1 expression.

In order to explore the direct effect and mechanism of action of HK-1, we did further studies on cultured primary sensory neurons. HK-1, but not SP, induced Ca^{2+}-influx into these neurons. HK-1-induced direct Ca^{2+}-influx could be seen during PTX administration and also in sensory neurons derived from *NK1R*$^{-/-}$ animals. The main finding of our experiments was that the Ca^{2+}-influx was coming from the extracellular space in an NK1R-independent manner since the signal disappeared in Ca^{2+}-free extracellular solution. It suggests an ion channel-coupled receptorial mechanism, but not TRPV1- or TRPA1-mediated mechanism, since the TRPV1 receptor antagonist AMG9810 and the TRPA1 receptor antagonist HC 030031 did not influence the HK-1-induced Ca^{2+} influx response. Furthermore, even lower concentrations of both HK-1 (similarly to SP) diminished desensitization of the TRPV1 receptor that upon repeated capsaicin administration could also contribute to the peripheral pain generating and maintaining effect of HK-1. The neuronal activating potential of HK-1 is supported by earlier data showing the ability of HK-1 to evoke direct post-synaptic activation of cholinergic hippocampal neurons in a tetrodotoxin-resistant manner. However, unlike sensory neurons, this response was not inhibited in Ca^{2+}-fee media and was similar to the effect of SP (Morozova et al., 2008).

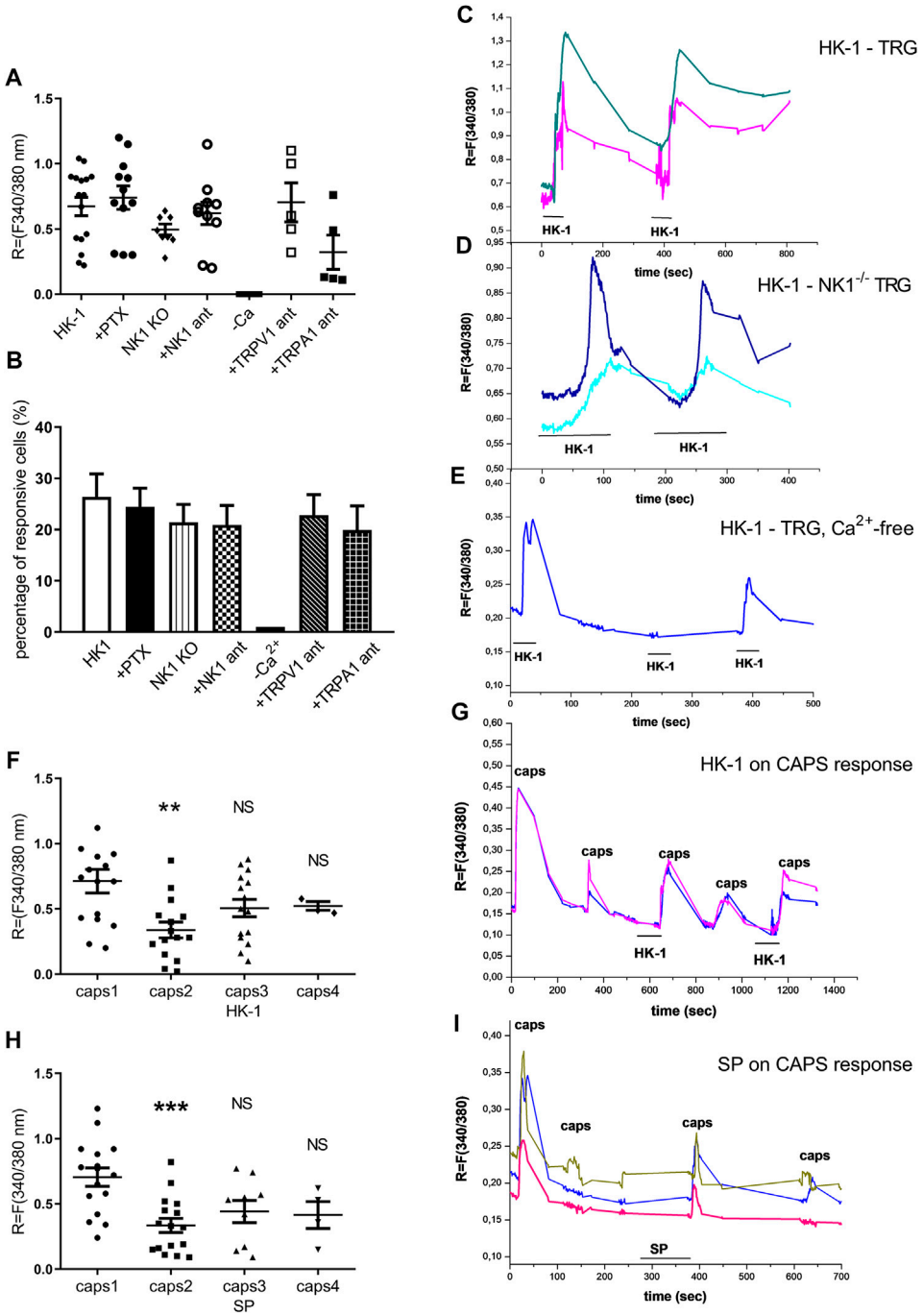

FIGURE 6 | Effect of HK-1 and SP in cultured primary sensory neurons. Change in the fluorescence ratio (R = F340/F380) in HK-1-sensitive cells (●) is presented. ●: HK-1 and PTX co-administration, ◆: fluorescence signal in neurons from *NK1R*$^{-/-}$ animals, ○: HK-1 and CP99994 NK1 receptor antagonist administration, □: HK-1 and AMG9810 TRPV1 receptor antagonist, ■: HK-1 and HC 030031 TRPA1 receptor antagonist. No signal was detected in Ca^{2+}-free extracellular solution. N = 19–49 cells/group **(A)**. The percentage of responsive cells to HK-1, HK-1+PTX, HK-1 in Ca^{2+}-free condition, HK-1+NK1 receptor antagonist CP99994 and HK-1 in TG from *NK1R*$^{-/-}$ animals, HK-1 + TRPV1 receptor antagonist AMG9810 and HK-1 + TRPA1 receptor antagonist HC 030031 is presented. Ca^{2+}-responses are presented in % of total number of examined neurons. N = 19–49 cells per group **(B)**. Original Ca^{2+}-imaging registrations after HK-1 administration. Increases of R = 340/380 fluorescence in fura-2 loaded cultured TG neurons **(C)**. Original Ca^{2+}-imaging registrations after HK-1 administration in TG neurons from NK1 gene deficient mice **(D)**. Original Ca^{2+}-imaging registrations after HK-1 administration in Ca^{2+}-free solution **(E)**. Effect of HK-1 on capsaicin-induced Ca^{2+}-influx. Increases of R = 340/380 fluorescence in fura-2 loaded neurons are presented, $^{**}p < 0.01$, NS (vs. caps1, one-way ANOVA with Bonferroni's multiple comparison post hoc test, n = 16) **(F)**. Effect of HK-1 on capsaicin-induced Ca^{2+}-influx. Original Ca^{2+}-imaging registrations after capsaicin and HK-1 administration **(G)**. Effect of SP on capsaicin-induced Ca^{2+}-influx. Increases of R = 340/380 fluorescence in fura-2 loaded neurons are presented, $^{***}p < 0.001$, NS (vs. caps1, one-way ANOVA with Bonferroni's multiple comparison post hoc test, n = 17) **(H)**. Effect of SP on capsaicin-induced Ca^{2+}-influx. Original Ca^{2+}-imaging registrations after capsaicin and SP administration **(I)**.

Some limitations of the present study are that we only performed our experiments on male mice to avoid the influencing factors of the estrus cycle and that we could detect HK-1 neither qualitatively by immunohistochemistry nor quantitatively by immune assays due to the lack of antibodies able to differentiate it from SP.

In conclusion, we provide the first evidence using three different mouse models mimicking distinct mechanisms of rheumatoid arthritis and integrative methodology (functional, *in vivo* optical imaging, cell cultures) that HK-1 mediates several arthritic inflammatory mechanisms and pain by direct activation of primary sensory neurons not via its classical NK1 receptor. The main translational value is that we modeled the late neuropathic component of arthritic pain related to neuropathic mechanisms without inflammatory symptoms and describe the involvement of HK-1 in this process. These findings add to the growing evidence that HK-1 has another, so far unidentified target initiating further research in this direction.

DATA AVAILABILITY STATEMENT

The original contributions presented in the study are included in the article/**Supplementary Material**, further inquiries can be directed to the corresponding author.

ETHICS STATEMENT

The animal study was reviewed and approved by Ethics Committee on Animal Research of the University of Pécs.

AUTHOR CONTRIBUTIONS

All authors were involved in drafting the article or revising it critically for important intellectual content, and all authors approved the final version to be published. ZH and AH had full access to all the data in the study and take responsibility for the integrity of the data and the accuracy of the data analysis. ÉB and AH, and also ÉS and ZH contributed equally to this work, respectively.

FUNDING

This work was supported by EFOP-3.6.2-16-2017-00008 "The role of the neuroinflammation in neurodegeneration: from molecules to clinics", 2017-1.2.1-NKP-2017-00002 (NAP-2; Chronic Pain Research Group), EFOP-3.6.1.-16-2016-0004 and GINOP 2.3.2-15-2016-00050 "PEPSYS". ÉB 2019 and ÉS 2017 were supported by the János Bolyai Research Scholarship of the Hungarian Academy of Sciences. KP was supported by GYTK-KA-2020-01, University of Pécs Faculty of Pharmacy and the New National Excellence Program of the Ministry for Innovation and Technologies from the source of the National Research, Development and Innovation Fund ÚNKP-20-4-II-PTE-465. BB 2019 was supported by the János Bolyai Research Scholarship of The Hungarian Academy of Sciences and the ÚNKP-20-5-PTE-540 New National Excellence Program of the Ministry for Innovation and Technology. The University of Pécs is acknowledged for a support from the 17886-4/23018/FEKUTSTRAT excellence grant. AM was supported by the "Élvonal" program from the Hungarian National Agency for Research, Development and Innovation (KKP 129954).

ACKNOWLEDGMENTS

We would like to thank Tamás Kiss, Anikó Perkecz, László Kereskai and Katinka Békefi for their assistance in the experiments, Ágnes Kemény for preparing the histology images for publication, Kata Bölcskei for revising the manuscript as well as Alexandra Berger, Christopher J. Paige and John P. Quinn for providing the original breeding pairs of the KO mice. The *in vivo* imaging studies were performed in the Small Animal *In Vivo* Imaging Core Facility of the Szentágothai Research Center (University of Pécs, Hungary).

SUPPLEMENTARY MATERIAL

The Supplementary Material for this article can be found online at: https://www.frontiersin.org/articles/10.3389/fphar.2020.594479/full#supplementary-material.

REFERENCES

Aczél, T., Kecskés, A., Kun, J., Szenthe, K., Bánáti, F., Szathmary, S., et al. (2020). Hemokinin-1 gene expression is upregulated in trigeminal ganglia in an inflammatory orofacial pain model: potential role in peripheral sensitization. *Int. J. Mol. Sci.* 21 (8), 2938. doi:10.3390/ijms21082938

Agalave, N. M., Larsson, M., Abdelmoaty, S., Su, J., Baharpoor, A., Lundbäck, P., et al. (2014). Spinal HMGB1 induces TLR4-mediated long-lasting hypersensitivity and glial activation and regulates pain-like behavior in experimental arthritis. *Pain* 155, 1802–1813. doi:10.1016/j.pain.2014.06.007

Arnhold, J., and Flemmig, J. (2010). Human myeloperoxidase in innate and acquired immunity. *Arch. Biochem. Biophys.* 500, 92–106. doi:10.1016/j.abb.2010.04.008

Berger, A., Benveniste, P., Corfe, S. A., Tran, A. H., Barbara, M., Wakeham, A., et al. (2010). Targeted deletion of the tachykinin 4 gene ($TAC4^{-/-}$) influences the early stages of B lymphocyte development. *Blood* 116, 3792–3801. doi:10.1182/blood-2010-06-291062

Berger, A., Tran, A. H., and Paige, C. J. (2007). Co-regulated decrease of Neurokinin-1 receptor and Hemokinin-1 gene expression in monocytes and macrophages after activation with pro-inflammatory cytokines. *J. Neuroimmunol.* 187, 83–93. doi:10.1016/j.jneuroim.2007.04.019

Billiau, A., and Matthys, P. (2001). Modes of action of Freund's adjuvants in experimental models of autoimmune diseases. *J. Leukoc. Biol.* 70, 849–860. doi:10.1189/jlb.70.6.849

Borbély, E., Hajna, Z., Sándor, K., Kereskai, L., Tóth, I., Pintér, E., et al. (2013). Role of tachykinin 1 and 4 gene-derived neuropeptides and the neurokinin 1 receptor in adjuvant-induced chronic arthritis of the mouse. *PloS One* 8, e61684. doi:10.1371/journal.pone.0061684

Borbély, É., and Helyes, Z. (2017). Role of hemokinin-1 in health and disease. *Neuropeptides* 64, 9–17. doi:10.1016/j.npep.2016.12.003

Borbély, É., Sándor, K., Markovics, A., Kemény, Á., Pintér, E., Szolcsányi, J., et al. (2016). Role of capsaicin-sensitive nerves and tachykinins in mast cell tryptase-

induced inflammation of murine knees. *Inflamm. Res.* 65, 725–736. doi:10.1007/s00011-016-0954-x

Botz, B., Bölcskei, K., and Helyes, Z. (2017). Challenges to develop novel anti-inflammatory and analgesic drugs. *Wiley Interdiscip. Rev. Nanomed. Nanobiotechnol.* 9, e1427. doi:10.1002/wnan.1427

Botz, B., Bölcskei, K., Kemény, Á., Sándor, Z., Tékus, V., Sétáló, G., et al. (2015). Hydrophobic cyanine dye-doped micelles for optical *in vivo* imaging of plasma leakage and vascular disruption. *J. Biomed. Optic.* 20, 016022. doi:10.1117/1.JBO.20.1.016022

Buma, P., Elmans, L., Berg, W. B. V. D., and Schrama, L. H. (2000). Neurovascular plasticity in the knee joint of an arthritic mouse model. *Anat. Rec.* 260, 51–61. doi:10.1002/1097-0185(20000901)260:1<51::AID-AR60>3.0.CO;2-9

Chancay, M. G., Guendsechadze, S. N., and Blanco, I. (2019). Types of pain and their psychosocial impact in women with rheumatoid arthritis. *Womens Midlife Health.* 5, 3. doi:10.1186/s40695-019-0047-4

Christianson, C. A., Corr, M., Firestein, G. S., Mobargha, A., Yaksh, T. L., and Svensson, C. I. (2010). Characterization of the acute and persistent pain state present in K/BxN serum transfer arthritis. *Pain* 151, 394–403. doi:10.1016/j.pain.2010.07.030

Day, A. L., and Curtis, J. R. (2019). Opioid use in rheumatoid arthritis: trends, efficacy, safety, and best practices. *Curr. Opin. Rheumatol.* 31, 264–270. doi:10.1097/BOR.0000000000000602

De Felipe, C., Herrero, J. F., O'Brien, J. A., Palmer, J. A., Doyle, C. A., Smith, A. J., et al. (1998). Altered nociception, analgesia and aggression in mice lacking the receptor for substance P. *Nature* 392, 394–397. doi:10.1038/32904

Donaldson, L. F., McQueen, D. S., and Seckl, J. R. (1995). Neuropeptide gene expression and capsaicin-sensitive primary afferents: maintenance and spread of adjuvant arthritis in the rat. *J. Physiol.* 486, 473–482. doi:10.1113/jphysiol.1995.sp020826

Ebbinghaus, M., Müller, S., Banchet, G. S. von., Eitner, A., Wank, I., Hess, A., et al. (2019). Contribution of inflammation and bone destruction to pain in arthritis: a study in murine glucose-6-phosphate isomerase–induced arthritis. *Arth. Rheum.* 71, 2016–2026. doi:10.1002/art.41051

Fu, C.-Y., Kong, Z.-Q., Wang, K.-R., Yang, Q., Zhai, K., Chen, Q., et al. (2005). Effects and mechanisms of supraspinal administration of rat/mouse hemokinin-1, a mammalian tachykinin peptide, on nociception in mice. *Brain Res.* 1056, 51–58. doi:10.1016/j.brainres.2005.07.020

Herrero, J. F., Laird, J. M., and López-García, J. A. (2000). Wind-up of spinal cord neurones and pain sensation: much ado about something? *Prog. Neurobiol.* 61, 169–203. doi:10.1016/s0301-0082(99)00051-9

Horváth, Á., Tékus, V., Boros, M., Pozsgai, G., Botz, B., Borbély, É., et al. (2016). Transient receptor potential ankyrin 1 (TRPA1) receptor is involved in chronic arthritis: *in vivo* study using TRPA1-deficient mice. *Arthritis Res. Ther.* 18, 6. doi:10.1186/s13075-015-0904-y

Hunyady, Á., Hajna, Z., Gubányi, T., Scheich, B., Kemény, Á., Gaszner, B., et al. (2019). Hemokinin-1 is an important mediator of pain in mouse models of neuropathic and inflammatory mechanisms. *Brain Res. Bull.* 147, 165–173. doi:10.1016/j.brainresbull.2019.01.015

Jakus, Z., Simon, E., Balázs, B., and Mócsai, A. (2010). Genetic deficiency of Syk protects mice from autoantibody-induced arthritis. *Arthritis Rheum.* 62, 1899–1910. doi:10.1002/art.27438

Keeble, J., Blades, M., Pitzalis, C., Castro da Rocha, F. A., and Brain, S. D. (2005). The role of substance P in microvascular responses in murine joint inflammation. *Br. J. Pharmacol.* 144, 1059–1066. doi:10.1038/sj.bjp.0706131

Kecskés, A., Pohóczky, K., Kecskés, M., Varga, Z. V., Kormos, V., Szöke, É., et al. (2020). Characterization of neurons epressing the novel analgesic drug target somatostatin receptor 4 in mouse and human brains. *Int. J. Mol. Sci.* 21 (20), 7788. doi:10.3390/ijms21207788

Klassert, T. E., Pinto, F., Hernández, M., Candenas, M. L., Hernández, M. C., Abreu, J., et al. (2008). Differential expression of neurokinin B and hemokinin-1 in human immune cells. *J. Neuroimmunol.* 196, 27–34. doi:10.1016/j.jneuroim.2008.02.010

Kobayashi, Y., and Okunishi, H. (2002). Mast cells as a target of rheumatoid arthritis treatment. *Jpn. J. Pharmacol.* 90, 7–11. doi:10.1254/jjp.90.7

Krock, E., Jurczak, A., and Svensson, C. I. (2018). Pain pathogenesis in rheumatoid arthritis-what have we learned from animal models?. *Pain* 159 (Suppl. 1), S98–S109. doi:10.1097/j.pain.0000000000001333

Makino, A., Sakai, A., Ito, H., and Suzuki, H. (2012). Involvement of tachykinins and NK1 receptor in the joint inflammation with collagen type II-specific monoclonal antibody-induced arthritis in mice. *J. Nippon Med. Sch.* 79, 129–138. doi:10.1272/jnms.79.129

Malcangio, M. (2020). Translational value of preclinical models for rheumatoid arthritis pain 161, 1399–1400. *Pain* doi:10.1097/j.pain.0000000000001851

Matsumura, T., Sakai, A., Nagano, M., Sawada, M., Suzuki, H., Umino, M., et al. (2008). Increase in hemokinin-1 mRNA in the spinal cord during the early phase of a neuropathic pain state. *Br. J. Pharmacol.* 155, 767–774. doi:10.1038/bjp.2008.301

McWilliams, D. F., and Walsh, D. A. (2019). Pain mechanisms in rheumatoid arthritis. Available at: https://www.clinexprheumatol.org/abstract.asp?a=12176 (Accessed December 3, 2019).

Millward-Sadler, S. J., Mackenzie, A., Wright, M. O., Lee, H.-S., Elliot, K., Gerrard, L., et al. (2003). Tachykinin expression in cartilage and function in human articular chondrocyte mechanotransduction. *Arthritis Rheum.* 48, 146–156. doi:10.1002/art.10711

Morozova, E., Wu, M., Dumalska, I., and Alreja, M. (2008). Neurokinins robustly activate the majority of septohippocampal cholinergic neurons. *Eur. J. Neurosci.* 27, 114–122. doi:10.1111/j.1460-9568.2007.05993.x

Morteau, O., Lu, B., Gerard, C., and Gerard, N. P. (2001). Hemokinin 1 is a full agonist at the substance P receptor. *Nat. Immunol.* 2, 1088. doi:10.1038/ni1201-1088

Nakamura-Craig, M., and Smith, T. W. (1989). Substance P and peripheral inflammatory hyperalgesia. *Pain* 38, 91–98. doi:10.1016/0304-3959(89)90078-x

Onaga, T. (2014). Tachykinin: recent developments and novel roles in health and disease. *Biomol. Concepts* 5, 225–243. doi:10.1515/bmc-2014-0008

Pfaffl, M. W. (2001). A new mathematical model for relative quantification in real-time RT-PCR. *Nucleic Acids Res.* 2001, 29. doi:10.1093/nar/29.9.e45

Pinho-Ribeiro, F. A., Verri, W. A., Jr, and Chiu, I. M. (2017). Nociceptor sensory neuron-immune interactions in pain and inflammation. *Trends Immunol. Jan.* 38 (1), 5–19. doi:10.1016/j.it.2016.10.001

Prokopowicz, Z., Marcinkiewicz, J., Katz, D. R., and Chain, B. M. (2012). Neutrophil myeloperoxidase: soldier and statesman. *Arch. Immunol. Ther. Exp.* 60 (1), 43–54. doi:10.1007/s00005-011-0156-8

Smith, J. B., and Haynes, M. K. (2002). Rheumatoid arthritis—a molecular understanding. *Ann. Intern. Med.* 136, 908. doi:10.7326/0003-4819-136-12-200206180-00012

Sommer, C., and Kress, M. (2004). Recent findings on how proinflammatory cytokines cause pain: peripheral mechanisms in inflammatory and neuropathic hyperalgesia. *Neurosci. Lett.* 361, 184–187. doi:10.1016/j.neulet.2003.12.007

Sparks, J. A. (2019). Rheumatoid arthritis. *Ann. Intern. Med.* 170, ITC1–ITC16. doi:10.7326/AITC201901010

Sun, W.-H., and Dai, S.-P. (2018). Tackling pain associated with rheumatoid arthritis: proton-sensing receptors. *Adv. Exp. Med. Biol.* 1099, 49–64. doi:10.1007/978-981-13-1756-9_5

Szoke, E., Börzsei, R., Tóth, D. M., Lengl, O., Helyes, Z., Sándor, Z., et al. (2010). Effect of lipid raft disruption on TRPV1 receptor activation of trigeminal sensory neurons and transfected cell line. *Eur. J. Pharmacol.* 628, 67–74. doi:10.1016/j.ejphar.2009.11.052

Tóth, D. M., Ocskó, T., Balog, A., Markovics, A., Mikecz, K., Kovács, L., et al. (2019). Amelioration of autoimmune arthritis in mice treated with the DNA methyltransferase inhibitor 5′-azacytidine. *Arthritis Rheum.* 71, 1265–1275. doi:10.1002/art.40877

Watanabe, C., Mizoguchi, H., Bagetta, G., and Sakurada, S. (2016). Involvement of spinal glutamate in nociceptive behavior induced by intrathecal administration of hemokinin-1 in mice. *Neurosci. Lett.* 617, 236–239. doi:10.1016/j.neulet.2016.02.027

Watanabe, C., Mizoguchi, H., Yonezawa, A., and Sakurada, S. (2010). Characterization of intrathecally administered hemokinin-1-induced nociceptive behaviors in mice. *Peptides* 31, 1613–1616. doi:10.1016/j.peptides.2010.04.025

Willcockson, H. H., Chen, Y., Han, J. E., and Valtschanoff, J. G. (2010). Effect of genetic deletion of the vanilloid receptor TRPV1 on the expression of Substance P in sensory neurons of mice with adjuvant-induced arthritis. *Neuropeptides* 44, 293–297. doi:10.1016/j.npep.2010.02.003

Zhang, Y., Lu, L., Furlonger, C., Wu, G. E., and Paige, C. J. (2000). Hemokinin is a hematopoietic-specific tachykinin that regulates B lymphopoiesis. *Nat. Immunol.* 1, 392–397. doi: doi:10.1038/80826

Zhang, Y., and Paige, C. J. (2003). T-cell developmental blockage by tachykinin antagonists and the role of hemokinin 1 in T lymphopoiesis. *Blood* 102, 2165–2172. doi:10.1182/blood-2002-11-3572

Zieglgänsberger, W. (2019). Substance P and pain chronicity. *Cell Tissue Res*. 375, 227–241. doi:10.1007/s00441-018-2922-y

Conflict of Interest: Zsuzsanna Helyes is the strategic director and shareholder of PharmInVivo Ltd. (Pécs, Hungary) and shareholder of Algonist Biotechnologies Gmbh, (Wien, Austria). Eva Szoke is also a shareholder of Algonist Biotechnologies Gmbh, (Wien, Austria), but there is no conflict of interest with the present work. These companies were not involved in the study design, funding, collection, analysis, interpretation of data, the writing of this article or the decision to submit it for publication.

The remaining authors declare that the research was conducted in the absence of any commercial or financial relationships that could be construed as a potential conflict of interest.

GLOSSARY

AITC allyl isothiocyanate

CAIA collagen antibody induced arthritis

CFA complete Freund's adjuvant

DMARD disease-modifying antirheumatic drugs

D-MEM Dulbecco's-Modified Eagle Medium-low glucose

DMSO dimethyl sulfoxide

DPE dynamic plantar esthesiometer

DRG dorsal root ganglion

ECS extracellular solution

GPCR G-protein-coupled receptor

HK-1 hemokinin-1

i.p. intraperitoneal

i.v. intravenous

KO knockout

MCT mast cell tryptase

MPO Myeloperoxidase

NGF nerve growth factor

NK1R tachykinin neurokinin-1 receptor

NK2R tachykinin neurokinin-2 receptor

NK3R tachykinin neurokinin-3 receptor

NMDA N-metil-d-aspartic acid

NSAID nonsteroidal anti-inflammatory drugs

PAR2 protease-activated receptor two

PBS phosphate-buffered saline

PCR Polymerase chain reaction

PTX pertussis toxin

RA rheumatoid arthritis

ROI region of interest

SP substance P

Tac4 preprotachykinin-4 gene

Tacr1 tachykinin receptor one gene, encodes NK1R

TG trigeminal ganglion

TRPA1 transient receptor potential cation channel subfamily A member one

TRPV1 transient receptor potential cation channel subfamily V member one

WT wild type